



**icat
mar**

Institut Català de
Recerca per a la
Governança del Mar

State of fisheries in Catalonia 2021, Part 2: Stock assessment



Generalitat de Catalunya
Departament d'Acció Climàtica,
Alimentació i Agenda Rural



EUROPEAN UNION
European Maritime
and Fisheries Fund



Institut
de Ciències
del Mar



CSIC
CONSEJO SUPERIOR DE INVESTIGACIONES CIENTÍFICAS

This report presents the state of fisheries in Catalonia in 2021 and is the second volume to State of fisheries in Catalonia 2021, Part II: report on the monitoring of the commercial fishing fleet.

Scientific team: Joan B. Company and Laura Recasens (coord.), John G. Ramírez and Mariona Garriga-Panisello (stock assessment analyses coord.).

Technical team: Marta Blanco, Eve Galimany, Marc Balcells, Ferran Bustos, Marta Carreton, Mauro Gómez, Cristina López-Pérez, Sara Mohamed, David Nos, Xènia Puigcerver, Marta Pujol, Jordi Ribera, Alberto J. Rico, Alba Rojas, Joan Sala-Coromina, Ricardo Santos-Bethencourt and Mireia Silvestre

How to cite this document

Institut Català de Recerca per a la Governança del Mar (ICATMAR). State of fisheries in Catalonia 2021, Part 2: stock assessment (ICATMAR, 22-05) 110 pp, Barcelona. DOI: 10.2436/10.8080.05.15

Image credits:

Front page (Marc Balcells and Mariona Garriga), 1 (Marta Blanco and David Nos), 2 (Marc Balcells and Ricardo Santos), 3 (David Nos), 4 (Marc Balcells and Mariona Garriga).

Table of contents

Index of figures and tables	7
Glossary	13
Executive summary	15
1. Introduction	17
2. Material and Methods	23
Data	24
Models	26
3. Results by stock	29
Red mullet (<i>Mullus barbatus</i>) MUT	30
Stock assessment by model (without discards)	33
LBSPR	33
LBPA	36
Stock assessment indicators	38
Stock assessment by model (with discards)	39
LBSPR	39
LBPA	42
Stock assessment indicators	45
Hake (<i>Merluccius merluccius</i>) HKE	46
Stock assessment by model (without discards)	49
LBSPR	49
LBPA	52
LIME	54
Stock assessment indicators	56
Stock assessment by model (with discards)	57
LBSPR	57
LBPA	60
LIME	62

Stock assessment indicators	64
Deep-water rose shrimp (<i>Parapenaeus longirostris</i>) DPS	66
Stock assessment by model (without discards)	69
LBSPR	69
LBPA	72
Stock assessment indicators	74
Stock assessment by model (with discards)	75
LBSPR	75
LBPA	78
Stock assessment indicators	80
Norway lobster (<i>Nephrops norvegicus</i>) NEP	82
Stock assessment by model	85
LBSPR	85
LBPA	88
LIME	90
Stock assessment indicators	93
Blue and red shrimp (<i>Aristeus antennatus</i>) ARA	94
Stock assessment by model	97
LBSPR	97
LBPA	100
LIME	102
4. Conclusions and Comments	105
References	107

Index of figures and tables

Figure 1. Spawning potential ratio (SPR) for the five stock evaluated.	13
Figure 2. Kobeplot for the five stock evaluated.	14
Figure 3. Raising scenarios to obtain the annual length frequencies distributions.	23
Figure 4. Spatial distribution of landings per unit effort (LPUE) for Red mullet.	28
Figure 5. Characterization of red mullet landings.	29
Figure 6. Annual length-frequency distributions for red mullet.	30
Figure 7. Annual length-frequency distributions for red mullet (with discards).	30
Figure 8. Fitting data by LBSPR model for red mullet.	32
Figure 9. Red mullet length maturity and selectivity outputs by the LBSPR model.	33
Figure 10. Estimated SPR values for red mullet.	33
Figure 11. Estimated F/M values for red mullet.	34
Figure 12. Fitting data by LBPR model for red mullet.	35
Figure 13. Graphs plotting the maturity-at-length curve and the estimated selectivity-at-length curve for each year by LBPR model for red mullet.	35
Figure 14. Graphs plotting the estimates of SPR and F by LBPR model for red mullet.	36
Figure 15. Fitted data by LBSPR model for red mullet (with discards).	37
Figure 16. Red mullet length maturity and selectivity by LBSPR model (with discards).	38
Figure 17. Estimated SPR values for red mullet (with discards).	39
Figure 18. Estimated F/M values for red mullet (with discards).	39
Figure 19. Fitting data by LBPR model for red mullet (with discards).	40
Figure 20. Graphs plotting the maturity-at-length curve and the estimated selectivity-at-length curve for each year by LBPR model for red mullet (with discards).	41
Figure 21. Graphs plotting the estimates of SPR and F by LBPR model for red mullet (with discards).	42
Figure 22. Spatial distribution of landings per unit effort (LPUE) for hake.	44
Figure 23. Characterization of hake landings.	45
Figure 24. Annual length-frequency distributions for hake.	46
Figure 25. Annual length-frequency distributions for hake (with discards).	46
Figure 26. Fitting of the data by LBSPR model for hake.	47

Figure 27. Hake length maturity and selectivity outputs by the LBSPR model.	48
Figure 28. Estimated SPR values for hake.	49
Figure 29. Estimated F/M values for hake.	49
Figure 30. Fitting of the data by LBPR model hake.	50
Figure 31. Graphs plotting the maturity-at-length curve and the estimated selectivity-at-length curve for each year by LBPR model for hake.	51
Figure 32. Graphs plotting the estimates of SPR and F by LBPR model for hake.	51
Figure 33. Fitting of the data by LIME model for hake.	52
Figure 34. Graphs plotting the selectivity-at-length curve by LIME model for hake.	53
Figure 35. Graphs plotting the estimates of SPR by LIME model for hake.	53
Figure 36. Graphs plotting the estimates of F by LIME model for hake.	54
Figure 37. Fitting of the data by LBSPR model for hake (with discards).	55
Figure 38. European hake length maturity and selectivity outputs by the LBSPR model (with discards).	56
Figure 39. Estimated SPR values for hake (with discards).	57
Figure 40. Estimated F/M values for hake (with discards).	57
Figure 41. Fitting of the data by LBPR model for hake (with discards).	58
Figure 42. Graphs plotting the maturity-at-length curve and the estimated selectivity-at-length curve for each year by LBPR model for hake (with discards).	59
Figure 43. Graphs plotting the estimates of SPR and F by LBPR model for hake (with discards).	59
Figure 44. European hake length frequency fit by LIME model for hake (with discards).	60
Figure 45. Graphs plotting the estimated selectivity-at-length curve by LIME model for hake (with discards).	61
Figure 46. Graphs plotting the estimates of SPR by LIME model for hake (with discards).	61
Figure 47. Graphs plotting the estimates of F by LIME model for hake (with discards).	62
Figure 48. Spatial distribution of landings per unit effort (LPUE) for deep-water rose shrimp.	64
Figure 49. Characterization of deep-water rose shrimp landings.	65
Figure 50. Annual length-frequency distributions for deep-water rose shrimp.	66

Figure 51. Annual length-frequency distributions for deep-water rose shrimp.	66
Figure 52. Fitness of the length-frequency data by LBSPR model for deep-water rose shrimp.	67
Figure 53. Deep-water rose shrimp length maturity and selectivity outputs by LBSPR model for deep-water rose shrimp.	68
Figure 54. Estimated SPR values for deep-water rose shrimp.	69
Figure 55. Estimated F/M values for deep-water rose shrimp.	69
Figure 56. Fitting of the data by LBPR model for deep-water rose shrimp.	70
Figure 57. Graphs plotting the maturity-at-length curve and the estimated selectivity-at-length curve for each year by LBPR model for deep-water rose shrimp.	71
Figure 58. Graphs plotting the estimates of SPR and F by LBPR model for deep-water rose shrimp.	71
Figure 59. Fitness of the length-frequency data using LBSPR model for deep-water rose shrimp (with discards).	73
Figure 60. Deep-water rose shrimp length maturity and selectivity outputs by LBSPR model for deep-water rose shrimp (with discards).	74
Figure 61. Estimated SPR values for deep-water rose shrimp (with discards).	75
Figure 62. Estimated F/M values for deep-water rose shrimp (with discards).	75
Figure 63. Fitting of the data by LBPR model for deep-water rose shrimp (with discards)	76
Figure 64. Graphs plotting the maturity-at-length curve and the estimated selectivity-at-length curve for each year by LBPR model for deep-water rose shrimp (with discards).	77
Figure 65. Graphs plotting the estimates of SPR and F by LBPR model for deep-water rose shrimp (with discards).	77
Figure 66. Spatial distribution of landings per unit effort (LPUE) for Norway lobster.	80
Figure 67. Characterization of Norway lobster landings.	81
Figure 68. Annual length-frequency distributions for Norway lobster.	82
Figure 69. Fitting of the data by LBSPR model for Norway lobster.	83
Figure 70. Maturity-at-length curve and the estimated selectivity-at-length curve for each year by the LBSPR model for Norway lobster.	84
Figure 71. Estimated SPR values for Norway lobster.	85

Figure 72. Estimated F/M values for for Norway lobster.	85
Figure 73. Fitting of the data by LBPR model Norway lobster.	86
Figure 74. Maturity-at-length curve and the estimated selectivity-at-length curve for each year by LBPR model for Norway lobster.	87
Figure 75. Graphs plotting estimates of SPR and F by LBPR model for Norway lobster.	87
Figure 76. Fitting of the data by LIME model for Norway lobster.	88
Figure 77. Graphs plotting the estimated selectivity-at-length curve by LIME model for Norway lobster.	89
Figure 78. Estimated SPR values by LIME model for Norway lobster.	89
Figure 79. Estimated fishing mortality by LIME model for Norway lobster.	90
Figure 80. Spatial distribution of LPUE for blue and red shrimp.	92
Figure 81. Characterization of blue and red shrimp.	93
Figure 82. Annual length-frequency distributions for blue and red shrimp.	94
Figure 83. Fitting of the data for by LBSPR model for blue and red shrimp.	95
Figure 84. Graphs plot the maturity-at-length curve and the estimated selectivity-at-length curve for each year by LBSPR for blue and red shrimp.	96
Figure 85. Estimated SPR values for blue and red shrimp.	97
Figure 86. Estimated F/M values for blue and red shrimp.	97
Figure 87. Fitting of the data by LBPR model blue and red shrimp.	98
Figure 88. Graphs plotting the maturity-at-length curve and the estimated selectivity-at-length curve for each year by LBPR model for blue and red shrimp.	99
Figure 89. Graphs plotting the SPR and F by LBPR model for blue and red shrimp.	99
Figure 90. Fitting of the data for by LIME model for blue and red shrimp.	100
Figure 92. Estimated SPR values by LIME model for blue and red shrimp.	101
Figure 91. Graphs plotting the estimated selectivity-at-length curve by LIME model for blue and red shrimp.	101
Figure 93. Fishing mortality using LIME model for blue and red shrimp.	102

Table 1. Summary table of stock assessment results by stock in Catalonia.	21
Table 2. <i>Métier</i> allocation depending on deep water species presence.	24
Table 3. Assumptions of model scenarios.	27
Table 4. Biological parameters described for red mullet.	30
Table 5. Stock assessment indicators for red mullet.	38
Table 6. Stock assessment indicators for red mullet (with discards).	45
Table 7. Biological parameters described for hake.	46
Table 8. Stock assessment indicators for hake.	56
Table 8. Stock assessment indicators for hake (with discards).	64
Table 9. Biological parameters described for deep-water rose shrimp.	66
Table 10. Stock assessment indicators for deep-water rose shrimp.	74
Table 11. Stock assessment indicators for deep-water rose shrimp (with discards).	80
Table 12. Biological parameters described for Norway lobster.	82
Table 13. Stock assessment indicators for Norway lobster.	93
Table 14. Biological parameters described for blue and red shrimp.	94
Table 15. Stock assessment indicators for blue and red shrimp.	104

Glossary

a: scaling coefficient for the weight at length of the fish species from length-weight relationship $W = aL^b$

b: a shape parameter for the body form of the fish species from length-weight relationship $W = aL^b$

B_{lim}: Biomass limit

B_{th}: Biomass threshold

DCF: Data Collection Framework

F: Fishing mortality

F_{msy}: Fishing mortality at a maximum sustainable yield

GSA: Geographic Sub-Area

k: Growth rate (Von Bertalanffy Growth Function)

LFD: Length Frequency Distribution

L_{inf}: Length infinity or asymptotic length at which growth is zero (Von Bertalanffy Growth Function)

L_{mat50}: Length where 50% of individuals are mature

L_{mat95}: Length where 95% of individuals are mature

M: Natural mortality

SL50: Length where 50% of individuals are caught

SPR: Spawning Potential Ratio of a stock is defined as the proportion of the unfished reproductive potential left at any given level of fishing pressure.

t₀: age at which the organisms would have had zero size (Von Bertalanffy Growth Function)

Executive summary

This report presents the first results obtained by ICATMAR using their own data set to develop stock assessment of the area (N GSA06) using the data-poor models LBPA, LBSPR, and LIME. The results for the five target species from WMMAP (Western Mediterranean Multiannual Plan), i.e. red mullet (MUT), hake (HKE), deep-water rose shrimp (DPS), Norway lobster (NEP) and blue and red shrimp (ARA) estimate that the Spawning Potential Ratio (SPR) for all species but the Norway lobster was under the Blim, at least for the prediction of one model used (Fig. 1).

In detail, for each species the results are:

- Red mullet and hake SPR are under Blim for the three years evaluated and with the three models tested.
- Deep-water rose shrimp results differ depending on the model used. That is, with LBPA predict a SPR under Blim but LBSPR predicts a SPR was above the Blim. However, these results should consider that this resource is exploited since 2016 and the lack of catch historical data makes uncertainty on the models.

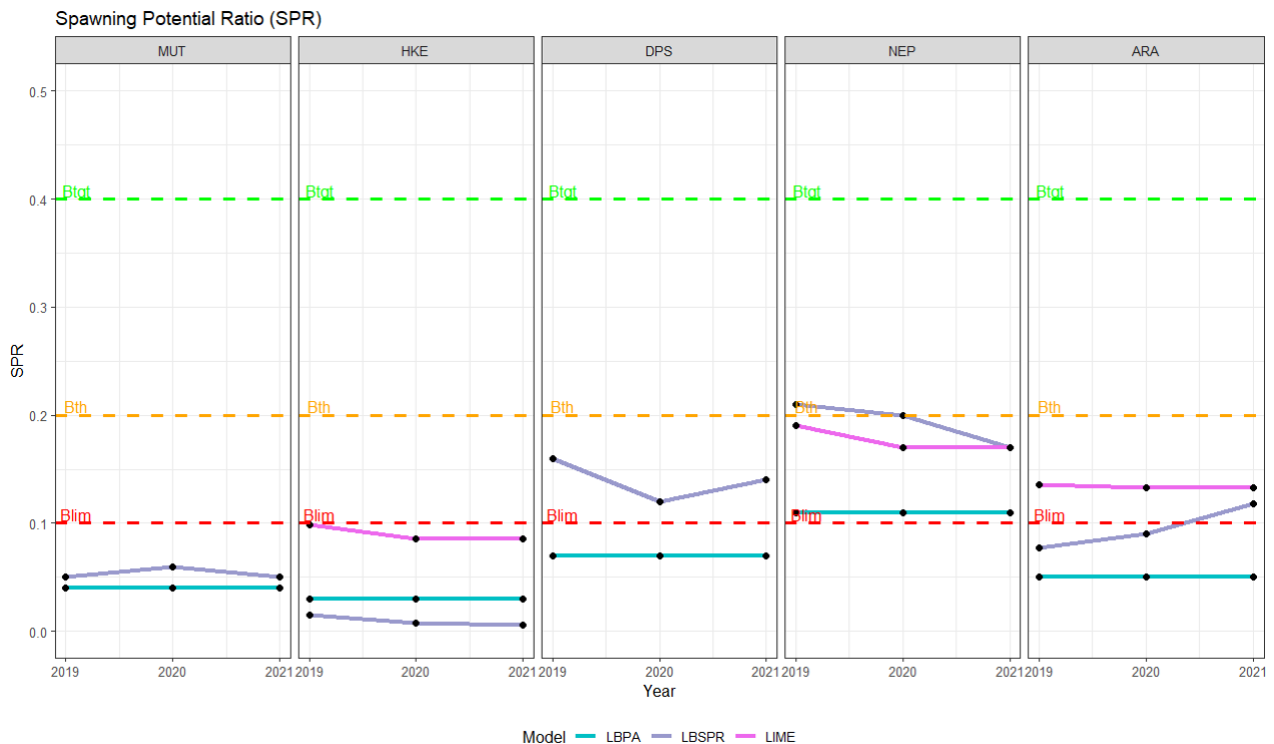


Figure 1. Spawning potential ratio (SPR) by year for the five stocks evaluated with three models tested. MUT: red mullet, HKE: hake, DPS: deep-water rose shrimp, NEP: Norway lobster and ARA: blue and red shrimp. LBSPR; Length-Based Spawning Potential Ratio, LBPA: Length-Based Pseudo-cohort Analysis and LIME: Length-based integrated mixed effects.

- Norway lobster estimates for all the models result in a SPR above the Blim, although LBSPR showed a decrease in 2021.

- Blue and red shrimp results vary according to each model evaluated. In detail, LBPA predicted a SPR under the Blim, LIME predicted a SPR above Blime, and LBSPR predicted a SPR above the Blim in 2021 but not for the previous years, indicating an improvement of this stock in the timespan of our data series (from 2019 to 2021).

As a summary, a Kobe plot (Figure 2) presenting all the data together, to visualize the results for the stock assessment models used, indicates that all stocks are overfished. However, results differ among stocks, and thus stock indicators are in better shape for the Norway lobster and the deep-sea blue and red shrimp, but the European hake does not show improvement of stock indicators over the years. For the deep-water rose shrimp, the model does not take into account previous years and the recent expansion of this species in the habitats of the Northern GSA6. Therefore, it is important to implement urgent management measures to improve the trends of the fishing stocks in the N GSA06.

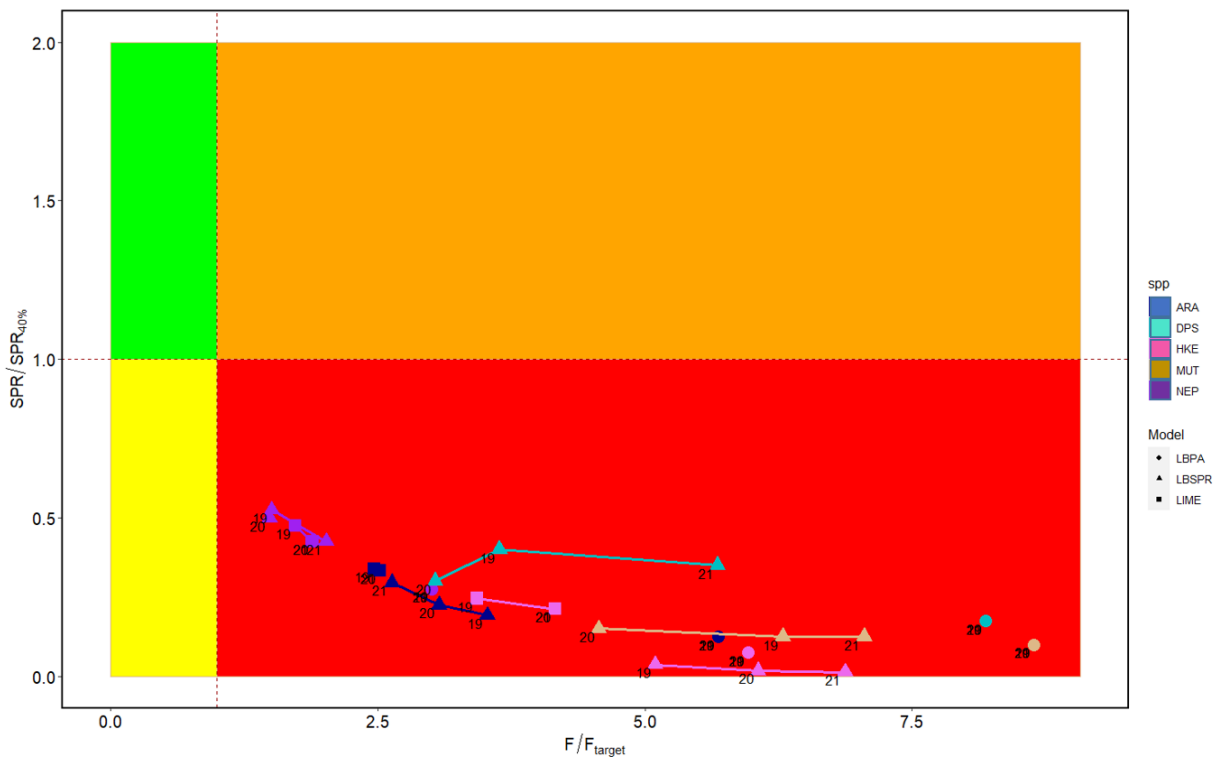


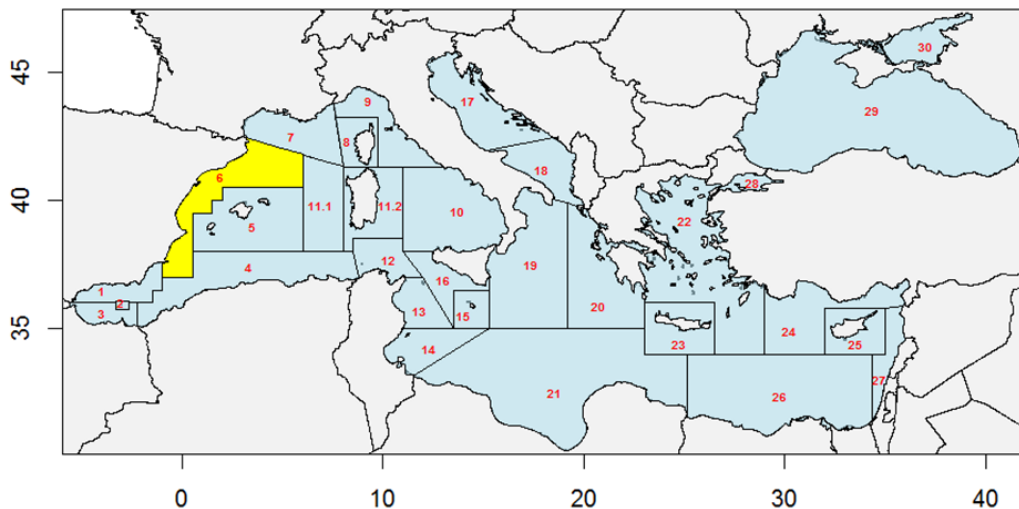
Figure 2. Kobeplot for the five stocks evaluated with three models tested. Colors indicate the species tested, MUT: red mullet, HKE: hake, DPS: deep-water rose shrimp, NEP: Norway lobster and ARA: blue and red shrimp. Shape indicates the model tested, LBSPR; Length-Based Spawning Potential Ratio, LBPA: Length-Based Pseudo-cohort Analysis and LIME: Length-based integrated mixed effects. SPR: spawning potential ratio, SPR0.4: SPR with 40%, F: fishing mortality and F_{target}: fishing mortality of target species.



1

Introduction

The European Union Data Collection Framework (DCF) establishes that the member states must collect, manage and annually report biological, environmental and socioeconomic data from fisheries to use as a base for scientific advice in management strategies (EU 2017/1004). In the Mediterranean and Black Seas, the data collection is structured in Geographical Sub-Areas (GSAs), defined by the General Fisheries Commission for the Mediterranean (GFCM, Resolution GFCM/33/2009/2). The GSA06 (Northern Spain) comprises the Spanish Mediterranean coast from Cartagena to the Spanish-French border.



01 – Northern Alboran Sea	07 – Gulf of Lion	13 – Gulf of Hammamet	19 – Western Ionian Sea	25 – Cyprus
02 – Alboran island	08 – Corsica	14 – Gulf of Gabès	20 – Eastern Ionian Sea	26 – Southern Levant Sea
03 – Southern Alboran Sea	09 – Ligurian Sea and northern Tyrrhenian Sea	15 – Malta	21 – Southern Ionian Sea	27 – Eastern Levant Sea
04 – Algeria	10 – Southern and central Tyrrhenian Sea	16 – Southern Sicily	22 – Aegean Sea	28 – Marmara Sea
05 – Balearic Islands	11.1 – Western Sardinia 11.2 – Eastern Sardinia	17 – Northern Adriatic Sea	23 – Crete	29 – Black Sea
06 – Northern Spain	12 – Northern Tunisia	18 – Southern Adriatic Sea	24 – Northern Levant Sea	30 – Azov Sea

Mediterranean fisheries are governed by the European Common Fisheries Policy (CFP), where control of fishing effort (fishing days), combined with specific technical measures such as gear regulation (Resolution GFCM/33/2009/2), the establishment of a minimum conservation reference size (EU Reg. 2019/1241) and the implementation of closure of areas and closed seasons (EU Reg. 2022/1614), are the main management strategies adopted in the western Mediterranean Sea. The current Western Mediterranean Multiannual Plan (WMMAP, EU reg. 2019/1022) establishes a series of management measures aimed, mainly, for the bottom trawling fleet. The bottom trawlers from the Spanish Mediterranean are allowed to fish between 50 and 1000 m depth or 3 miles far from shore when the seabed is shallow and five days per week with a maximum of 12 labour hours per day. The maximum power of the vessel may not exceed 500 hp and the vessel length is limited to a range between 12 and 24 meters (Real Decreto 1440/1999). In addition, the Ministry of Agriculture and Fisheries, Food and Environment may limit, by regulation, the number of days per year that a vessel may fish in order to regulate the total effort exerted in each of the fishing areas (EU Reg, 2019/1022).

Scientific data is needed to understand the state of the fisheries to establish scientific-based management strategies. For that, the EU Member States have been collecting fisheries data to support CFP since 2000. These data are collected through fisheries-dependent (fishing on board) and –independent methods (annual surveys), which periodicity varies throughout the year. The fisheries-dependent data occur monthly in some specific ports by on-board observers, whereas the fisheries-independent data is gathered once a year from the MEDiterranean Trawl Survey (MEDITS). To complete this monitoring program established by the DCF, and with the goal to get a more exhaustive data set to better manage marine resources, the Directorate-General for Fisheries and Maritime Affairs of the Government of Catalonia and the Institut de Ciències del Mar (ICM-CSIC) promoted the *Institut Català de Recerca per a la Governança del Mar* (ICATMAR), an autonomous organization whose main goal is to generate scientific advice for management purposes in the blue economy field. Since 2019, ICATMAR has developed and implemented a fisheries' monitoring program in Catalonia, which constitutes the northern part of the GSA06 (from the French border to the south of the Ebre delta). This program uses fisheries-dependent methods that also allow the collection of biological and stock parameters. The goal is to monitor the main target species of the Catalan commercial fleet of different fishing modalities, including bottom trawling, which is, economically, the most important fishing modality with a revenue of 95.86 M€ in 2021. Bottom trawlers target demersal species, such as those defined by the WMMAP including red mullet, European hake, deep-water rose shrimp, Norway lobster, and blue and red shrimp (EU reg. 2019/1022).

To provide scientific advice for management purposes in the northern GSA 6, the data gathered by ICATMAR during 2019, 2020 and 2021 has been used for stock assessment evaluations. Despite that the data is only from 3 years, it is possible to obtain results by using data

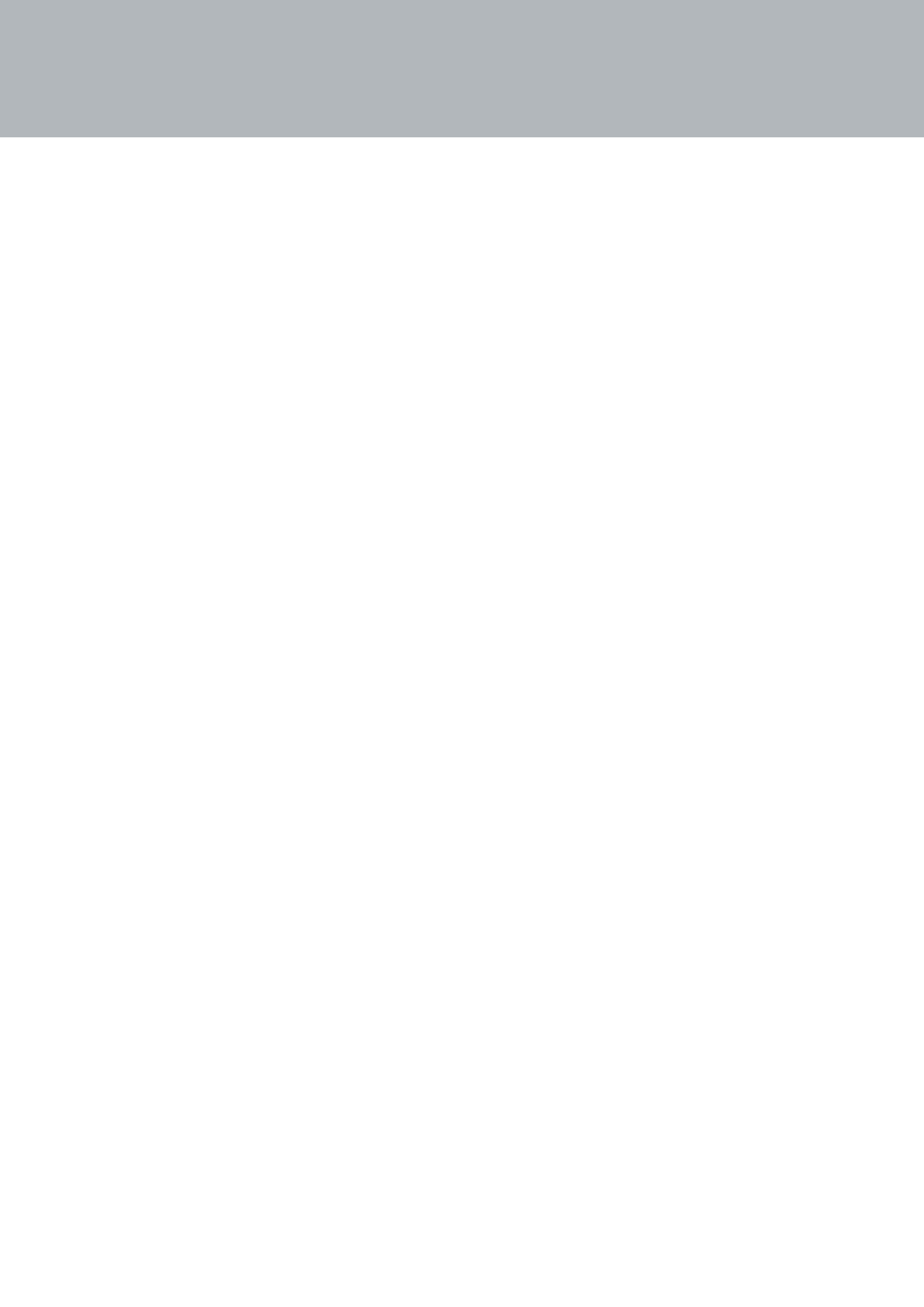
resource-limited (length-based) models. This report, though, is the first of many to come and, as ICATMAR will continue the intense monitoring program in the area, the long-term data collection will allow, in next years, the use of the models commonly used by the Scientific, Technical and Economic Committee for Fisheries (STECF).

Summary table by stock

A summary table 1 is provided to understand, in a glance, the results obtained from the stock assessment models. The species analysed are red mullet (MUT), European hake (HKE), deep-water rose shrimp (DPS), Norway lobster (NEP), and blue and red shrimp (ARA).

Table1. Stock assessment results for Catalonia in 2021. SPR: Spawning Potential Ratio. SPR0.4: SPR al 40%. SPR0.1: SPR al 10%. F: Fishing mortality. *different results according to the method: LBSPR Above, LBPA Below.

Area	Species	Method	Ref. Year	SPR /SPR _{0.4}	SPR/SPR _{0.1}	F/F _{target}
CAT	MUT	Data-Resource-limited (LB-SPR, LBPA)	2021	Below	Below	Above
CAT	HKE	Data-Resource-limited (LB-SPR, LBPA, LIME)	2021	Below	Below	Above
CAT	DPS	Data-Resource-limited (LB-SPR, LBPA)	2021	Below	Above/ Below*	Above
CAT	NEP	Data-Resource-limited (LB-SPR, LBPA, LIME)	2021	Below	Above	Above
CAT	ARA	Data-Resource-limited (LB-SPR, LBPA, LIME)	2021	Below	Above	Above





2

Material and Methods



Framework

The data used for the stock assessment models has been gathered in the northern GSA06 for years 2019, 2020, and 2021 obtained from onboard samplings with commercial bottom trawlers. Sampling occurred monthly in 3 different areas covering the whole Catalan coast (north, center and south), each containing three fishing ports, a total of nine ports.

Dataset

Length frequency distributions (LFD) for each target species, red mullet (*Mullus barbatus*), European hake (*Merluccius merluccius*), deep-water rose shrimp (*Parapenaeus longirostris*), Norway lobster (*Nephrops norvegicus*), and blue and red shrimp (*Aristeus antennatus*), were obtained yearly. This data is one of the main inputs for the selected stock assessment models. To obtain them, weighting and extrapolation are needed for the whole study area.

As the fishing fleet activity is defined by *métiers*, each fishing trip, which is linked to the fishing landings per day and vessel, is allocated to a specific *métier*. As a reminder, a *métier* is defined as a “group of fishing operations targeting a similar assemblage of species, using similar gear, during the same period of the year and/or within the same area and which are characterized by a similar exploitation pattern” (Reg. (EC) N° 949/2008 and Commission Decision 2010/93/UE). In this study area, the daily fishing landings of a vessel correspond to one effective fishing day, as vessels land their catch daily.

Therefore, as each sampling haul is allocated to a specific *métier*, the sampled length frequencies can be weighed and extrapolated to the fishing landings by *métier*. Several raisings - combinations of *métiers*, weightings and extrapolations - can be applied to obtain the annual length frequency distribution, thus different scenarios were considered.

Table 2. *Métier* allocation depending on deep water species presence. OTB: Bottom Otter Trawl.

<i>Métier</i> code	<i>Métier</i> name	Presence of <i>A. antennatus</i> and <i>A. foliacea</i>
OTB-DWS	Deep water species	> 20%
OTB-MDD	Mixed demersal species and deep water species	5% - 20% or ≥ 10 kg
OTB-DES	Demersal species	< 5% or < 10 kg

Two different groups of *métiers* for bottom trawling were used in this study:

ICATMAR *métiers*: Defined in “*the state of the fisheries Part I Section 3*” of this report. In summary, landings and revenues from 2002 to 2021 were used and at each port; then, dendrograms and cluster analysis were performed, and for each trip (vessel + day), the corresponding *métier* was assigned. A total of 8 *métiers* were defined according to different depths and zones.

DCF *métiers*: Defined by the European Data Collection Framework (Reg. (2008/949/EC and BOE-A-2020-5163)). The allocation of these *métiers* on a fishing trip depends on the presence of the species *Aristeus antennatus* and *Aristaeomorpha foliacea* versus the total landings, as described in the Table 2.

Two different raising approaches were used in this study:

ICATMAR raising: The factors month, season, port and area were considered in the raising process. The inclusion of these factors is important to account for the variability of the data.

DCF raising: This type of raising is used for the data that is delivered to DCF for European stock assessment analyses. The factor month and season are considered in the raising process, but the variability between ports or areas are not considered. In case there is no sampling in a certain month, the average length frequency of the season is used instead.

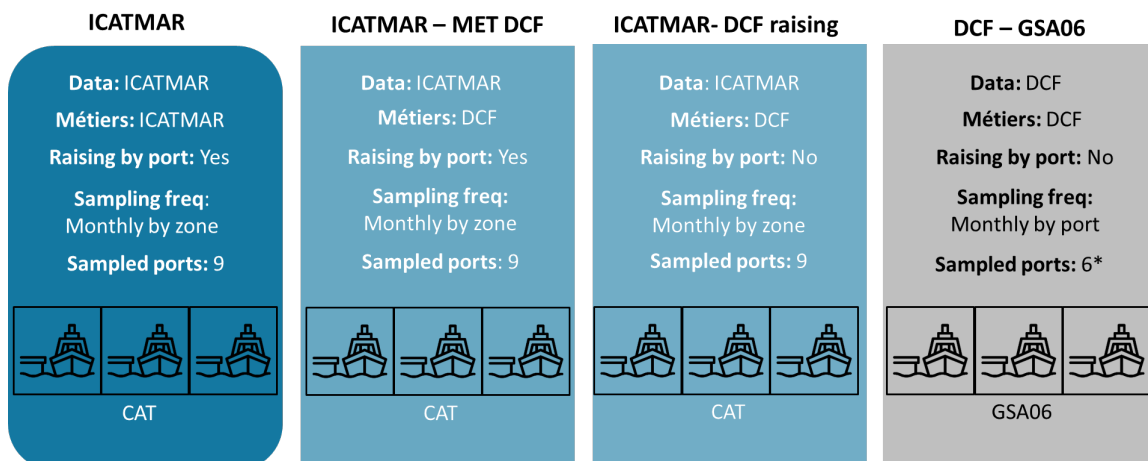


Figure 3. Raising scenarios to obtain the annual length frequencies. *ports sampled along the GSA06.

Four scenarios were used in this study (Figure 3):

ICATMAR: This scenario is based on ICATMAR data, *métiers* and raising. The evaluation area is Catalunya. From here onwards it is referred as Scenario 1.

ICATMAR – MET DCF: This scenario is based on ICATMAR data, DCF *métiers* and ICATMAR raising. The evaluation area is Catalunya.

ICATMAR – DCF raising: This scenario is based on ICATMAR data, DCF *métiers* and raising. The evaluation area is Catalunya.

DCF – GSA06: This scenario is currently used to evaluate GSA06, based on DCF data, *métiers* and raising. From here onwards it is referred as Scenario 2.

In this study, for each evaluated species, the sampling length frequencies from 2019 to 2021 are raised according the three first scenarios, as the “DCF – GSA06” data is already raised. The scenario 1 is the one that shows the best fit for the models according to the sensitivity analysis. Moreover, it also considers seasonal and spatial variability in the raising process. Therefore, in this study the results are shown according to scenario 1 and scenario 2, in order to compare with the current evaluations.

Sampling on board data was divided into commercial and discards to calculate each species' annual discard ratio by *métier*. This ratio was applied to the landings by port and used to raise the yearly discard length frequencies.

Stock assessment models

Data resource-limited (length-based) models were selected to perform the stock assessments. Three different models were selected regarding steady-state assumptions: LBSPR and LBPA assume equilibrium whereas LIME does not assume equilibrium*. The results of these models should be understood as tendencies (qualitative) more than precise indicators (quantitative) (Table 3).

*Equilibrium assumption: both mortality and recruitment remain constant.

LBSPR - Length-Based Spawning Potential Ratio (Hordyk et al., 2016)

LBPA - Length-Based Pseudo-cohort Analysis (Canales et al., 2021)

LIME - Length-based integrated mixed effects (Rudd & Thorson, 2018)

Table 3. Assumptions of model scenarios. LBSPR (Length-Based Spawning Potential Ratio), LBPA (Length-Based Pseudo-cohort Analysis) and LIME (Length-based integrated mixed effects).

	Assumptions
LBSPR	<p>Stock is in equilibrium Natural mortality and growth rates are constant Selectivity and maturity follow a logistic curve Both sexes have the same growth curve and the sex ratio is equal The lengths at each age are normally distributed around a mean length-at-age value.</p>
LBPA	<p>Reduction of equilibrium assumption merging length data Natural mortality and growth rates are constant Selectivity and maturity follow a logistic curve Both sexes have the same growth curve and the sex ratio is equal</p>
LIME	<p>Accounting for time-varying fishing mortality and recruitment Requirement of at least 1 year of length composition data of the catch, and assumptions about growth, natural mortality, and maturity Derivation of random effects for time-varying recruitment Fitting to multiple years of length composition data and/or catch and/or an abundance index time series, if available.</p>

A large pile of crayfish and other aquatic life caught in a woven mesh net. The net is made of a light-colored, diamond-shaped mesh. The catch includes many crayfish of various sizes and colors (red, orange, white), as well as several larger, spotted crayfish. There are also some smaller crustaceans and debris mixed in with the catch. The background is a bright, outdoor setting.

3

Results by stock

Red mullet (*Mullus barbatus*) MUT

The Red mullet (*Mullus barbatus*; FAO code MUT) growth parameters, length-weight relationship and maturity at L_{mat50} and L_{mat95} are shown in Table 4. These data are used as inputs for the models used.

The spawning area for red mullet is the continental shelf but the nursery is on coastal areas. The recruitment season is between October and December (Lombarte et al. 2000).

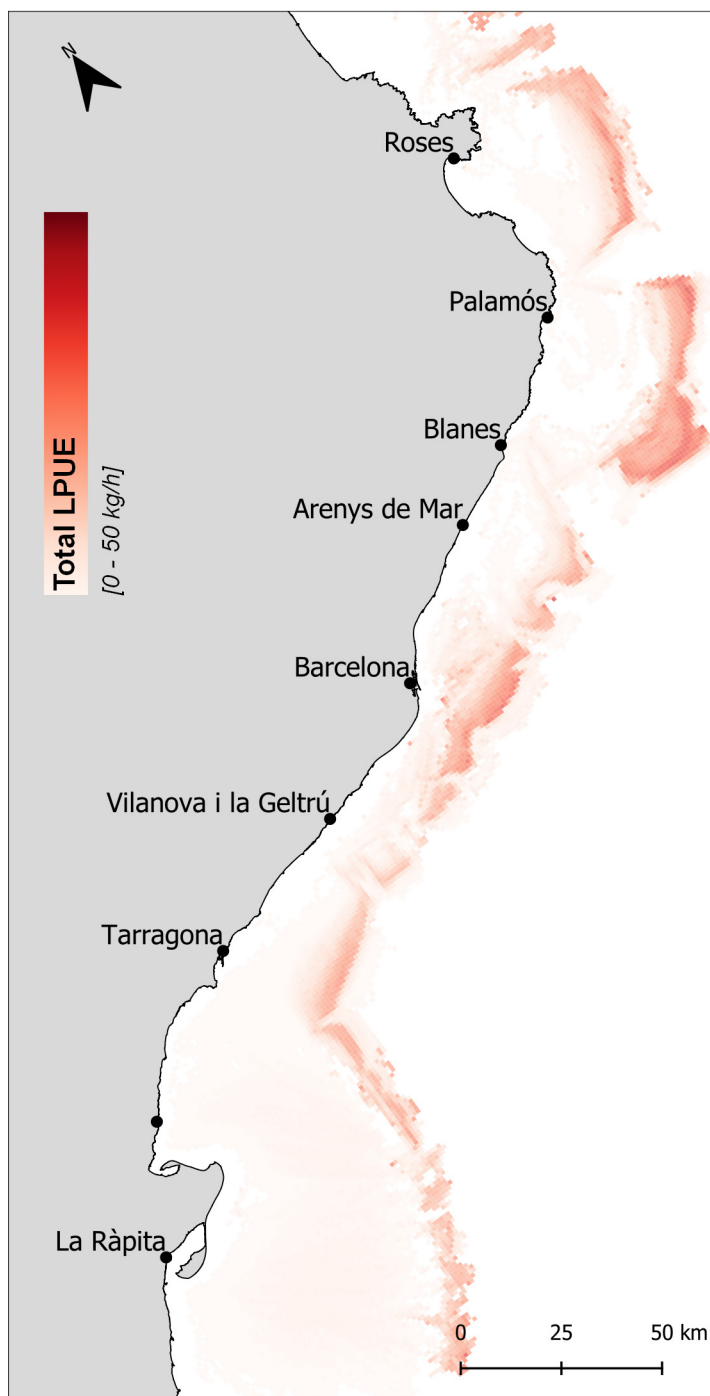


Figure 4. Spatial distribution of landings per unit effort (LPUE) for red mullet in the Catalan fishing grounds (N GSA6) in 2021.

Table 4. Biological parameters described for red mullet. Detailed information of each parameter can be found in the Glossary.

MUT	L_{inf} (mm)	K	t_0	a	b	M	L_{mat50} (mm)	L_{mat95} (mm)
Data source	345	0.34	-0.14	0.0096	3.218	0.42	137	144
	Demestre et al., 1997			GFCM RY2020		Chen and Watanabe (1989)	GFCM RY2020	

Catch (landings and discards)

Red mullet landings are predominantly from the métier OTB; only a small amount is reported for small-scale fishing gears (trammel-net). Red mullet discards are found in métier OTB.

Red mullet landings show a clear increasing trend from 2005 and until 2016 (Fig. 5a). Afterwards, landings declined until the present day. The red mullet is caught by different OTB métiers of the Catalan fishing fleet: OTB Coastal Delta shelf, OTB Coastal shelf and OTB Deeper shelf. These are the métiers that land the largest quantities of the species (Fig. 5b).

The length frequency distribution per year and métier after raising the data without including discards in the data analyses for both scenarios, that is, using ICATMAR and DCF GSA6 data sets, are shown in Fig. 6, which plots very similarly results. For both scenarios, the length struc-

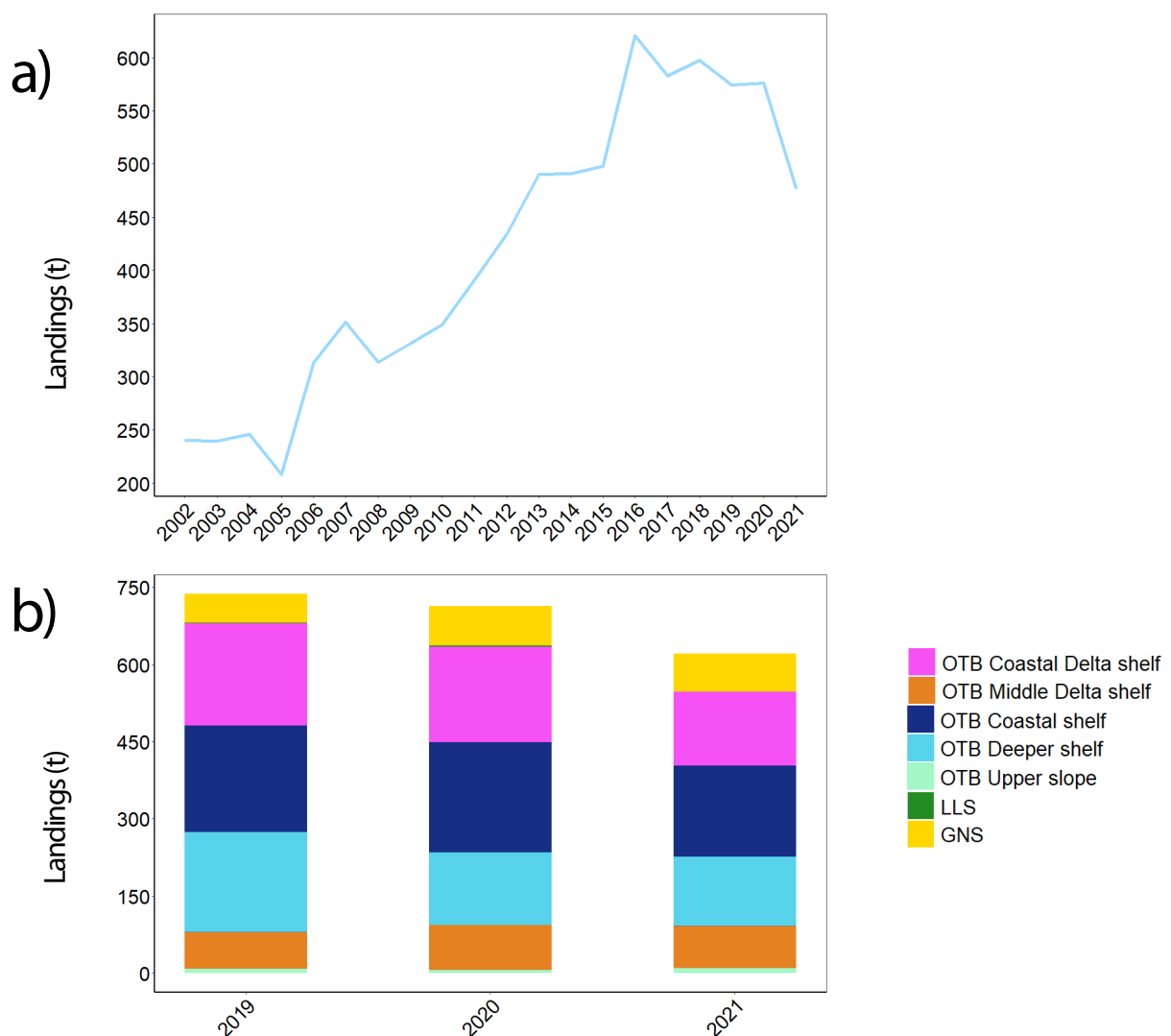


Figure 5. Characterization of red mullet landings. (a) Historical landings in the Catalan coast. (b) Landings per métier. (OTB) Bottom otter trawl, (LLS) Set longlines and (GNS) Set gillnet

tures are not similar among years and the number of individuals per size frequency decrease in time. In all cases, data from trawling and artisanal fisheries are included. On both scenarios, the 2019 size distribution is more homogeneous and with a larger number of individuals with the difference that, in scenario 2, the proportion of individuals is higher.

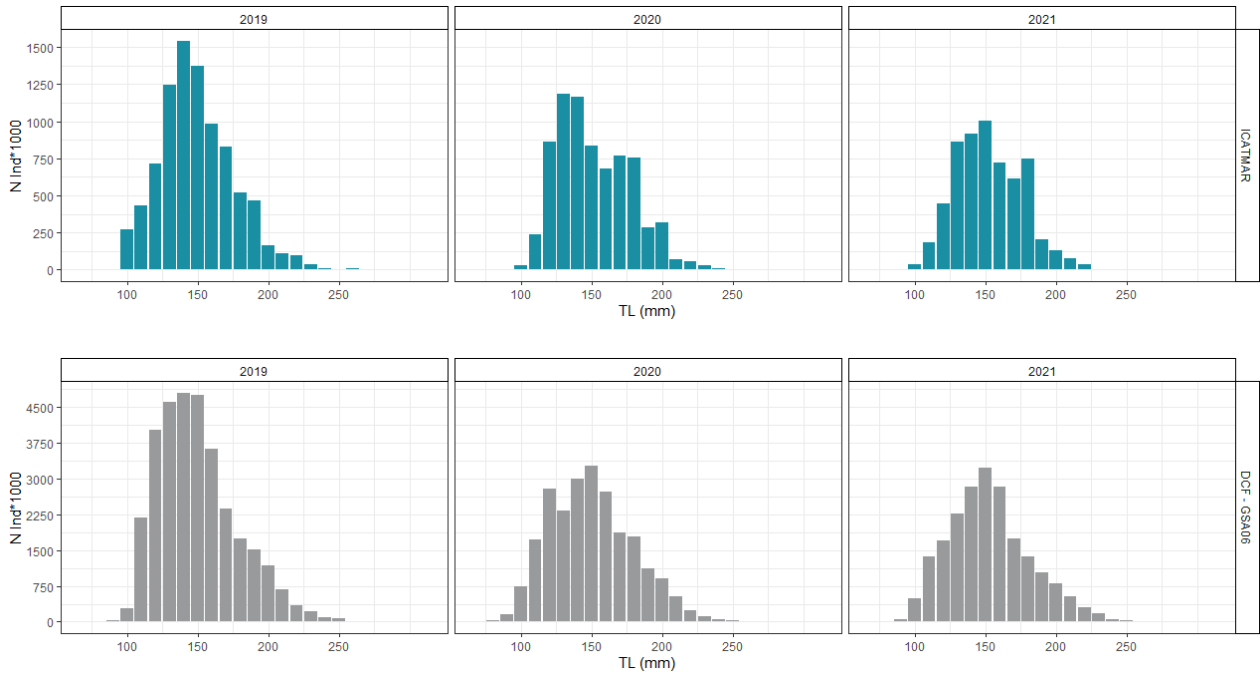


Figure 6. Annual length-frequency distributions for red mullet. Scenario 1 (top plots) using the ICATMAR data set and Scenario 2 (bottom plots) using DCF-GSA06 data data set. Data do not include discards.

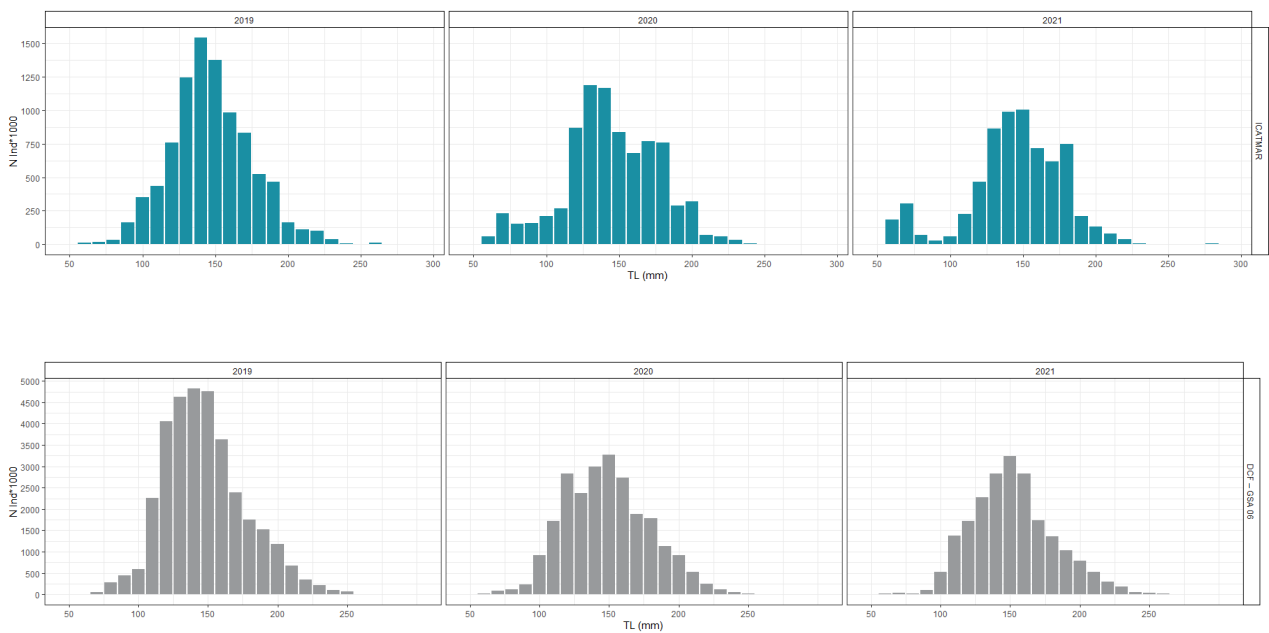


Figure 7. Annual length-frequency distributions for red mullet. Scenario 1 (top plots) using the ICATMAR data set and Scenario 2 (bottom plots) using DCF-GSA06 data data set. Data include discards.

The length frequency distribution per year and métier, including discards, after raising the data for both scenarios, are shown in Figure 7. On one side, for the first scenario (ICATMAR), there is no similarity in the length structure for the different years. In addition, the number of individuals per size frequency decreases over time. On the other side, for the second scenario (DCF GSA 6), there is a similarity among the length structure throughout the years but there are less individuals in years 2020 and 2021 than in 2019. On both scenarios, the number of individuals decreases over the years. However, in scenario 2 the proportion of individuals is higher with a greater presence of small-sized individuals.

Stock assessment by model (without discards)

LBSPR

Fitted data

The length frequency distribution fitted per year after raising the data for both scenarios, that is, using ICATMAR and DCF GSA6 data sets, are shown in Figure 8. In scenario 1, the best fit is in 2019, due to a more homogeneous size frequency. In the years 2020 and 2021 the length frequency adjustment worsens, especially for the larger size classes. In scenario 2, the best fit is in 2021. For both scenarios, sizes below and above the model fit (black line) are under and overestimated, respectively.

Maturity vs. selectivity (absolute and range of values)

The selectivity calculated by the model for the red mullet is plotted in Figure 9. For both scenarios, the estimated selectivity is under the size at first maturity. Over the years, selectivity has become closer to L_{mat50} , especially in scenario 1.

Precautionary advice based on SPR

On both scenarios, the calculated SPR values are below the Blim, as shown in Figure 10. There is no clear trend between years. In scenario 2 there are some values that are above Blim and Btgt.

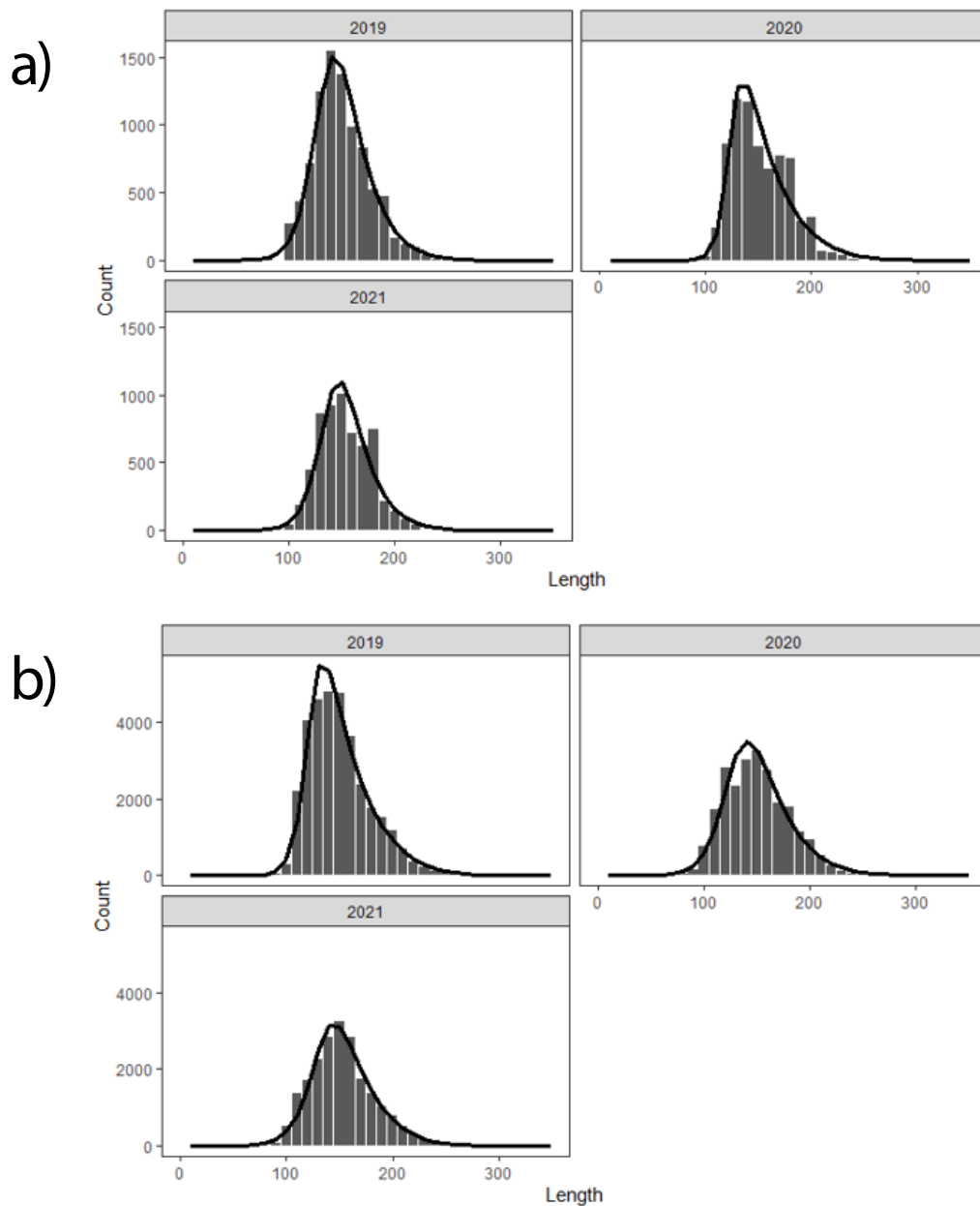


Figure 8. Fitting data by LBSPR model for red mullet. (a) Scenario 1 (ICatMar data), (b) Scenario 2 (DCF-GSA06 data). Data do not include discards.

Relative fishing mortality

Figure 11 plots F/M ratio values. On both scenarios, F/M ratios are above 1. There is no trend throughout the years and the range of values is wide, especially in scenario 1.

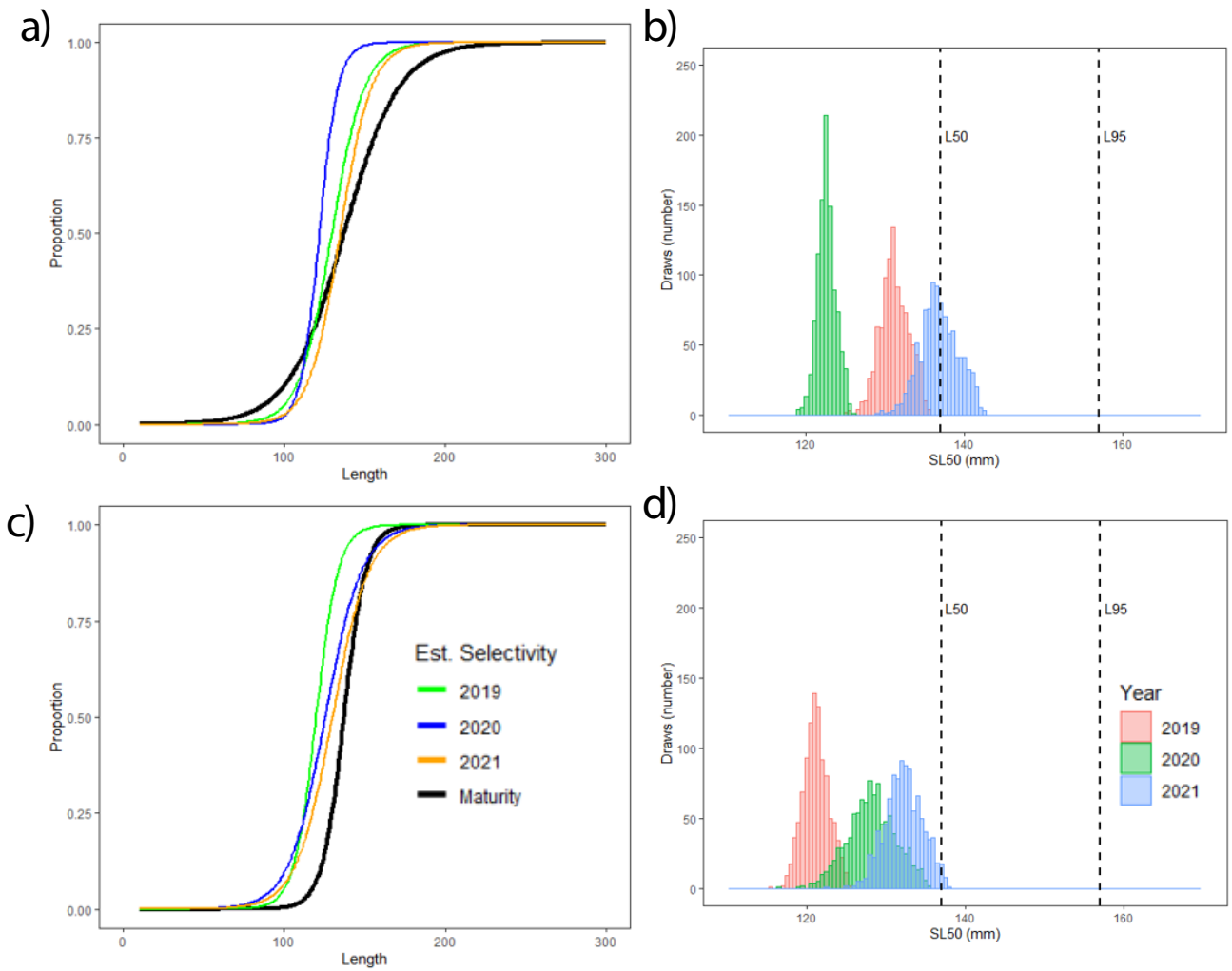


Figure 9. Left graphs plot the maturity-at-length curve and the estimated selectivity-at-length curve for each year by LBSPR forred mullet. Right graphs plot the SL50 values for each year; the bell shape is given by the number of draws estimated by the model. (a, b) Scenario 1 (ICatMar data), (c,d) Scenario 2 (DCF-GSA06 data). Data do not include discards.

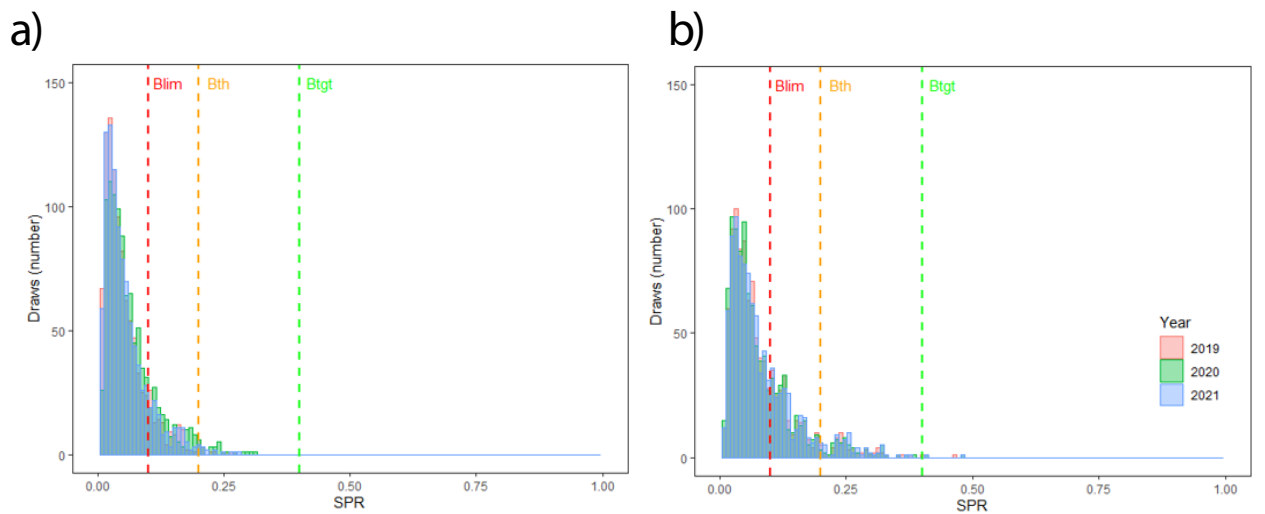


Figure 10. Estimates SPR values for red mullet. (a) Scenario 1 (ICatMar data), (b) Scenario 2 (DCF-GSA06 data). Data do not include discards.

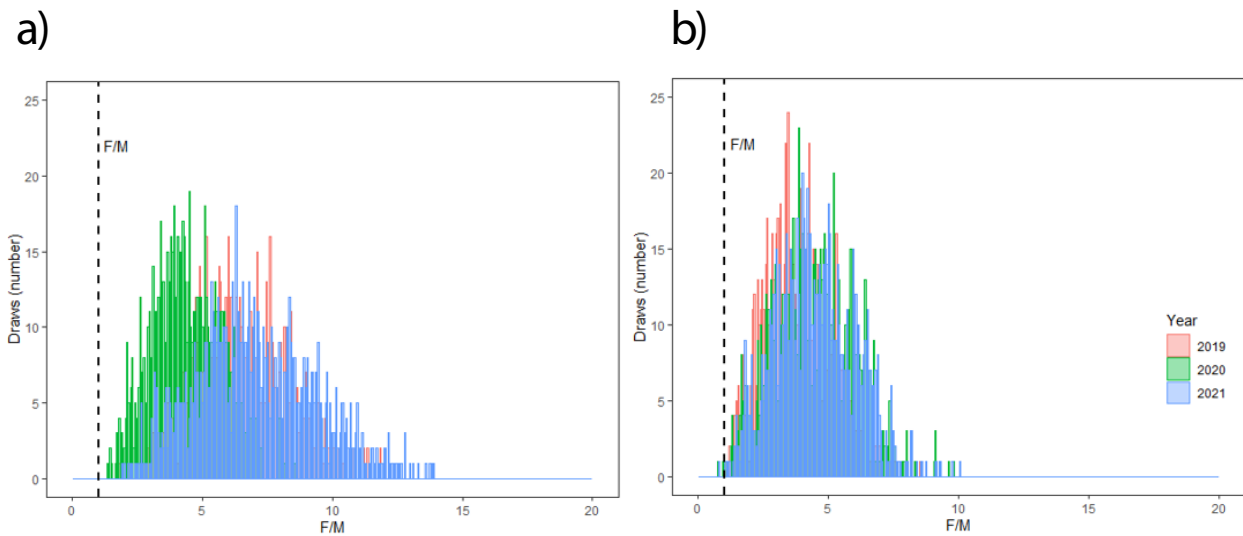


Figure 11. Estimated F/M values for red mullet. (a) Scenario 1 (ICatMar data), (b) Scenario 2 (DCF-GSA06 data). The bell shape is given by the number of draws estimated by the model. Data do not include discards.

LBPA

Fitted data

The length frequency distribution fitted per year after raising the data for both scenarios, that is, using ICATMAR and DCF GSA6 data sets, are shown in Figure 12. On both scenarios, sizes below the black line are underestimated and above the black line are overestimated. In scenario 1, the model does not quite fit the central size classes correctly. Therefore, the model underestimates small classes and overestimates individuals between 120 and 210 mm. In scenario 2, the model fits better, even though it underestimates the larger size classes.

Maturity vs. Selectivity

Maturity and Selectivity curves for red mullet are represented in Figure 13. In scenario 1, selectivity is below L_{mat50} but very close to it ($SL_{50}=130.7$ mm). In scenario 2, selectivity is above L_{mat50} ($SL_{50}=145.9$ mm).

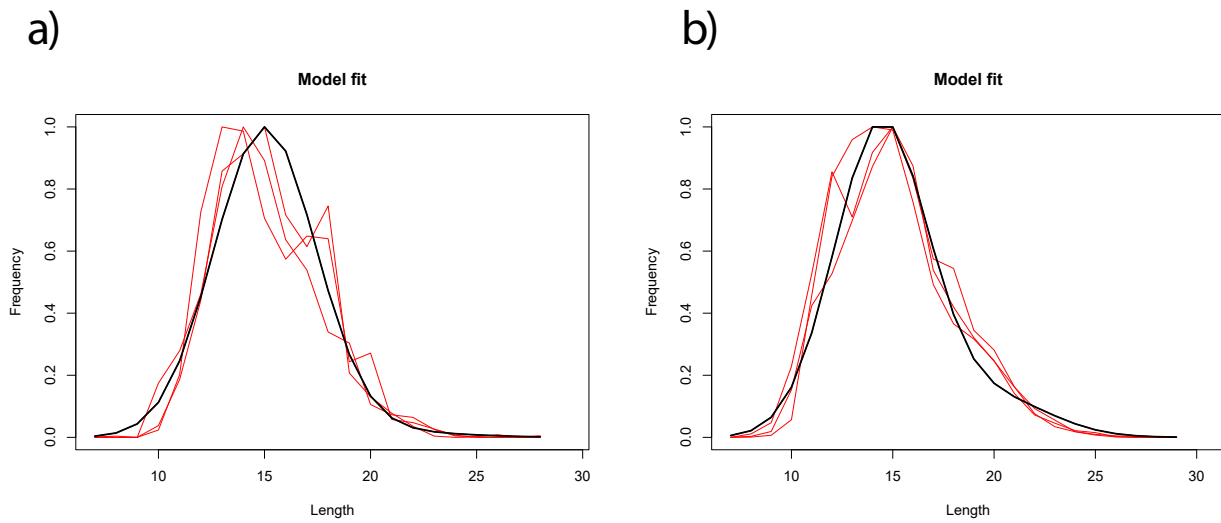


Figure 12. Fitting data by LBPR model for red mullet. (a) Scenario 1 (ICatMar data), (b) Scenario 2 (DCF-GSA06 data). Red lines represent the length frequency for the 3 studied years; the black line is the length frequency distribution estimated for the model. Data do not include discards.

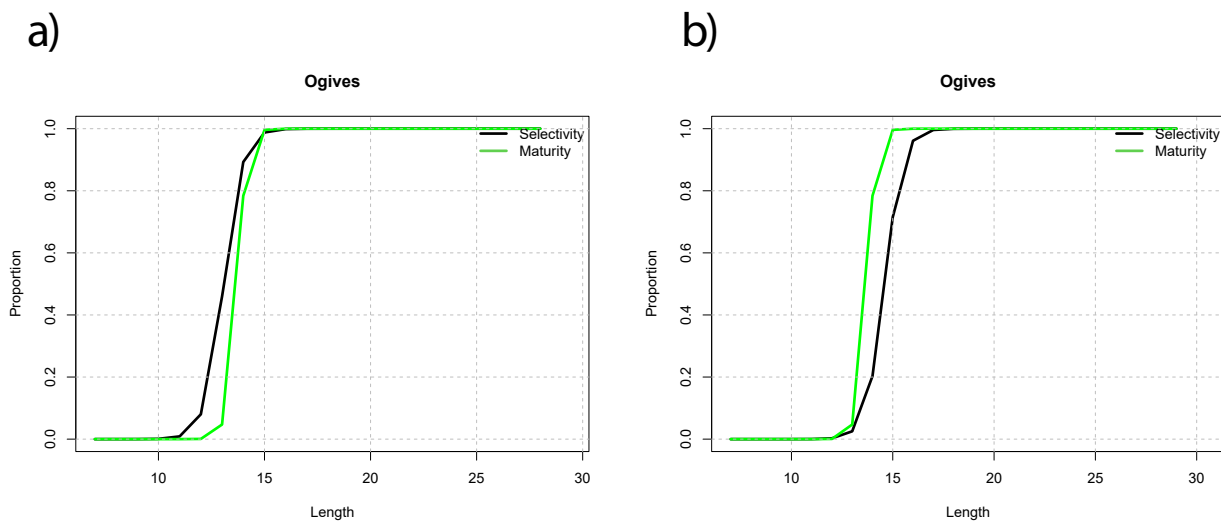


Figure 13. Graphs plotting the maturity-at-length curve and the estimated selectivity-at-length curve for each year by LBPR model for red mullet. (a) Scenario 1 (ICatMar data), (b) Scenario 2 (DCF-GSA06 data). Data do not include discards.

SPR and Fishing mortality estimations

SPR and F estimations are shown in Figure 14. In both scenarios, there is overexploitation and overfishing. In scenario 1, the SPR values are below the SPR_{tgt} (0.4), with a very narrow uncertainty range. In turn, F is above the F_{tar} and its values range between 2 and 5. In scenario 2, the estimations are similar to scenario 1 but fishing mortality has a very broad uncertainty range, with F ranging from 0 to 8.

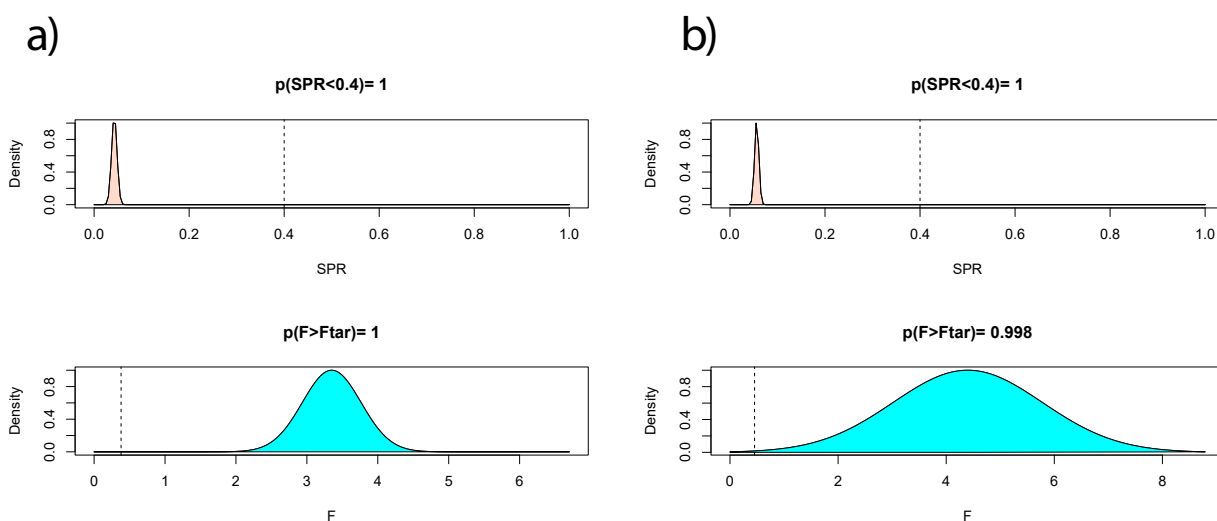


Figure 14. Graphs plotting the estimates of SPR and F by LBPR model for red mullet. (a) Scenario 1 (ICat-Mar data), (b) Scenario 2 (DCF-GSA06 data). Data do not include discards.

Stock assessment indicators

Table 5. Stock assessment indicators for red mullet. Detailed information of each parameter can be found in the Glossary. Data do not include discards.

Specie	Scenario	Method	Year	SPR	F/M or F/Fmsy*
MUT	ICATMAR	LBSPR	2019	0.05	6.29
MUT	ICATMAR	LBSPR	2020	0.06	4.57
MUT	ICATMAR	LBSPR	2021	0.05	7.05
MUT	ICATMAR	LBPA	2019	0.04	8.81*
MUT	ICATMAR	LBPA	2020	0.04	8.81*
MUT	ICATMAR	LBPA	2021	0.04	8.81*
MUT	DCF-GSA6	LBSPR	2019	0.08	3.81
MUT	DCF-GSA6	LBSPR	2020	0.08	4.32
MUT	DCF-GSA6	LBSPR	2021	0.08	4.49
MUT	DCF-GSA6	LBPA	2019	0.07	9.67*
MUT	DCF-GSA6	LBPA	2020	0.07	9.67*
MUT	DCF-GSA6	LBPA	2021	0.07	9.67*

Stock assessment by model (with discards)

LBSPR

Fitted data

The length frequency distribution fitted per year, including discards, after raising the data for both scenarios, that is, using ICATMAR and DCF GSA6 data sets, are shown in Figure 15. In

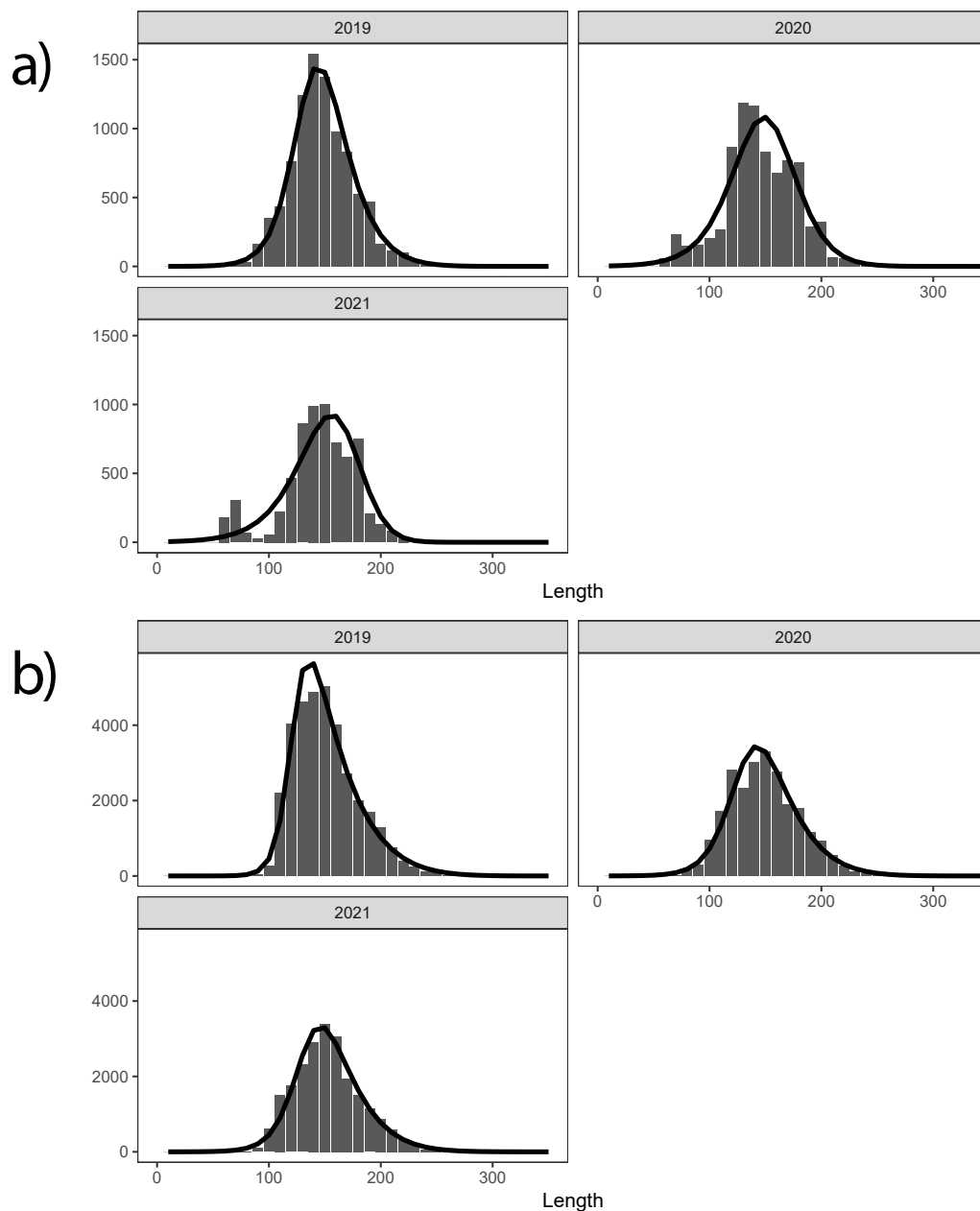


Figure 15. Fitting data by LBSPR model for red mullet. (a) Scenario 1 (ICatMar data), (b) Scenario 2 (DCF-GSA06 data). Data include discards.

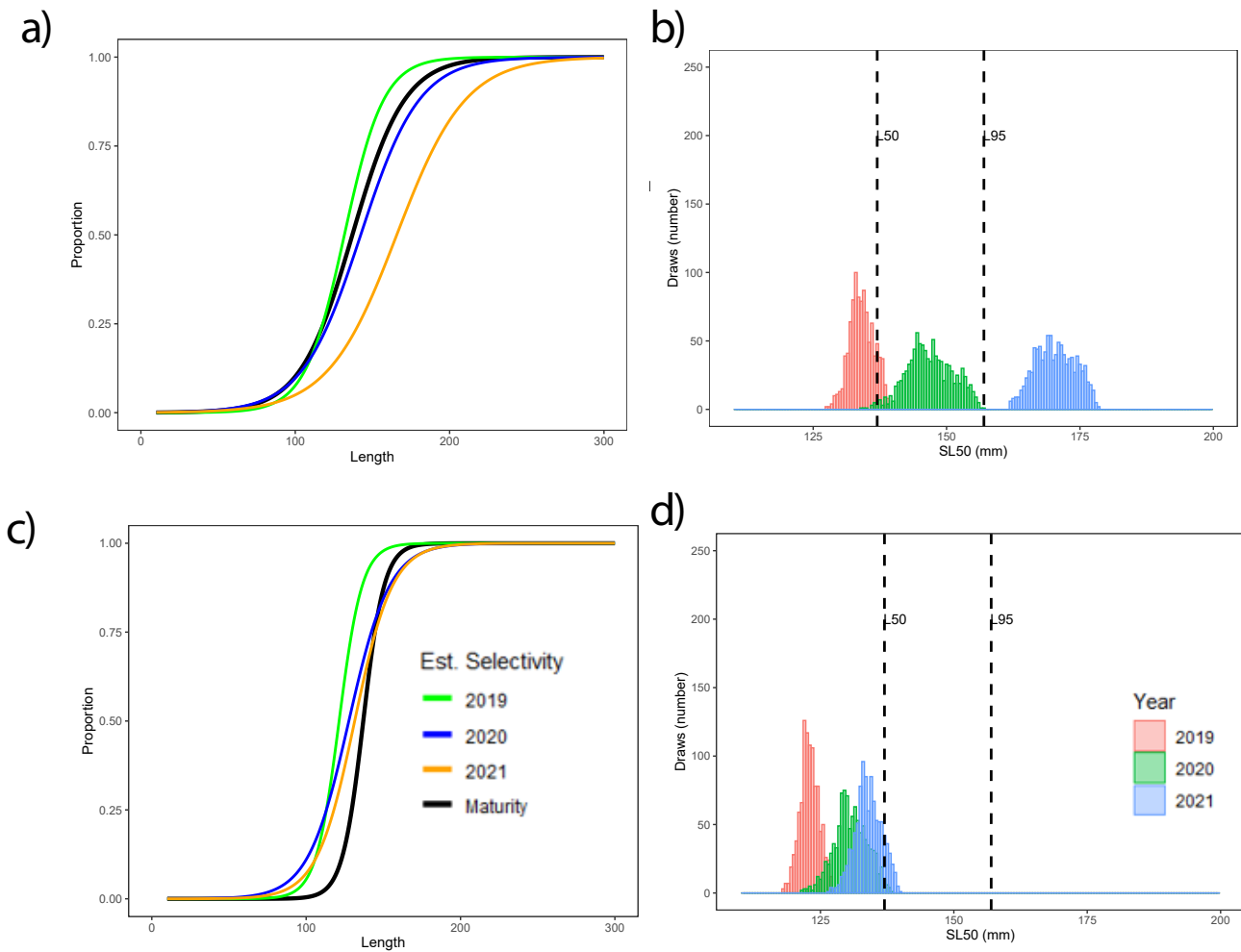


Figure 16. Left graphs plot the maturity-at-length curve and the estimated selectivity-at-length curve for each year by LBSPR for red mullet. Right graphs plot the SL50 values for each year; the bell shape is given by the number of draws estimated by the model. (a, b) Scenario 1 (ICatMar data), (c,d) Scenario 2 (DCF-GSA06 data). Data include discards.

scenario 1, the best fit is for 2019, due to a more homogeneous size frequency. In scenario 2, all the years have a good adjustment. On both scenarios, sizes below the black line are underestimated and above the black line are overestimated.

Maturity vs. selectivity (absolute and range of values)

The selectivity calculated by the model can be seen in Figure 16. On both scenarios, selectivity is increasingly improving. For example, in scenario 1, in 2019 the calculated selectivity is below the L_{mat50} ; in 2020 the calculated selectivity is between L_{mat50} and L_{mat95} ; and in 2021 S_{L50} is above L_{mat95} . However, in scenario 2, the calculated selectivity is below the L_{mat50} in the three years assessed.

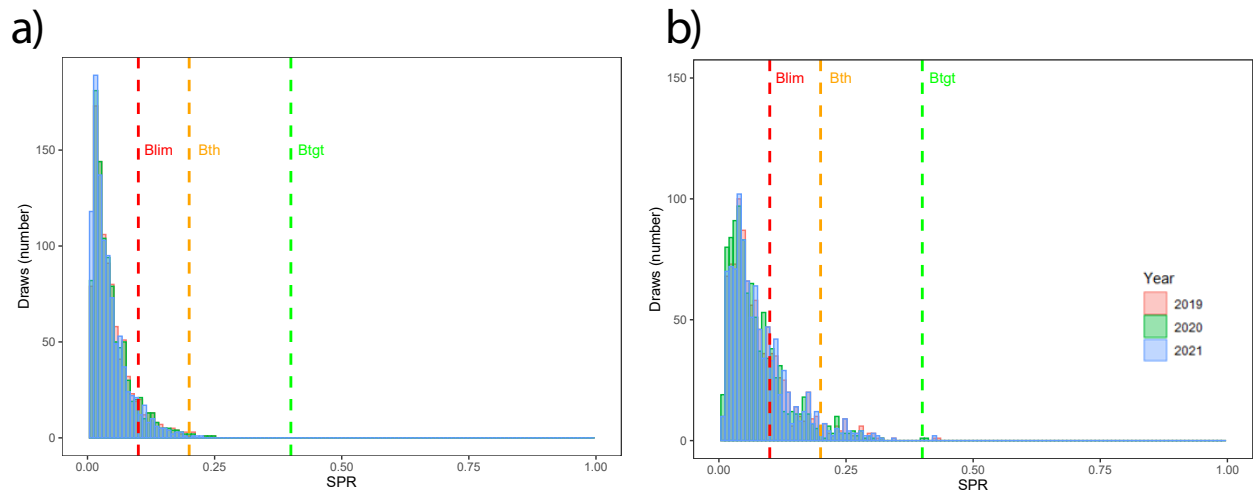


Figure 17. Estimated SPR values for red mullet. (a) Scenario 1 (ICatMar data), (b) Scenario 2 (DCF-GSA06 data). Data include discards.

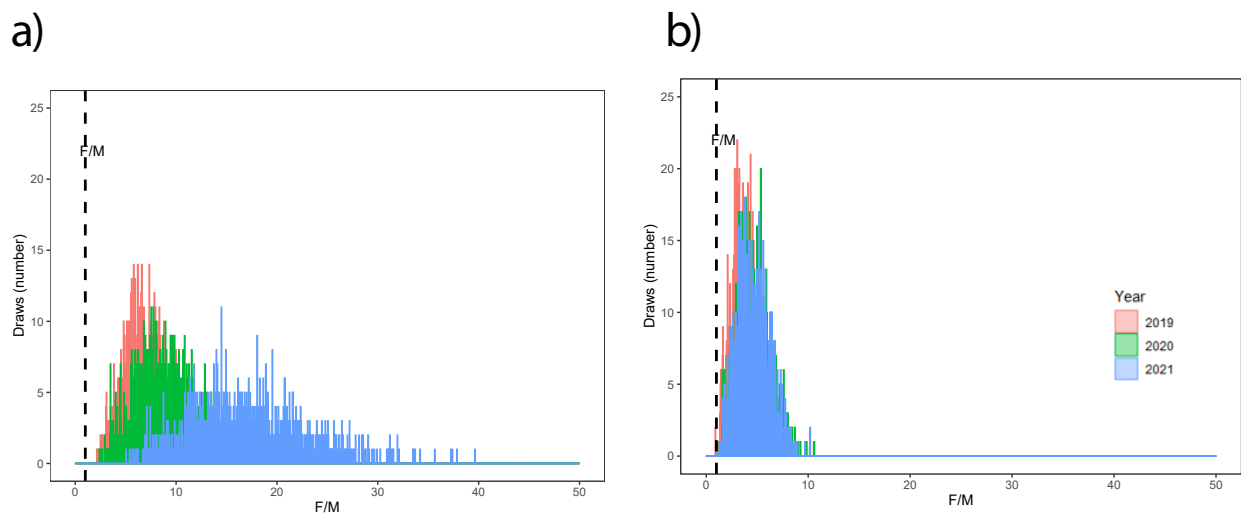


Figure 18. Estimated F/M values for red mullet. (a) Scenario 1 (ICatMar data), (b) Scenario 2 (DCF-GSA06 data). Data include discards.

Precautionary advice based on SPR

On both scenarios, the calculated SPR values are below the B_{lim} , as shown in Figure 17. There is no clear trend between years. In scenario 2 there are some values that are above the B_{lim} and B_{tgt} .

Relative fishing mortality

F/M ratio values are shown in Figure 18. On both scenarios, F/M ratio is above 1 with no trend between years. In scenario 1, the range of values of the F/M ratio are very wide (1 to 50) but in scenario 2 the range is narrow, with similar values among years. Ratio is also wide (1 to 10).

LBPA

Fitted data

The length frequency distribution fitted per year after raising the data for both scenarios, that is, using ICATMAR and DCF GSA6 data sets, are shown in Figure 19. On both scenarios, sizes below the black line are underestimated and above the black line are overestimated. In scenario 1, the model does not quite fit the size classes correctly. Therefore, the model underestimates small classes and overestimates individuals between 140 and 190 mm. The model fits better for scenario 2.

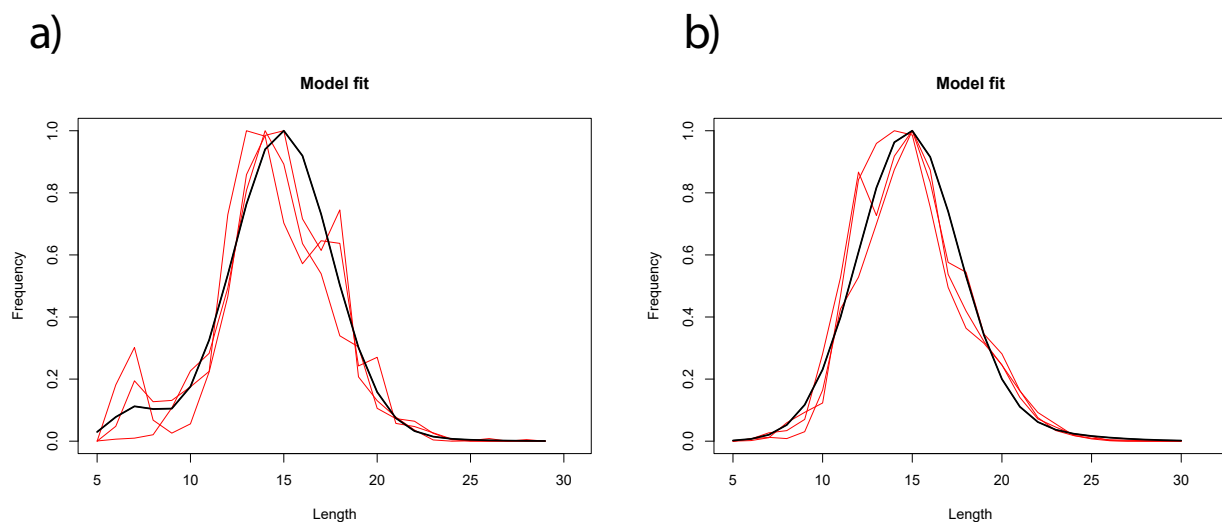


Figure 19. Fitting data by LBPR model for red mullet. (a) Scenario 1 (ICatMar data), (b) Scenario 2 (DCF-GSA06 data). Red lines represent the length frequency for the 3 studied years; the black line is the length frequency distribution estimated for the model. Data include discards.

Maturity vs. Selectivity

Maturity and Selectivity curves for the red mullet are represented in Figure 20. In scenario 1, selectivity is below $L_{\text{mat}50}$. In scenarios 2, selectivity is also below but much closer to $L_{\text{mat}50}$ ($SL_{50}=131$ mm).

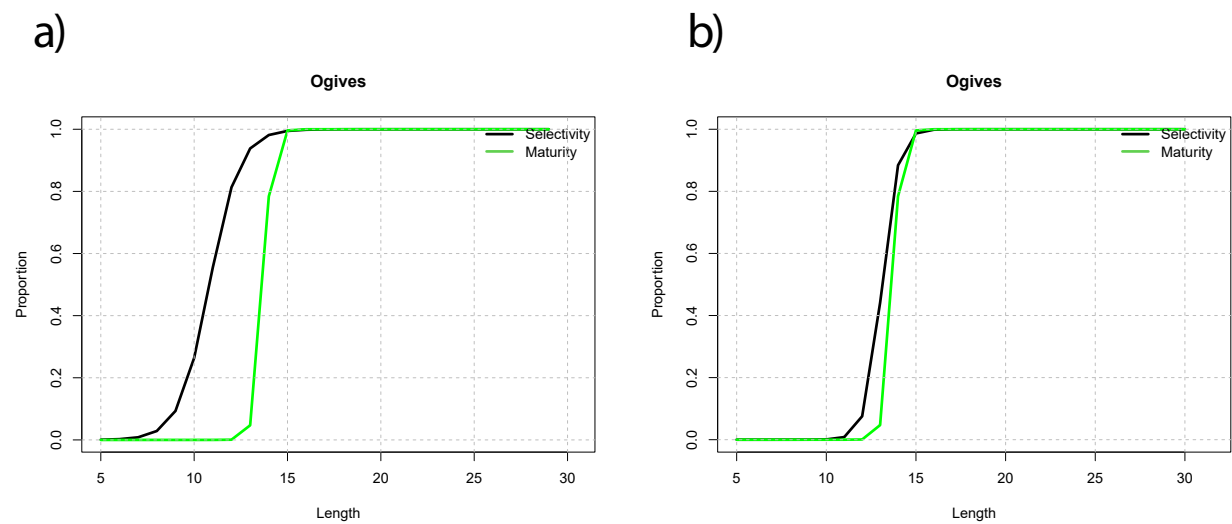


Figure 20. Graphs plotting the maturity-at-length curve and the estimated selectivity-at-length curve for each year by LBPR model for red mullet. (a) Scenario 1 (ICatMar data), (b) Scenario 2 (DCF-GSA06 data). Data include discards.

SPR and Fishing mortality estimations

SPR and F estimations are shown in Figure 21. In both scenarios, there is overexploitation and overfishing. In scenario 1, the SPR values are below the SPR_{tgt} (0.4) but the uncertainty range is very small. In turn, F is above the F_{tar} and its values range between 2 to 6, with high uncertainty. In scenario 2, SPR and fishing mortality estimations are similar to scenario 1 but fishing mortality has lower uncertainty, with F values ranging from 2 to 4.

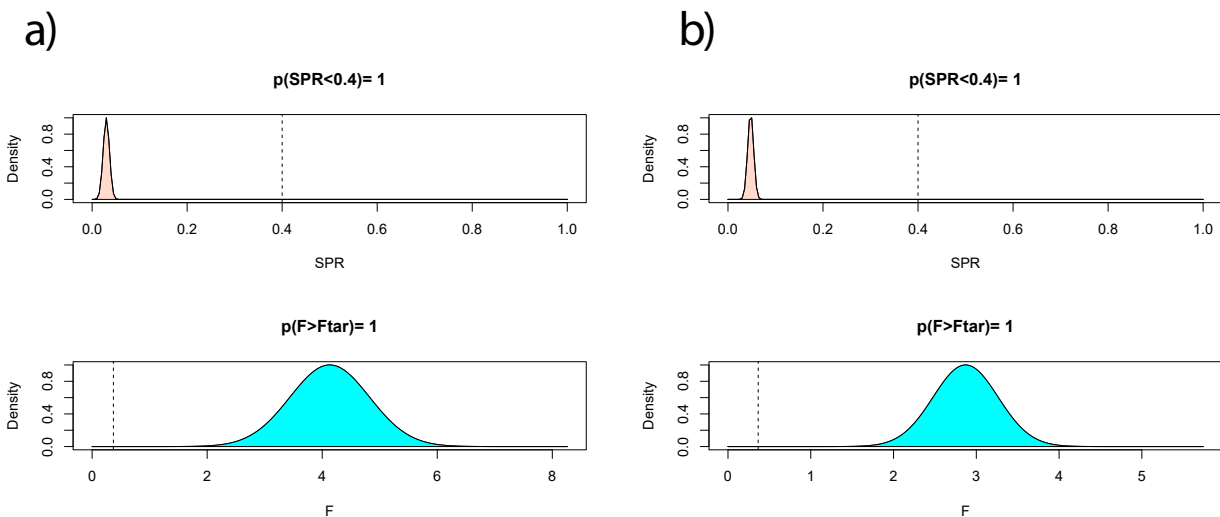


Figure 21. Graphs plotting the estimates of SPR and F by LBPR model for red mullet. (a) Scenario 1 (ICat-Mar data), (b) Scenario 2 (DCF-GSA06 data). Data include discards.

Stock assessment indicators

Table 6. Stock assessment indicators for red mullet. Detailed information of each parameter can be found in the Glossary. Data include discards.

Specie	Scenario	Method	Year	SPR	F/M or F/Fmsy*
MUT	ICATMAR	LBSPR	2019	0.05	7.06
MUT	ICATMAR	LBSPR	2020	0.05	8.93
MUT	ICATMAR	LBSPR	2021	0.04	17.10
MUT	ICATMAR	LBPA	2019	0.06	9.67*
MUT	ICATMAR	LBPA	2020	0.06	9.67*
MUT	ICATMAR	LBPA	2021	0.06	9.67*
MUT	DCF-GSA6	LBSPR	2019	0.08	3.82
MUT	DCF-GSA6	LBSPR	2020	0.08	4.43
MUT	DCF-GSA6	LBSPR	2021	0.08	4.57
MUT	DCF-GSA6	LBPA	2019	0.05	7.87*
MUT	DCF-GSA6	LBPA	2020	0.05	7.87*
MUT	DCF-GSA6	LBPA	2021	0.05	7.87*

Hake (*Merluccius merluccius*) HKE

The European hake (*Merluccius merluccius*; FAO code HKE) growth parameters, length-weight relationship and maturity at L_{mat50} and L_{mat95} are shown in Table 7.

The spawning area for European hake is the continental shelf and upper slope but the nursery area is only on the continental shelf. The recruitment season occurs all year round but with peaks in winter and spring (Recasens et al. 2008)

Catch (landings and discards)

European hake landings show a clear downward trend (Fig. 23). Likewise, landings in Catalan fishing ports have decreased from almost 2 500 t to less than 700 t at present. The European hake is caught by different métiers from the Catalan fishing fleet being OTB Middle Delta shelf, OTB Coastal shelf, OTB Deeper shelf and OTB Upper slope the métiers that land the largest quantities of this species (Fig. 23).

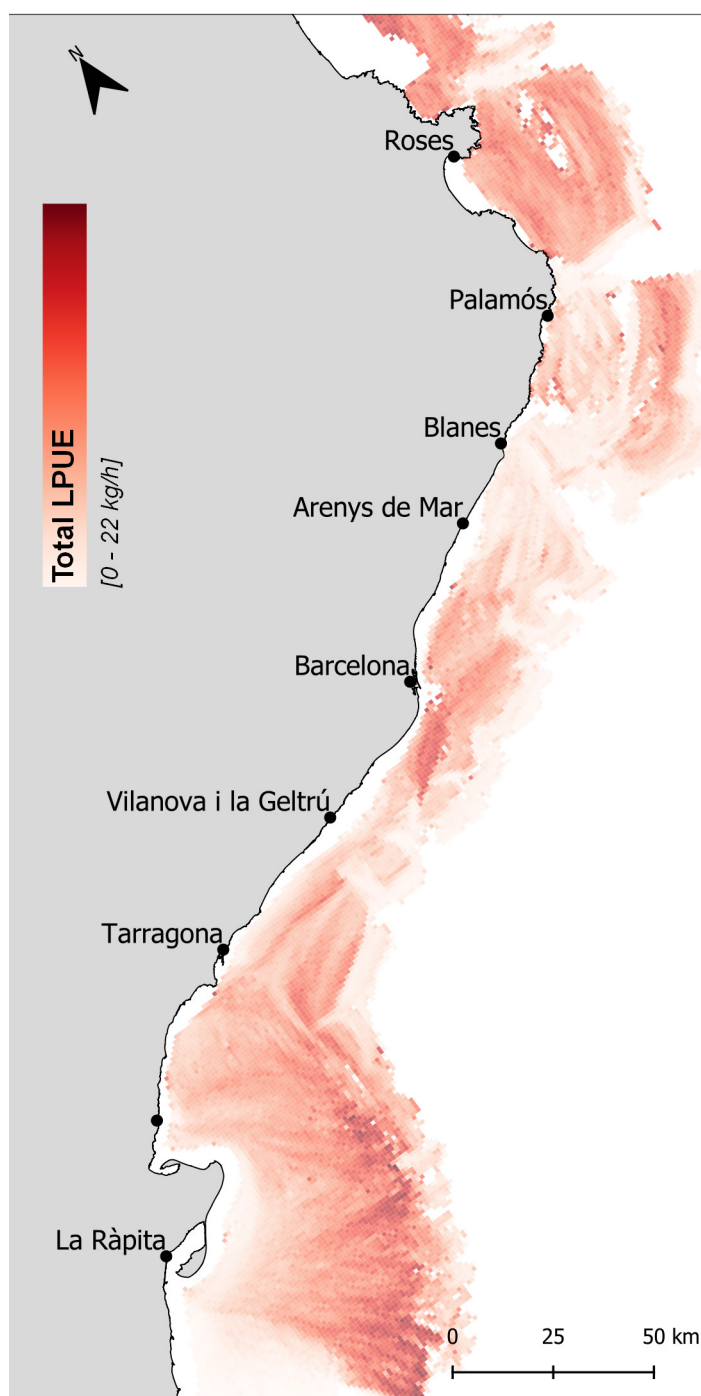


Figure 22. Spatial distribution of landings per unit effort (LPUE) for hake in the Catalan fishing grounds (N GSA6) in 2021.

Table 7. Biological parameters described for hake. Detailed information of each parameter can be found in the Glossary.

	L_{inf} (mm)	K	t_0	a	b	M	L_{mat50} (mm)	L_{mat95} (mm)
HKE	1100	0.178	-0.005	0.00677	3.035	0.4	260	310
Data source	Mellon-Duval et al. (2010)			DCF 2012	Abella et al. (1997)	García-Rodríguez M. and Fernández A.M. (2005)		

The length frequency distribution per year and métier after raising the data without including discards in the data analyses for both scenarios, that is, using ICATMAR and DCF GSA6 data sets, are shown in Figure 24. For the first scenario (ICATMAR), there is no similarity between length structures among years and the number of individuals per size frequency increases with time. For the second scenario (DCF GSA 6), there is a similarity among the length structure throughout the years, with less individuals in 2020. In 2021, there is an increase in the number of smaller sized individuals. For both scenarios, trawling and small-scale fisheries are included.

The length frequency distribution per year and métier, including discards, after raising the data for both scenarios, that is, using ICATMAR and DCF GSA6 data sets, are shown in Figure 25. For the first scenario (ICATMAR), there is no similarity for the length structure among years and

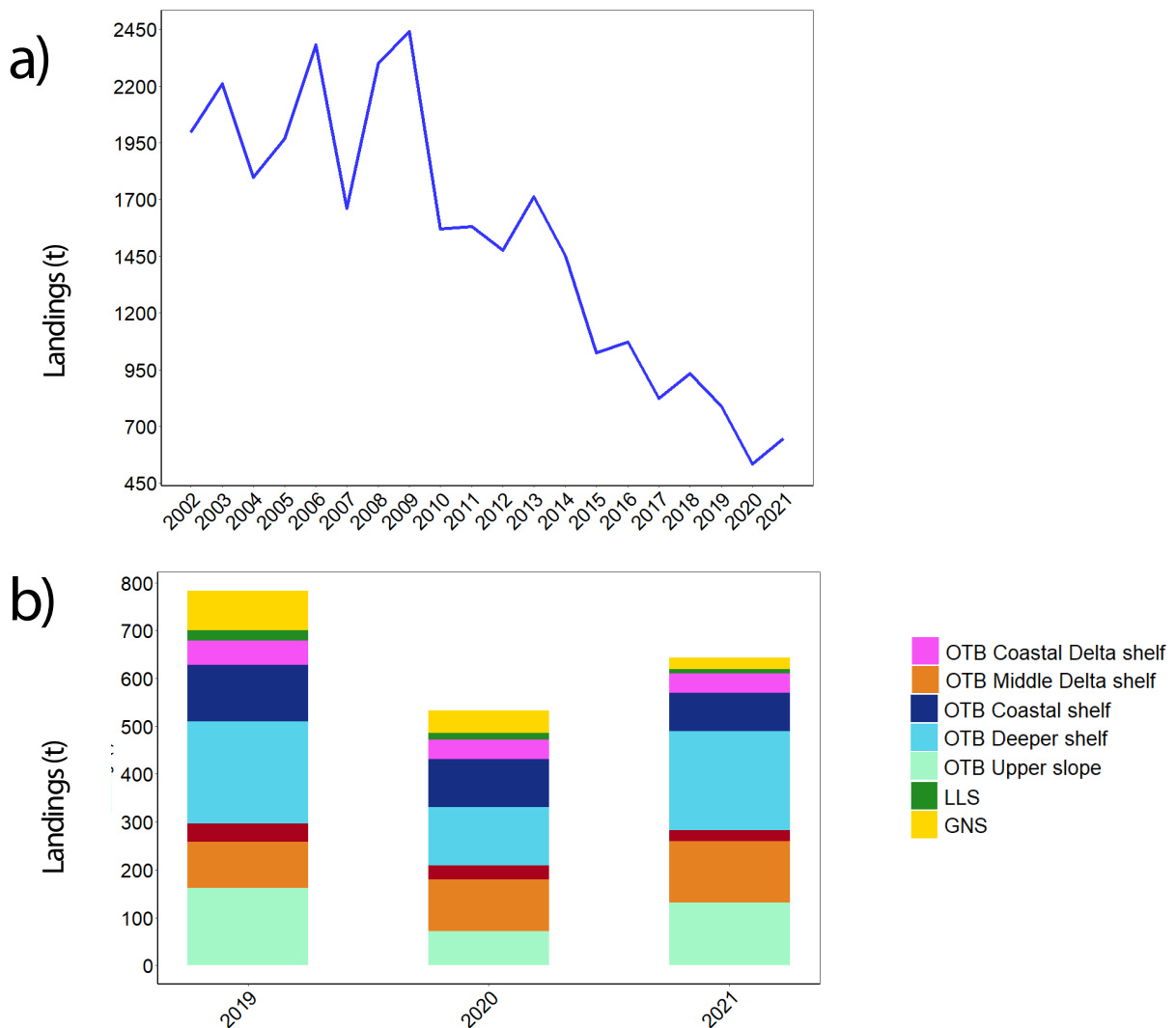


Figure 23. Characterization of hake landings. (a) Historical landings in Catalonia. (b) Landings for 2019, 2020 and 2021 for the different by métier and fishing gear (OTB) Bottom otter trawl, (LLS) Set longlines and (GNS) Set gillnet.

the number of individuals per size frequency increases with time. Similarly, for the second scenario (DCF GSA 6), there is no similarity among the length structure throughout the years and there are more individuals in 2021 than in 2019 and 2020. However, in scenario 2 the proportion of individuals is higher and there is a greater presence of small-sized individuals.

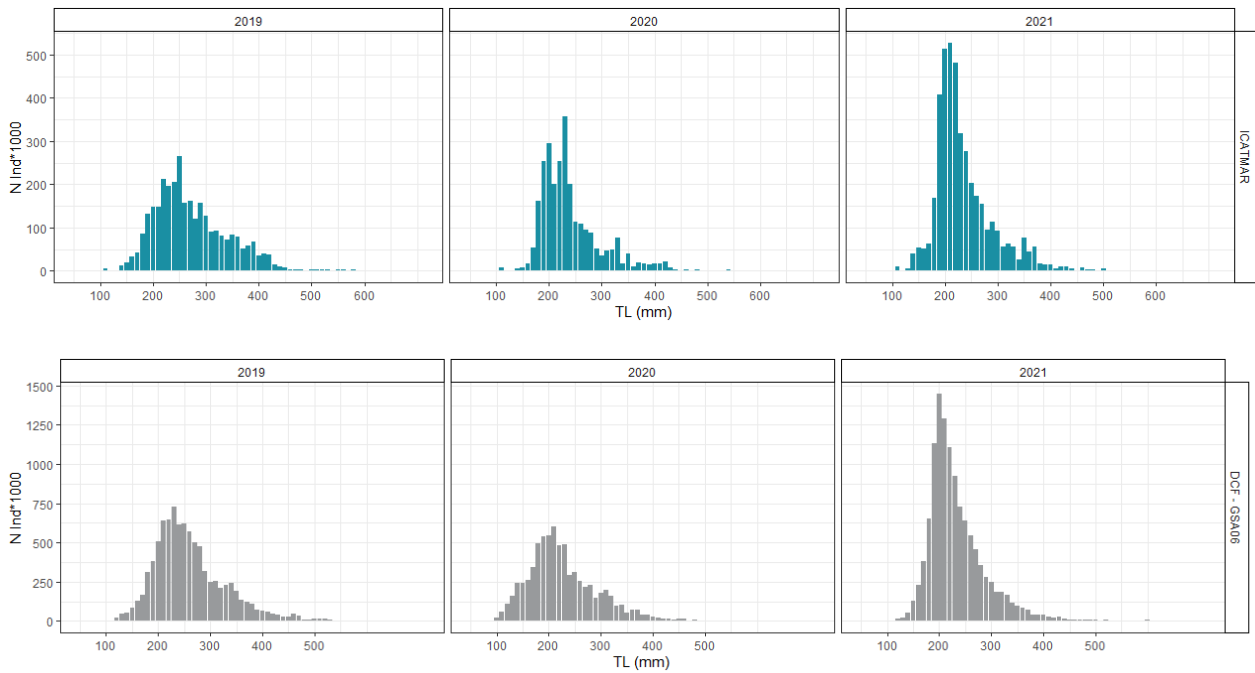


Figure 24. Annual length-frequency distributions for hake. Scenario 1 (top plots) using the ICATMAR data set and Scenario 2 (bottom plots) using DCF-GSA06 data data set. Data do not include discards.

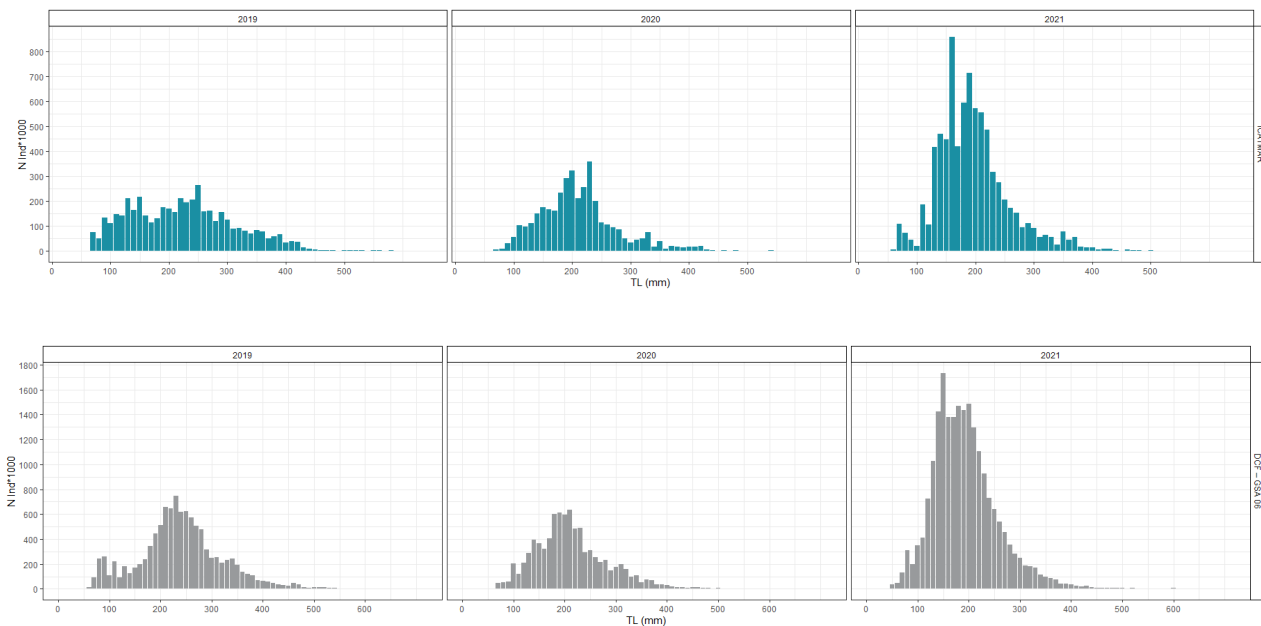


Figure 25. Annual length-frequency distributions for hake. Scenario 1 (top plots) using the ICATMAR data set and Scenario 2 (bottom plots) using DCF-GSA06 data data set. Data include discards.

Stock assessment by model (without discards)

LBSPR

Fitted data

The length frequency distribution fit per year after raising the data for both scenarios, that is, using ICATMAR and DCF GSA6 data sets, are shown in Figure 26. On both scenarios, sizes below the black line are underestimated and above the black line are overestimated. Scenario 1 is worse fitted than scenario 2 but both have under and overestimated values.

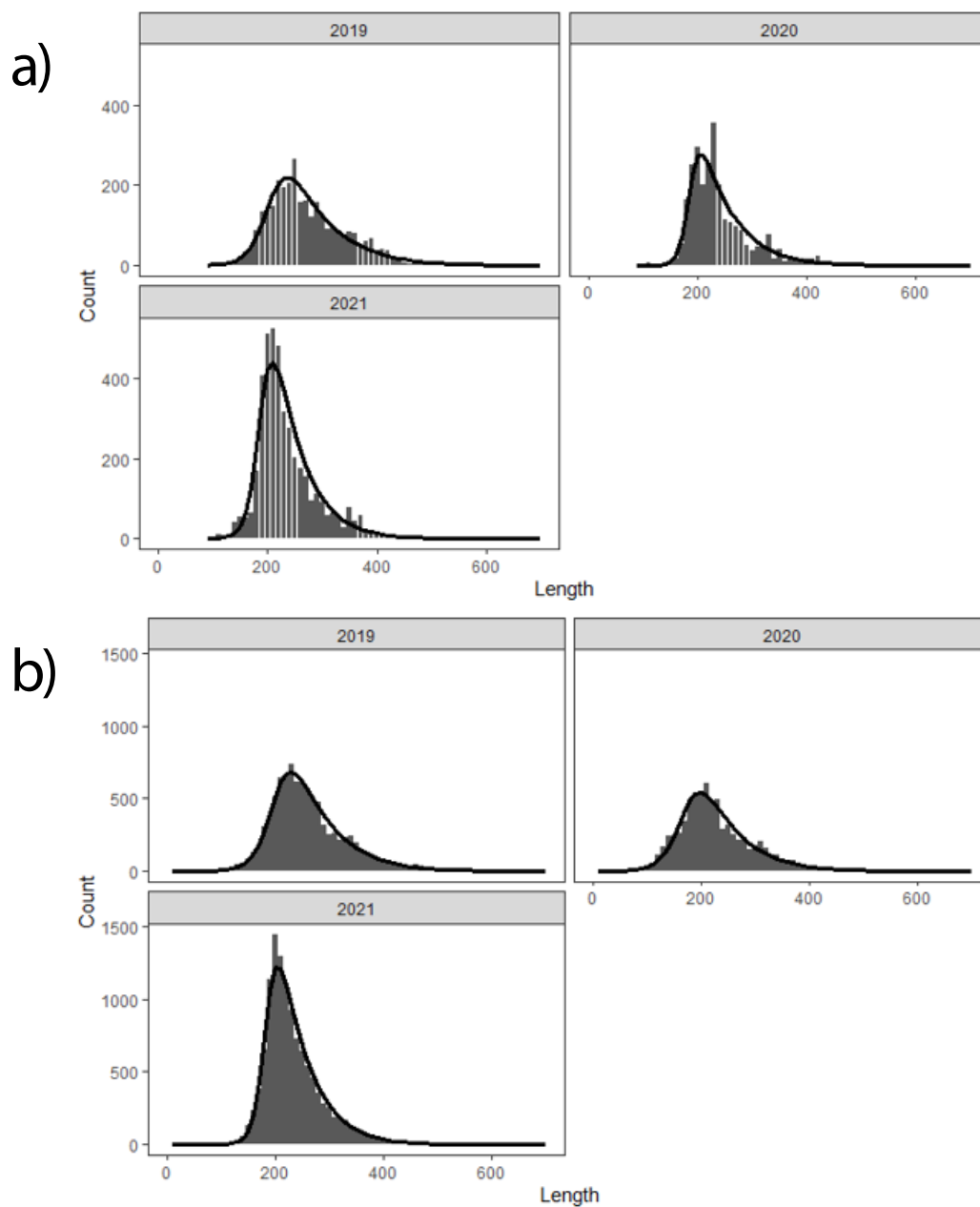


Figure 26. Fitting data by LBSPR model for hake. (a) Scenario 1 (ICatMar data), (b) Scenario 2 (DCF-GSA06 data). Data do not include discards.

Maturity vs. Selectivity (absolute and range of values)

The selectivity calculated by the model can be seen in the Figure 27. On both scenarios, the calculated selectivity is under the size at first maturity. Over the years, selectivity moved further away from L_{mat50} . Accordingly, for both scenarios, the estimated selectivity is closer to L_{mat50} in 2019 than the rest of the years assessed.

Precautionary advice based on SPR

On both scenarios, the calculated SPR values are below the B_{lim} , as shown in Figure 28. There is no clear trend between years.

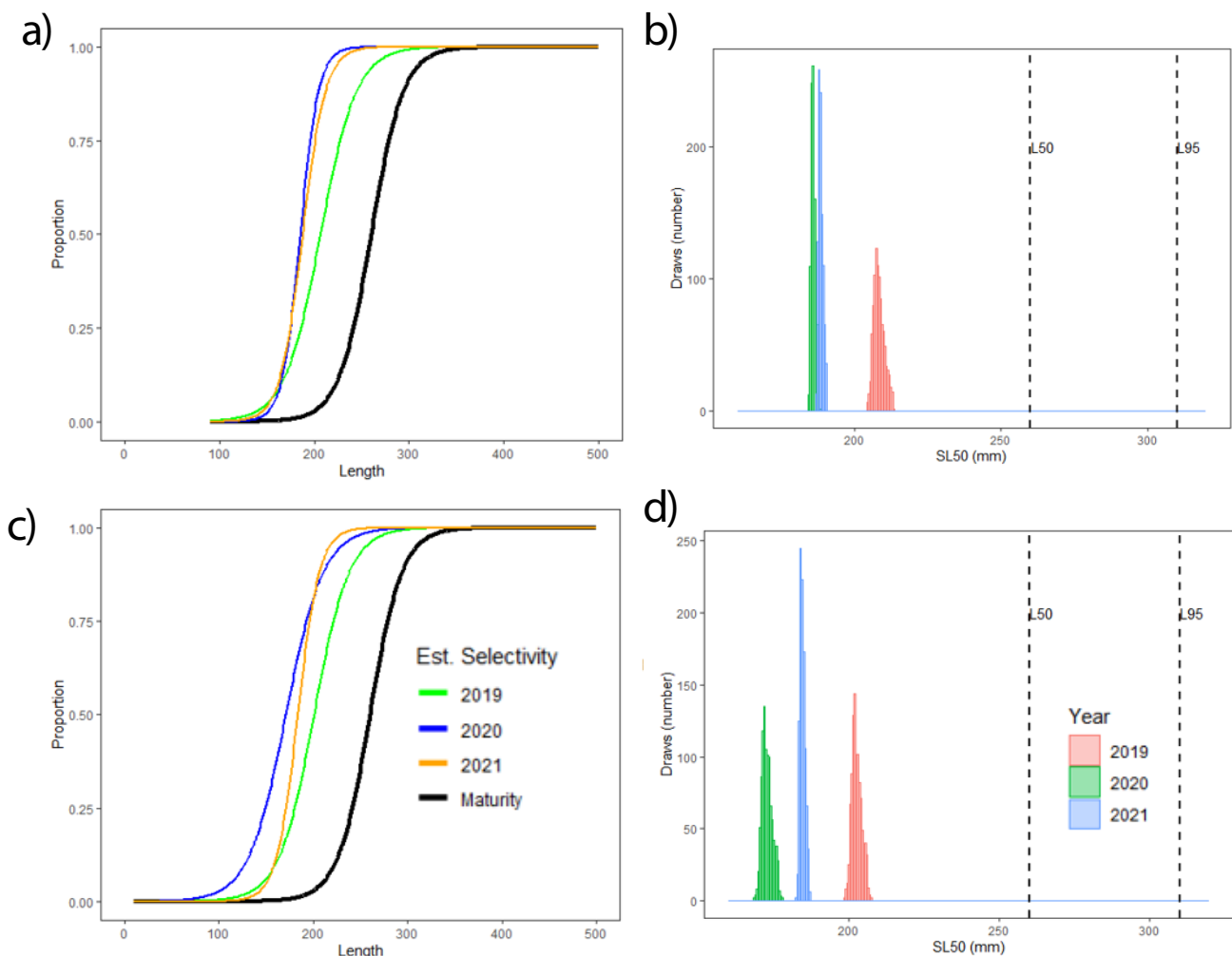


Figure 27. Left graphs plot the maturity-at-length curve and the estimated selectivity-at-length curve for each year by LBSPR for hake. Right graphs plot the SL50 values for each year; the bell shape is given by the number of draws estimated by the model. (a, b) Scenario 1 (ICatMar data), (c,d) Scenario 2 (DCF-GSA06 data). Data do not include discards.

Relative fishing mortality

F/M ratio values are shown in Figure 29. For both scenarios the F/M ratio is above 1, with a trend to increase over the years. The range of values for the F/M ratio is wide in for both scenarios.

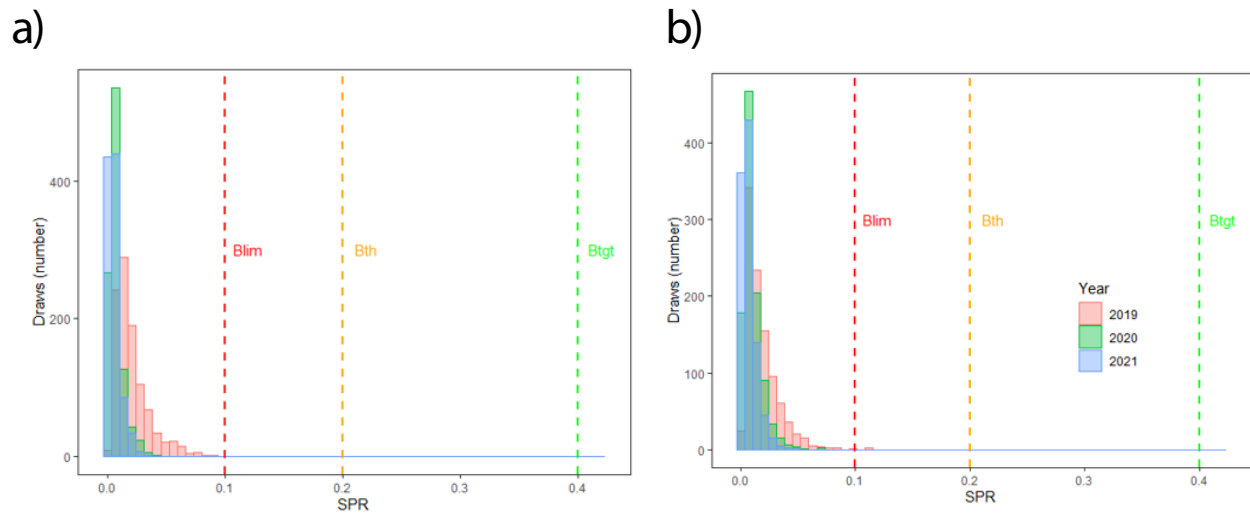


Figure 28. Estimated SPR values for hake. (a) Scenario 1 (ICatMar data), (b) Scenario 2 (DCF-GSA06 data). Data do not include discards.

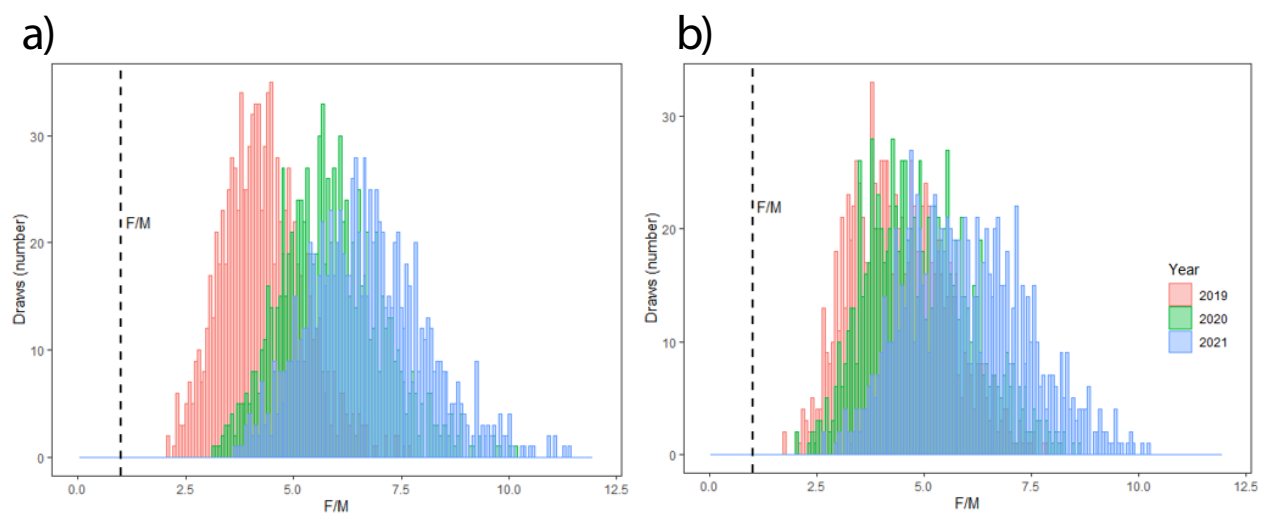


Figure 29. Estimated F/M values for hake. (a) Scenario 1 (ICatMar data), (b) Scenario 2 (DCF-GSA06 data). Data do not include discards.

LBPA

Fitted data

The length frequency distribution fitted per year after raising the data for both scenarios, that is, using ICATMAR and DCF GSA6 data sets, are shown in Figure 30. On both scenarios, sizes below the black line are underestimated and above the black line are overestimated. In scenario 1, the model does not quite fit the central size classes correctly overestimating small-central length classes and underestimating higher length classes. In scenario 2, the model does not have a good fit either underestimating the smallest size classes and overestimating the central length classes.

Maturity vs. Selectivity

Maturity and Selectivity curves for European hake are shown in Figure 31, with selectivity values below L_{mat50} for both scenarios. In detail, selectivity in scenario 1 and 2 are: $SL_{50} = 174.2$ mm and $SL_{50} = 203.2$ mm respectively.

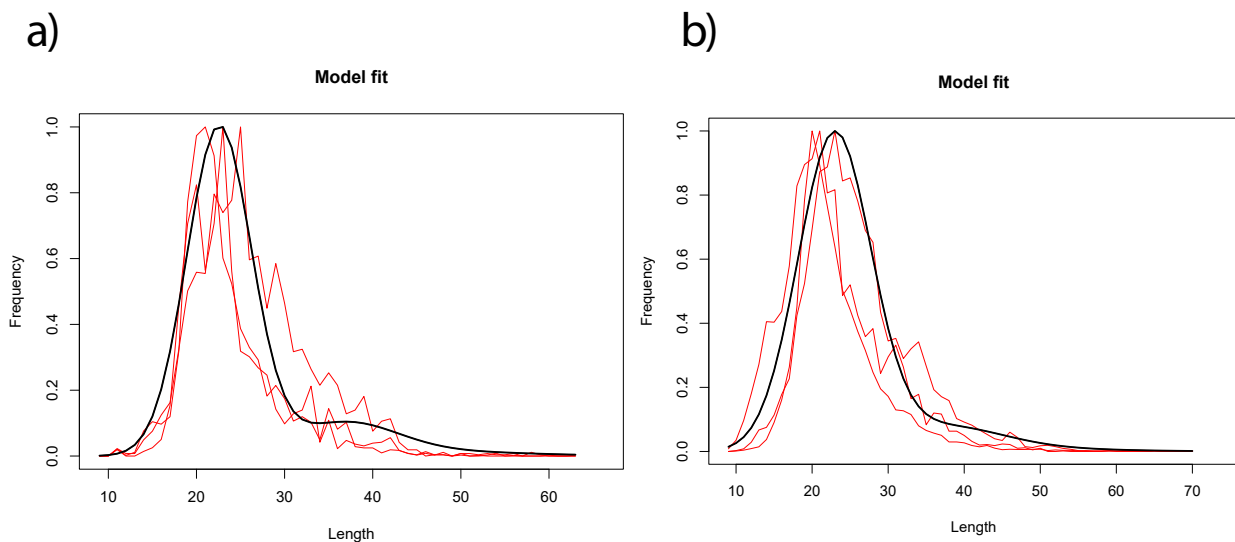


Figure 30. Fitting data by LBPR model hake. (a) Scenario 1 (ICatMar data), (b) Scenario 2 (DCF-GSA06 data). Red lines represent the length frequency for the 3 studied years; the black line is the length frequency distribution estimated for the model. Data do not include discards.

SPR and Fishing mortality estimations

SPR and F estimations are shown in Figure 32, where overexploitation and overfishing are defined for both scenarios. In scenario 1, the SPR values are below the SPR_{tgt} (0.4), with a narrow uncertainty range. Moreover, F is above the F_{tar} with values ranging between 1.22 and 2. Scenario 2 is very similar to scenario 1, with F values ranging from 1.5 to 2.

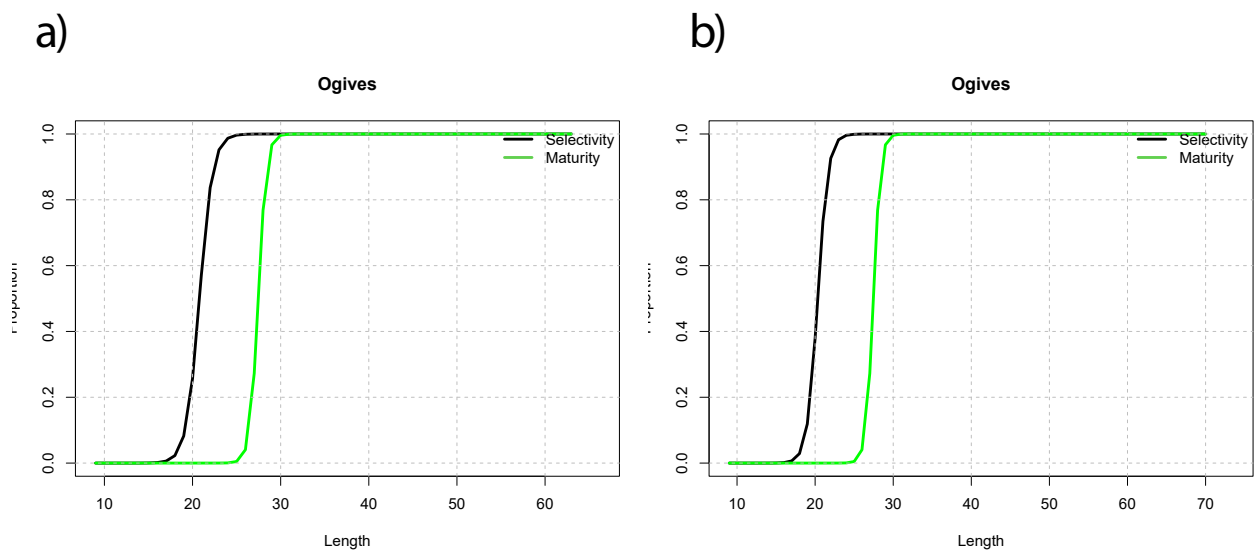


Figure 31. Graphs plotting the maturity-at-length curve and the estimated selectivity-at-length curve for each year by LBPR model for hake. (a) Scenario 1 (ICatMar data), (b) Scenario 2 (DCF-GSA06 data). Data do not include discards.

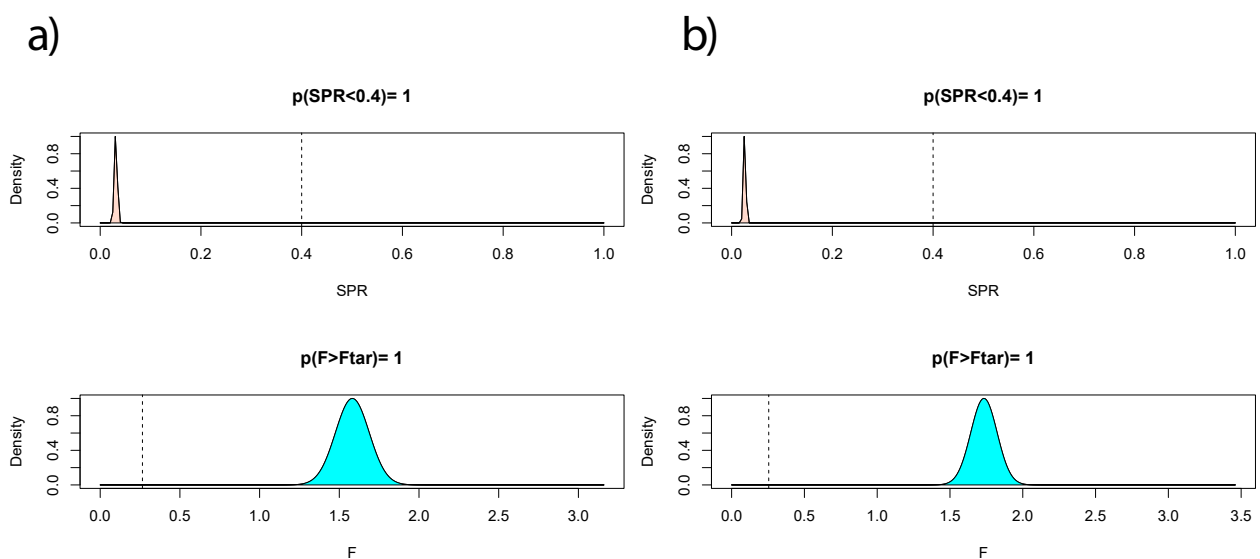


Figure 32. Graphs plotting the estimates of SPR and F by LBPR model for hake. (a) Scenario 1 (ICatMar data), (b) Scenario 2 (DCF-GSA06 data). Data do not include discards.

LIME

Fitted data

The length frequency distribution fit per year after raising the data for both scenarios, that is, using ICATMAR and DCF GSA6 data sets, are shown in Figure 33. For both scenarios, sizes below the red line are underestimated and above the red line are overestimated. In scenario 1, the model does not quite fit the central size classes correctly. Therefore, the model tends to overestimate the small-central length classes in 2019, underestimate the small-central length classes, and overestimate the central-larger length classes in 2020 and 2021. In scenario 2, the model does not have a good fit either, underestimating the smallest size classes and overestimating the central length for all years. Finally, the model estimates one single mode for the Scenario 1 and two modes for the Scenario 2.

Selectivity:

Selectivity-at-length is represented in Figure 34. Scenario 1 shows a higher selectivity-at-length than scenario 2.

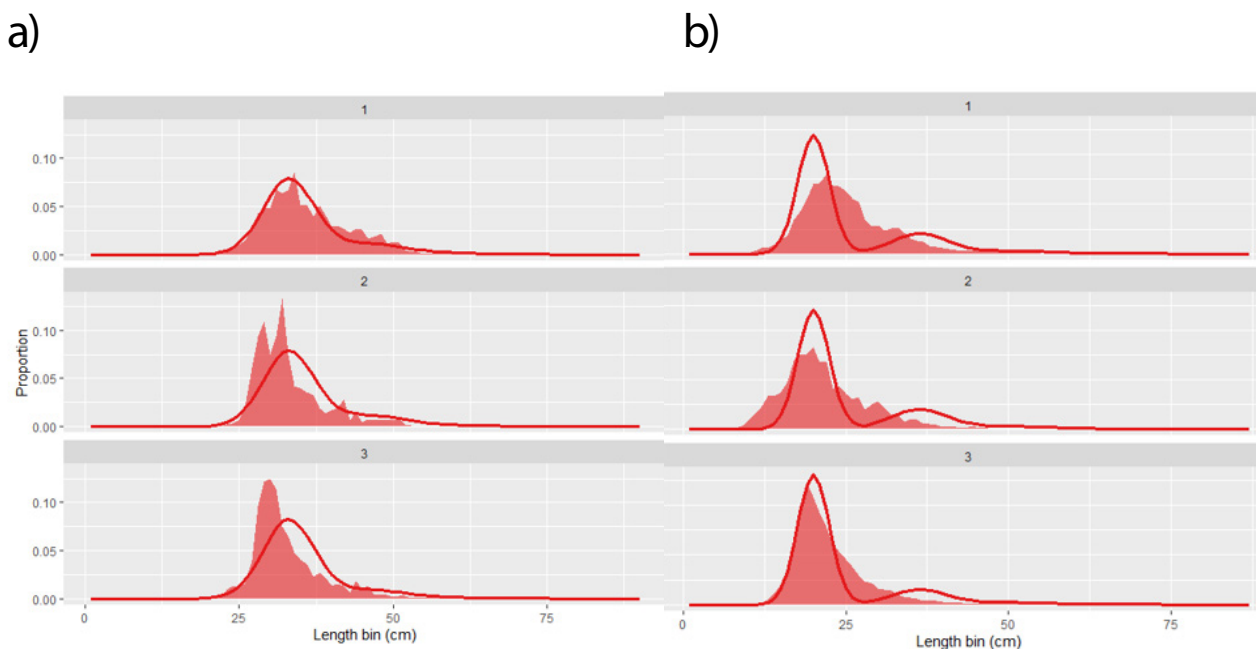


Figure 33. Fitting data by LIME model for hake. (a) Scenario 1 (ICatMar data), (b) Scenario 2 (DCF-GSA06 data). Top graph (1) plot year 2019, middle graphs (2) plot year 2020, and bottom graphs (3) plot year 2021. Data do not include discards.

Precautionary advice based on SPR

SPR estimations are shown in Figure 35. In both scenarios, there is a marked overexploitation in all years assessed.

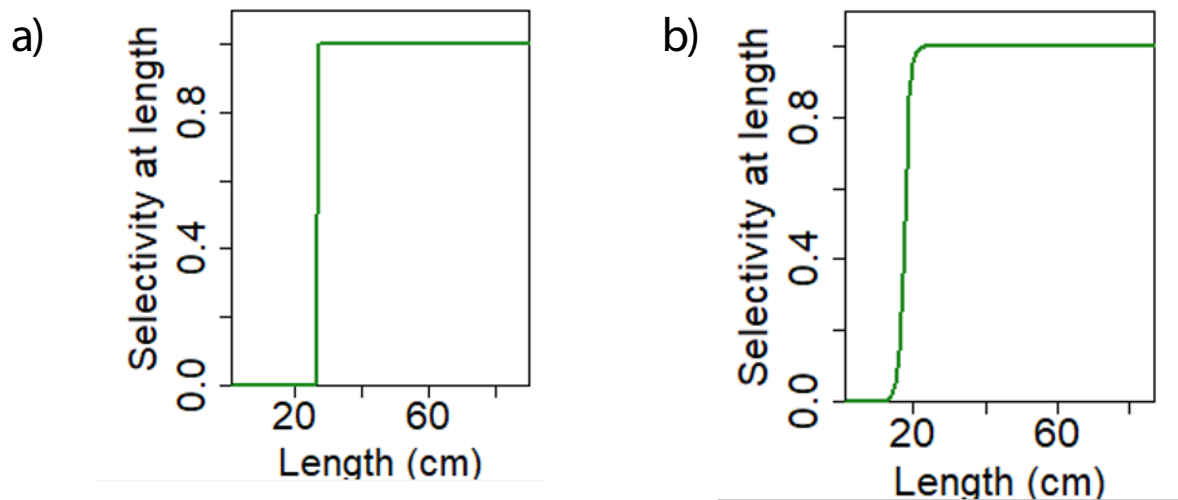


Figure 34. Graphs plotting the estimated selectivity-at-length curve by LIME model for hake. (a) Scenario 1 (ICatMar data), (b) Scenario 2 (DCF-GSA06 data). Data do not include discards.

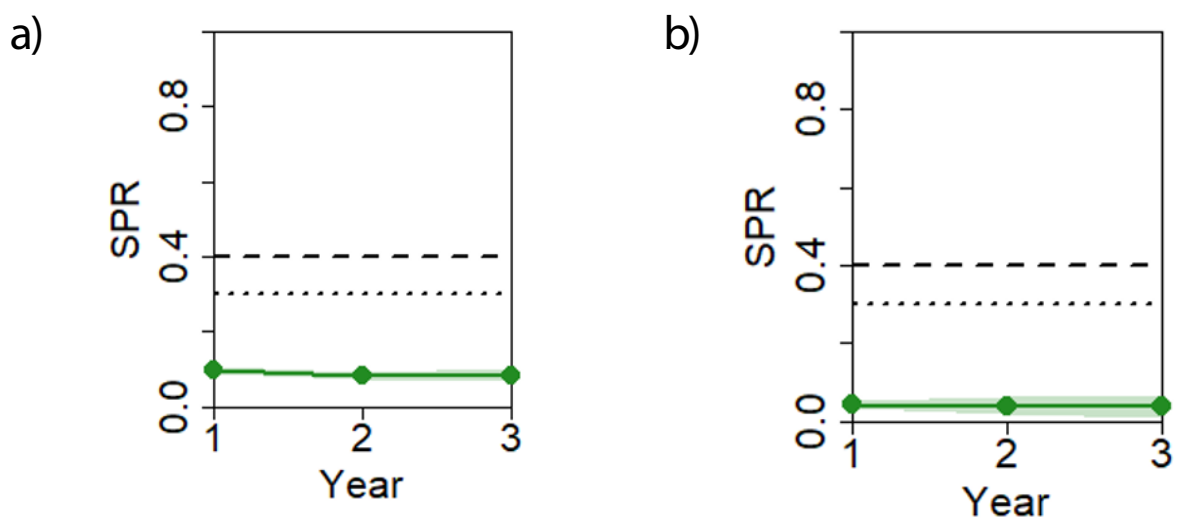


Figure 35. Graphs plotting the estimates of SPR by LIME model for hake. (a) Scenario 1 (ICatMar data), (b) Scenario 2 (DCF-GSA06 data). The uncertainty is shown by the green shade on both sides of the estimation. Data do not include discards.

Fishing mortality

F estimations are shown in Figure 36. In both scenarios, there is overfishing in all years assessed. Scenario 1 has a higher F than scenario 2.

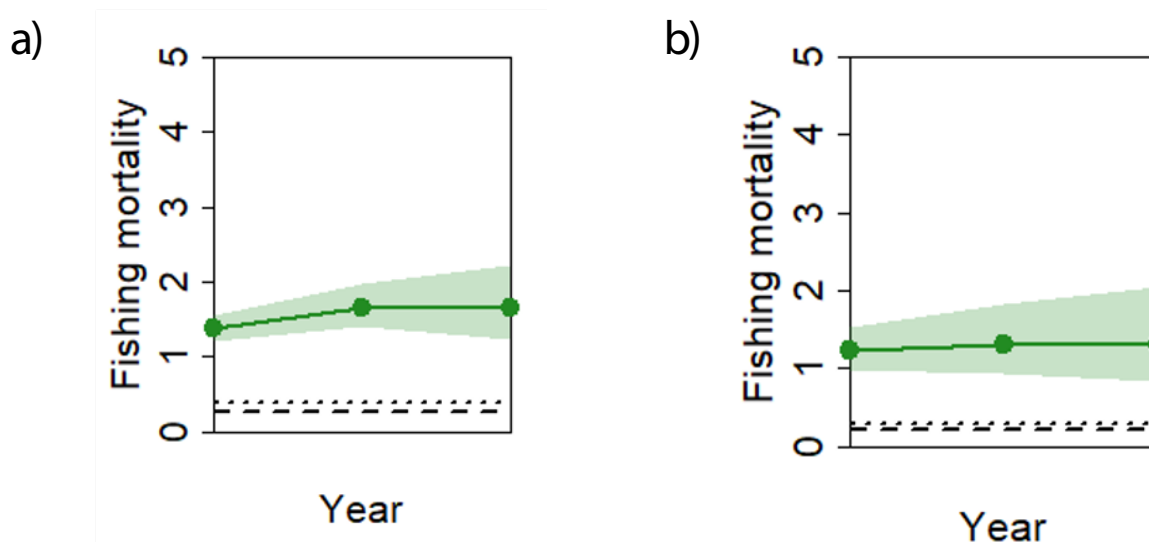


Figure 36. Estimated fishing mortality by LIME model for hake. (a) Scenario 1 (ICatMar data), (b) Scenario 2 (DCF-GSA06 data). Data does not include discards. The uncertainty is shown by the green shade on both sides of the estimation. Dotted line is the F_{msy} whereas the striped line a precautionary F value. Data do not include discards.

Stock assessment indicators

Table 8. Stock assessment indicators for hake. Detailed information of each parameter can be found in the Glossary. Data do not include discards.

Specie	Scenario	Method	Year	SPR	F/M or F/Fmsy*
HKE	ICATMAR	LBSPR	2019	0.02	4.30
HKE	ICATMAR	LBSPR	2020	0.01	5.90
HKE	ICATMAR	LBSPR	2021	0.01	6.71
HKE	ICATMAR	LBPA	2019	0.03	5.97*
HKE	ICATMAR	LBPA	2020	0.03	5.97*
HKE	ICATMAR	LBPA	2021	0.03	5.97*
HKE	ICATMAR	LIME	2019	0.10	3.43
HKE	ICATMAR	LIME	2020	0.09	4.16
HKE	ICATMAR	LIME	2021	0.09	4.16
HKE	DCF-GSA6	LBSPR	2019	0.02	4.42
HKE	DCF-GSA6	LBSPR	2020	0.01	4.92
HKE	DCF-GSA6	LBSPR	2021	0.01	5.98
HKE	DCF-GSA6	LBPA	2019	0.05	6.21*
HKE	DCF-GSA6	LBPA	2020	0.05	6.21*
HKE	DCF-GSA6	LBPA	2021	0.05	6.21*
HKE	DCF-GSA6	LIME	2019	0.12	6.70
HKE	DCF-GSA6	LIME	2020	0.12	6.65
HKE	DCF-GSA6	LIME	2021	0.12	6.65

Stock assessment by model (with discards)

LBSPR

Fitted data

The length frequency distribution fitted per year, including discards after raising the data for both scenarios, that is, using ICATMAR and DCF GSA6 data sets, are shown in Figure 37. On both scenarios, sizes below the black line are underestimated and above the black line are over-

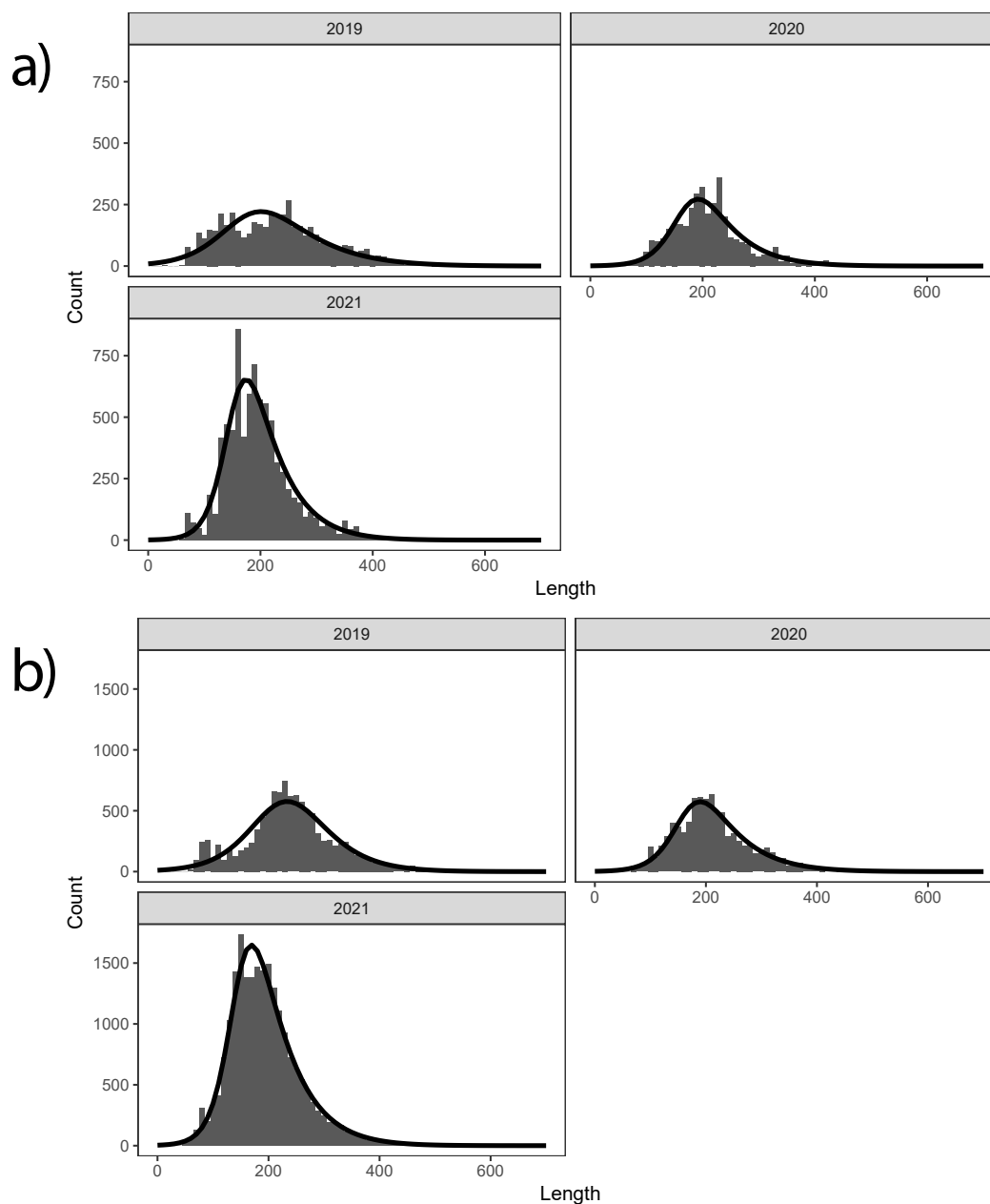


Figure 37. Fitting data by LBSPR model for hake. (a) Scenario 1 (ICatMar data), (b) Scenario 2 (DCF-GSA06 data). Data include discards.

estimated. Scenario 1 is worse fitted than scenario 2 but both have under and overestimated values, especially for years 2019 and 2021. The number of individuals increase with time.

Maturity vs. Selectivity (absolute and range of values)

The selectivity calculated by the model can be seen in the Figure 38. For both scenarios, the calculated selectivity is under the size of first maturity. Over the years, selectivity moves further away from L_{mat50} . In scenario 2, the closest calculated selectivity to the L_{mat50} is in 2019.

Precautionary advice based on SPR

For both scenarios, the calculated SPR values are below the B_{lim} , as shown in the Figure 39. There is no clear trend between years. Scenario 1 shown the closest values to B_{lim} in 2019.

Relative fishing mortality

F/M ratio values are shown in Figure 40. For both scenarios, F/M ratio is above 1.5. In scenario

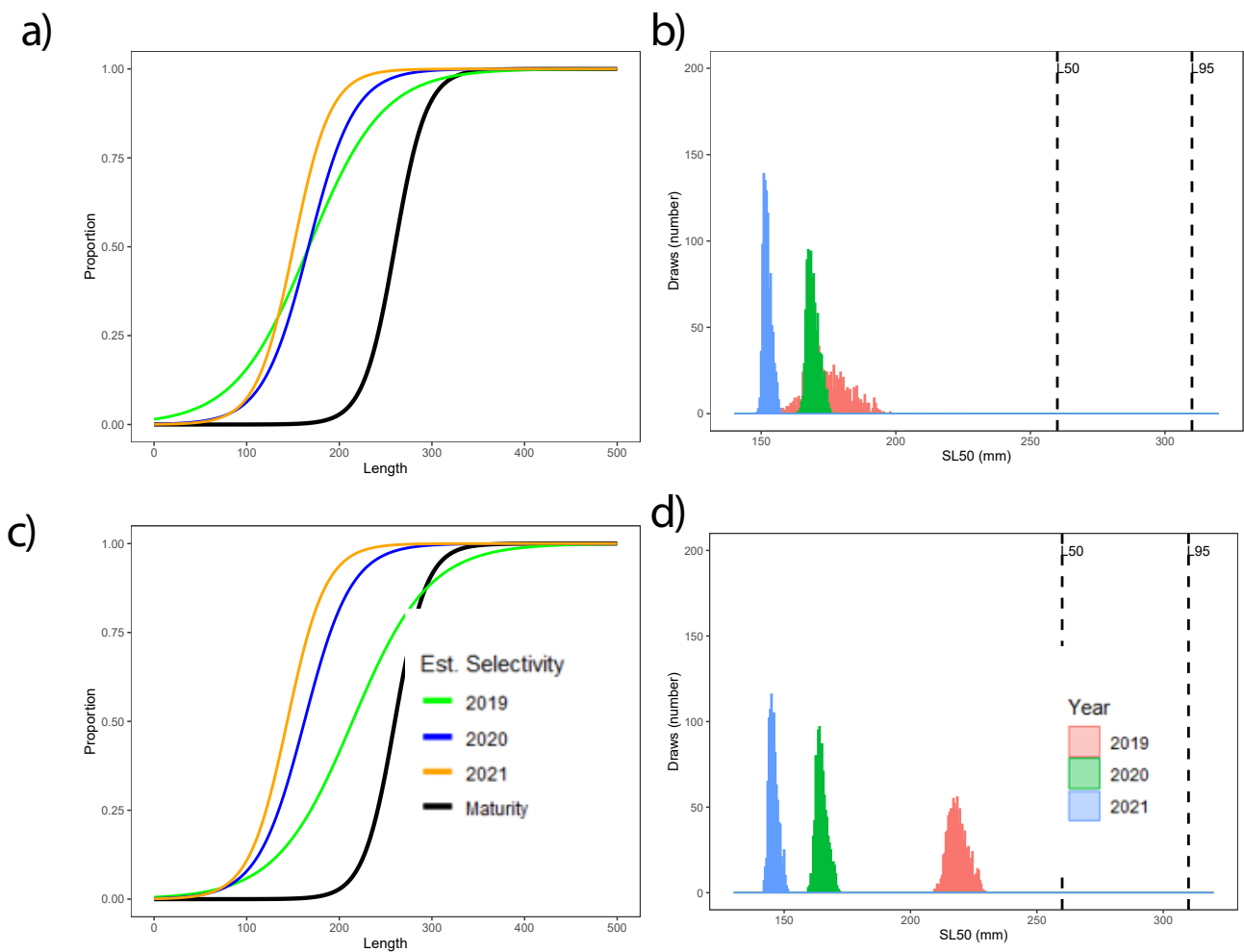


Figure 38. Left graphs plot the maturity-at-length curve and the estimated selectivity-at-length curve for each year by LBSPR for hake. Right graphs plot the SL50 values for each year; the bell shape is given by the number of draws estimated by the model. (a, b) Scenario 1 (ICatMar data), (c,d) Scenario 2 (DCF-GSA06 data). Data include discards.

1, the range of values of the F/M ratio are very wide (1.5 to 11), with is a slight increase in the F/M through time. In scenario 2, there is no trend through time but the values between years are similar to scenario 1 (3 to 10).

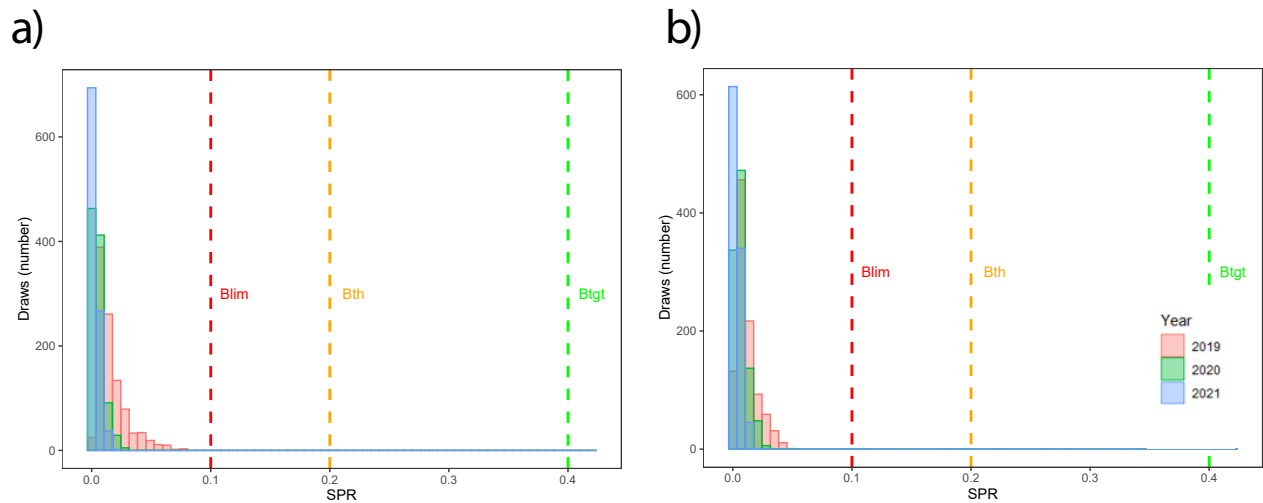


Figure 39. Estimated SPR values for hake. (a) Scenario 1 (ICatMar data), (b) Scenario 2 (DCF-GSA06 data). The bell shape is given by the number of draws estimated by the model. Data include discards.

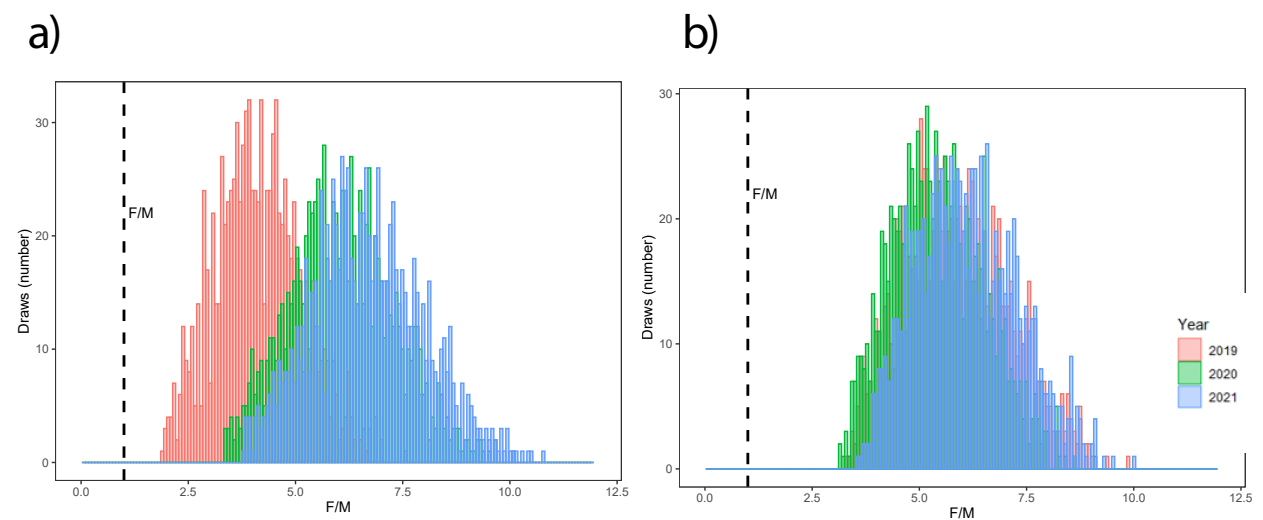


Figure 40. Estimated F/M values for hake. (a) Scenario 1 (ICatMar data), (b) Scenario 2 (DCF-GSA06 data). The bell shape is given by the number of draws estimated by the model. Data include discards.

LBPA

Fitted data

The length frequency distribution fit per year after raising the data for both scenarios, that is, using ICATMAR and DCF GSA6 data sets, are shown in Figure 41. On both scenarios, sizes below the black line are underestimated and above the black line are overestimated. In scenario 1, the model does not quite fit the central size classes correctly and overestimates them. Therefore, the model overestimates small-central length classes and underestimates higher length classes. In scenario 2 (Fig. 41 Right), the model fits also bad, even though it overestimates the central length classes.

Maturity vs. Selectivity

Maturity and Selectivity curves for hake are represented in Figure 42. On both scenarios, selectivity is below L_{mat50} . Selectivity in scenario 1 and 2 are: $SL_{50}=174.2$ mm and $SL_{50}=179.7$ mm respectively.

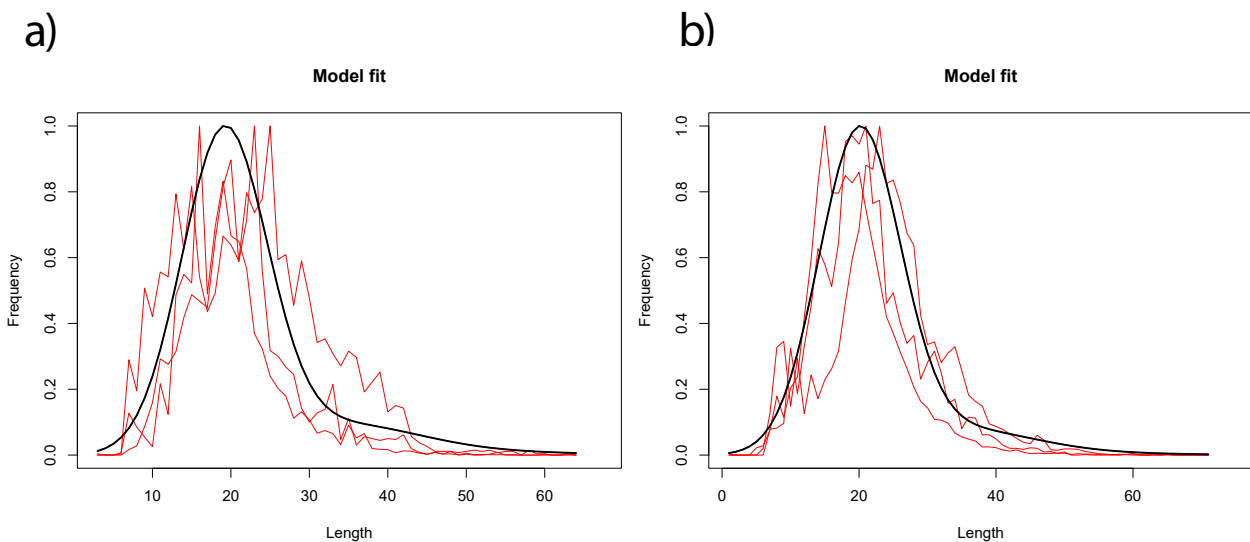


Figure 41. Fitting data by LBPR model for hake. (a) Scenario 1 (ICatMar data), (b) Scenario 2 (DCF-GSA06 data). Red lines represent the length frequency for the 3 studied years; the black line is the length frequency distribution estimated for the model. Data include discards.

SPR and Fishing mortality estimations

SPR and F estimations are shown in Figure 43. In both scenarios, there is a marked overexploitation and overfishing. In scenario 1 (Fig. 43 Left), the SPR values are below the SPR_{tgt} (0.4) but the uncertainty range is very small. In turn, F is above the F_{tar} and its values range between 1.4 and 2 with few uncertainty. In scenario 2 (Fig 43 right), SPR estimation is similar to scenario 1. For fishing mortality, the model shows few uncertainty values, with F ranging from 1.5 to 2.

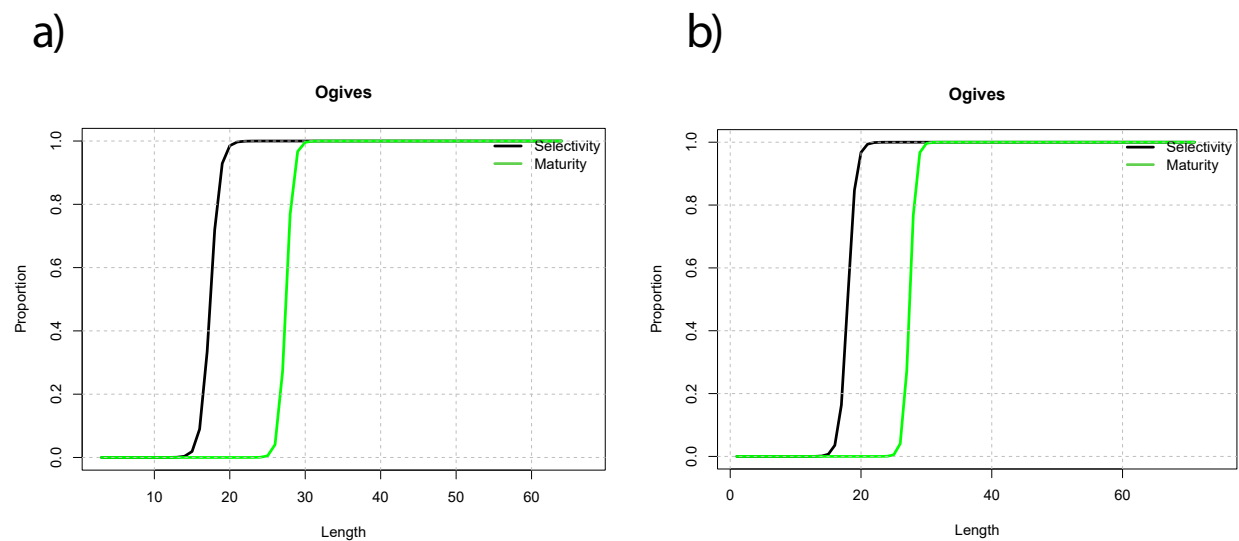


Figure 42. Graphs plotting the maturity-at-length curve and the estimated selectivity-at-length curve for each year by LBPR model for hake. (a) Scenario 1 (ICatMar data), (b) Scenario 2 (DCF-GSA06 data). Data include discards.

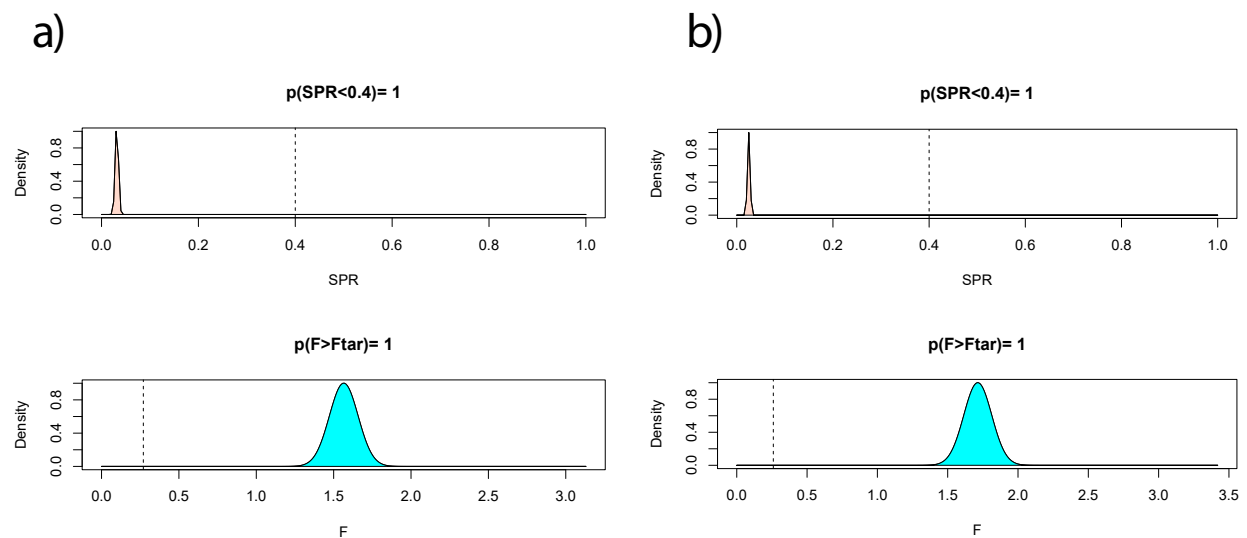


Figure 43. Graphs plotting the estimates of SPR and F by LBPR model for hake. (a) Scenario 1 (ICatMar data), (b) Scenario 2 (DCF-GSA06 data). Data include discards.

LIME

Fitted data

The length frequency distribution fit per year after raising the data for both scenarios, that is, using ICATMAR and DCF GSA6 data sets, are shown in Figure 44. On both scenarios, sizes below the red line are underestimated and above the red line are overestimated. In scenario 1 (Fig. 44 Left), the model does not quite fit the central size classes correctly. Therefore, the model overestimates small-central length classes in 2019, underestimates the small-central length classes and overestimates the central-larger length classes in 2020 and 2021. In scenario 2 (Fig. 44 Right), the model fits also bad, even though it overestimates the smallest size classes in 2019 and subestimates the central length classes in 2020 and 2021.

Selectivity:

Selectivity-at-length is represented in Figure 45. Both scenarios have a similar selectivity-at-length.

Precautionary advice based on SPR

SPR estimations are shown in Figure 46. In both scenarios, there is a marked overexploitation in all years assessed.

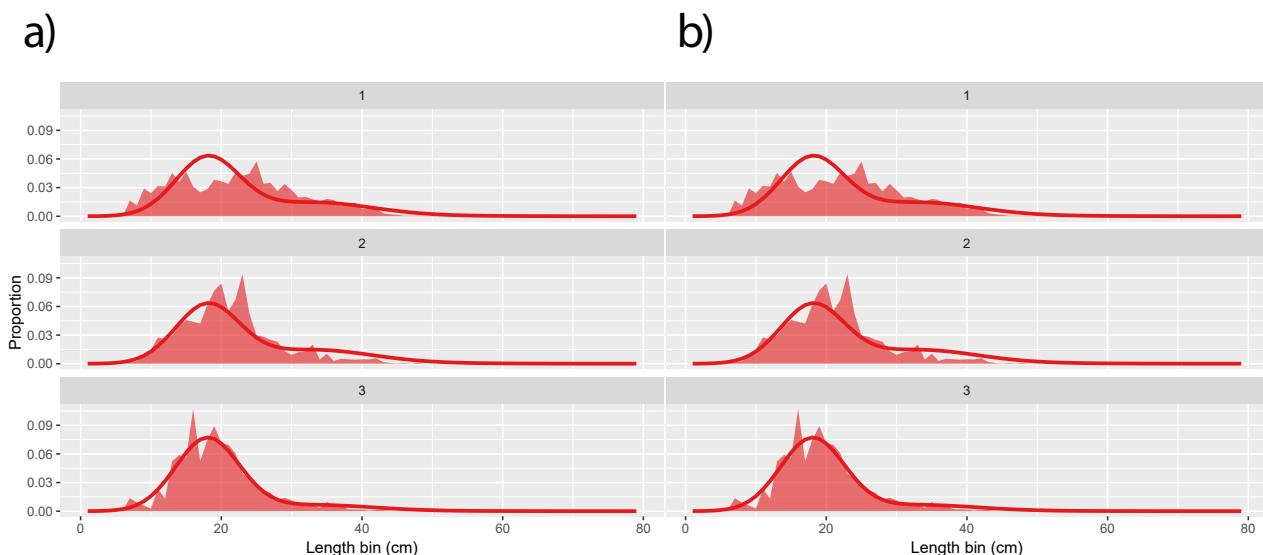


Figure 44. Fitting data by LIME model for hake. (a) Scenario 1 (ICatMar data), (b) Scenario 2 (DCF-GSA06 data). Top graph (1) plot year 2019, middle graphs (2) plot year 2020, and bottom graphs (3) plot year 2021. Data include discards.

Fishing mortality

F estimations are shown in Figure 47. In both scenarios, there is a slight overfishing in all years assessed. Scenario 1 has a higher F than scenario 2.

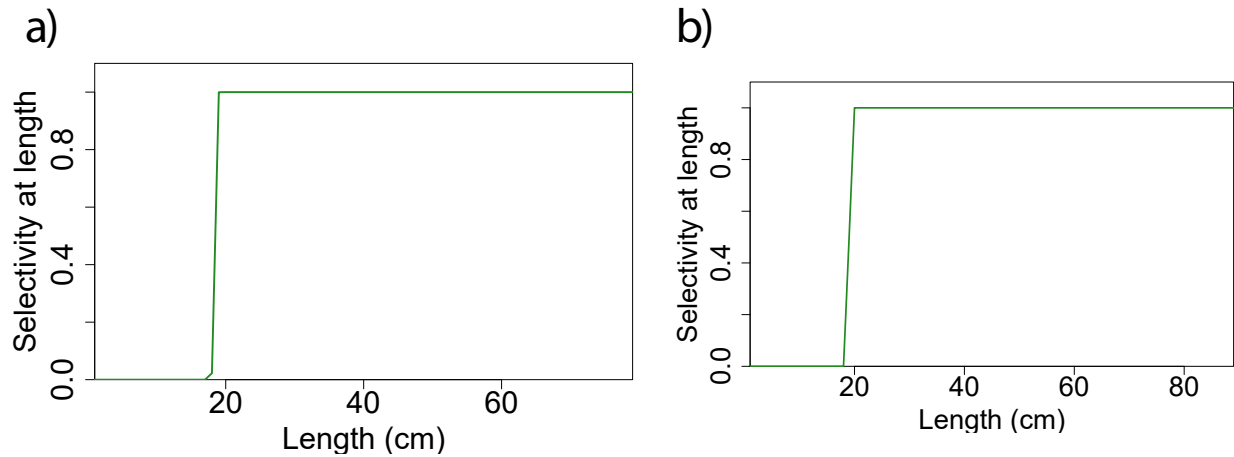


Figure 45. Graphs plotting the estimated selectivity-at-length curve by LIME model for hake. (a) Scenario 1 (ICatMar data), (b) Scenario 2 (DCF-GSA06 data). Data include discards.

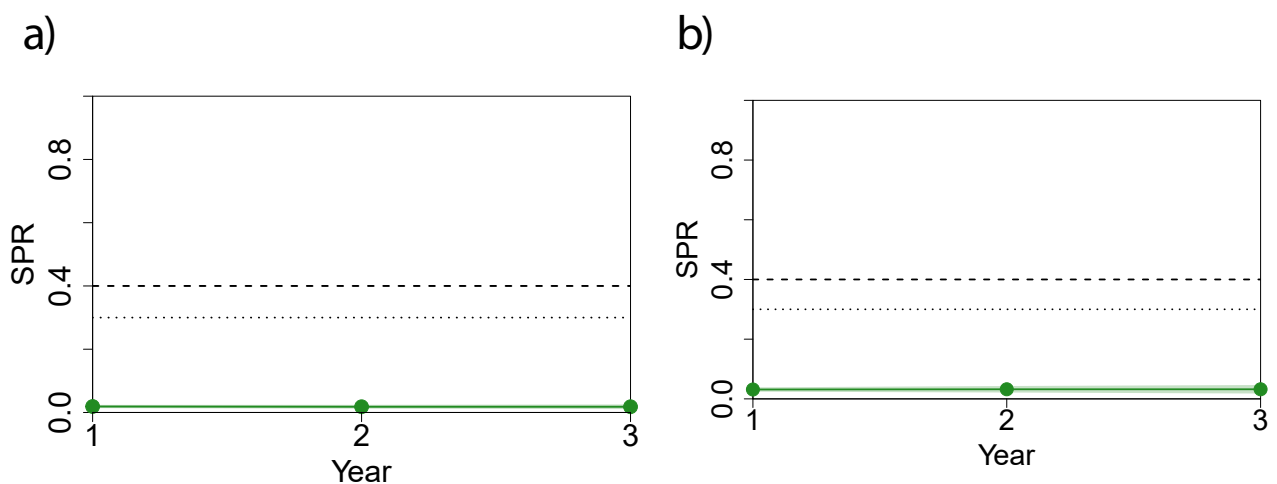


Figure 46. Graphs plotting the estimates of SPR by LIME model for hake. (a) Scenario 1 (ICatMar data), (b) Scenario 2 (DCF-GSA06 data). The uncertainty is shown by the green shade on both sides of the estimation. Data include discards.

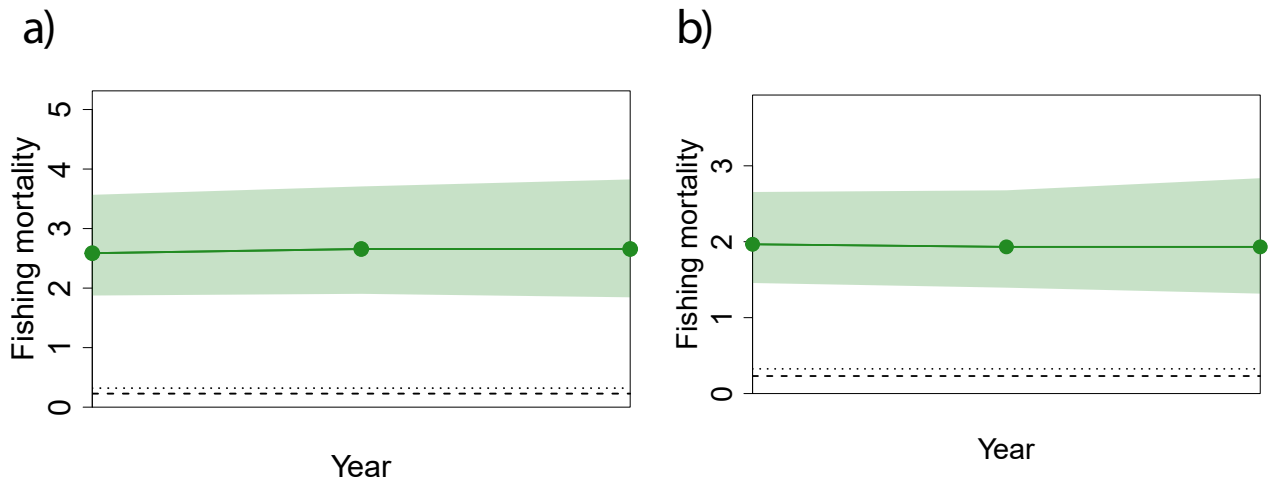


Figure 47. Estimated fishing mortality by LIME model for hake. (a) Scenario 1 (ICatMar data), (b) Scenario 2 (DCF-GSA06 data). The uncertainty is shown by the green shade on both sides of the estimation. Dotted line is the F_{msy} whereas the striped line a precautionary F value. Data include discards.

Stock assessment indicators

Table 8. Stock assessment indicators for hake. Detailed information of each parameter can be found in the Glossary. Data include discards.

Specie	Scenario	Method	Year	SPR	F/M or F/Fmsy*
HKE	ICATMAR	LBSPR	2019	0.02	4.14
HKE	ICATMAR	LBSPR	2020	0.01	6.08
HKE	ICATMAR	LBSPR	2021	0.01	6.67
HKE	ICATMAR	LBPA	2019	0.03	5.78*
HKE	ICATMAR	LBPA	2020	0.03	5.78*
HKE	ICATMAR	LBPA	2021	0.03	5.78*
HKE	ICATMAR	LIME	2019	0.02	6.47
HKE	ICATMAR	LIME	2020	0.02	6.64
HKE	ICATMAR	LIME	2021	0.02	6.64
HKE	DCF-GSA6	LBSPR	2019	0.01	5.86
HKE	DCF-GSA6	LBSPR	2020	0.01	5.47
HKE	DCF-GSA6	LBSPR	2021	0.01	6.10
HKE	DCF-GSA6	LBPA	2019	0.02	6.59*
HKE	DCF-GSA6	LBPA	2020	0.02	6.59*
HKE	DCF-GSA6	LBPA	2021	0.02	6.59*
HKE	DCF-GSA6	LIME	2019	0.03	4.92
HKE	DCF-GSA6	LIME	2020	0.03	4.83
HKE	DCF-GSA6	LIME	2021	0.03	4.83

Deep-water rose shrimp (*Parapenaeus longirostris*) DPS

The deep-water rose shrimp (*Parapenaeus longirostris*; FAO code DPS) growth parameters, length-weight relationship and maturity at L_{mat50} and L_{mat95} are shown in Table 9.

The spawning season occurs between January and November with a peak between April and September (DCF 2019), and recruitment is observed afterwards.

Catch (landings and discards)

Landings of deep-water rose shrimp show a clear upward trend (Fig. 49a). This means that landings in Catalan fishing ports have increased exponentially since 2015 until now. The deep water rose shrimp is caught by different métiers of the Catalan fishing fleet. In detail, OTB Deeper shelf and OTB Upper slope are the métiers that land the largest quantities of this species (Fig. 49b).

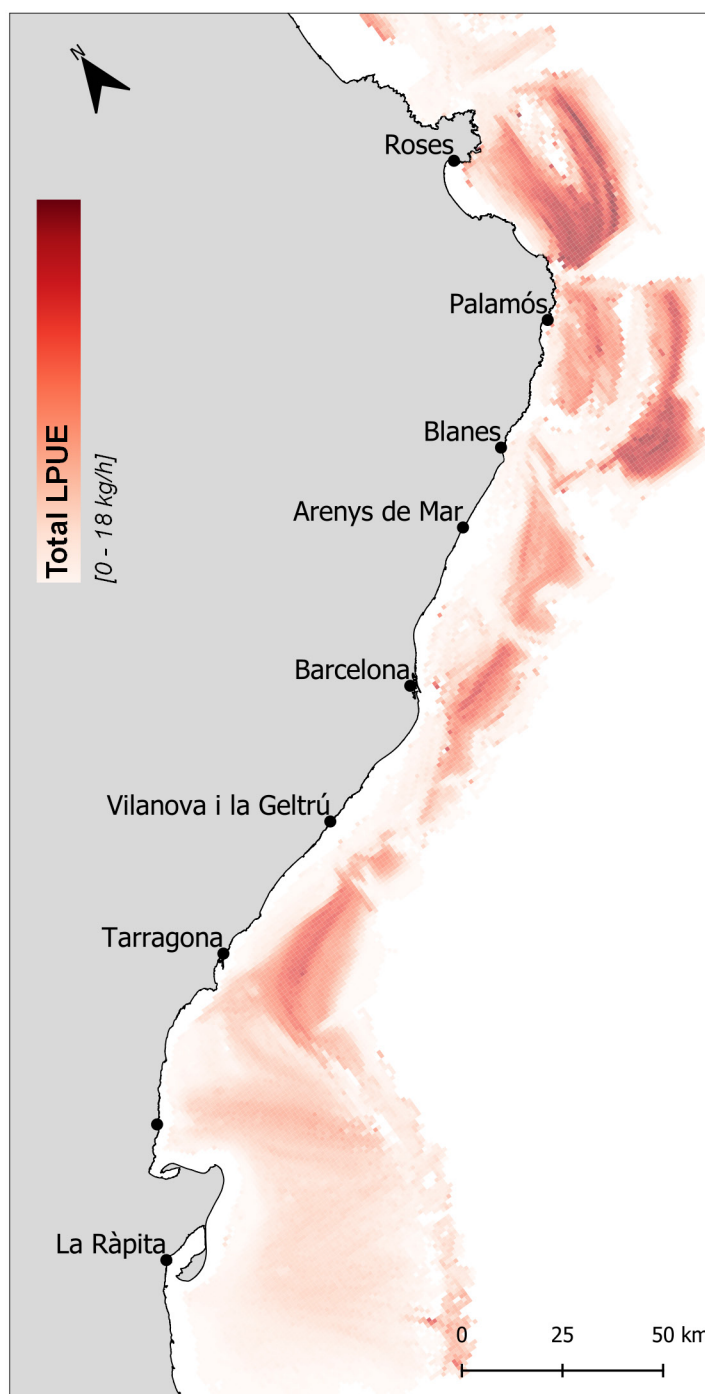


Figure 48. Spatial distribution of landings per unit effort (LPUE) for deep-water rose shrimp in the Catalan fishing grounds (N GSA6) in 2021.

Table 9. Biological parameters described for deep-water rose shrimp. Detailed information of each parameter can be found in the Glossary.

	L_{inf} (mm)	K	t_0	a	b	M	L_{mat50} (mm)	L_{mat95} (mm)
DPS	44	0.67	-0.08	0.00262	2.594	0.76	25.6	27.6
Data source	STECF EWG 22-09					Chen and Watanabe (1989)	(paper riki)	

The length frequency distributions per year and métier after raising the data without including discards in the data analyses for both scenarios, that is, using ICATMAR and DCF GSA6 data sets, are shown in Figure 50. For both scenarios 1 there are no similarities among the length structure throughout the years and there are less individuals from central length classes in 2020.

The length frequency distribution per year and métier, including discards, after raising the data for both scenarios, that is, using ICATMAR and DCF GSA6 data sets, are shown in Figure 51. In general, for both scenarios 1 and 2, there are not many differences in the length frequency distribution resulting from data with or without discards. This means that the proportion of discards for this specie is low.

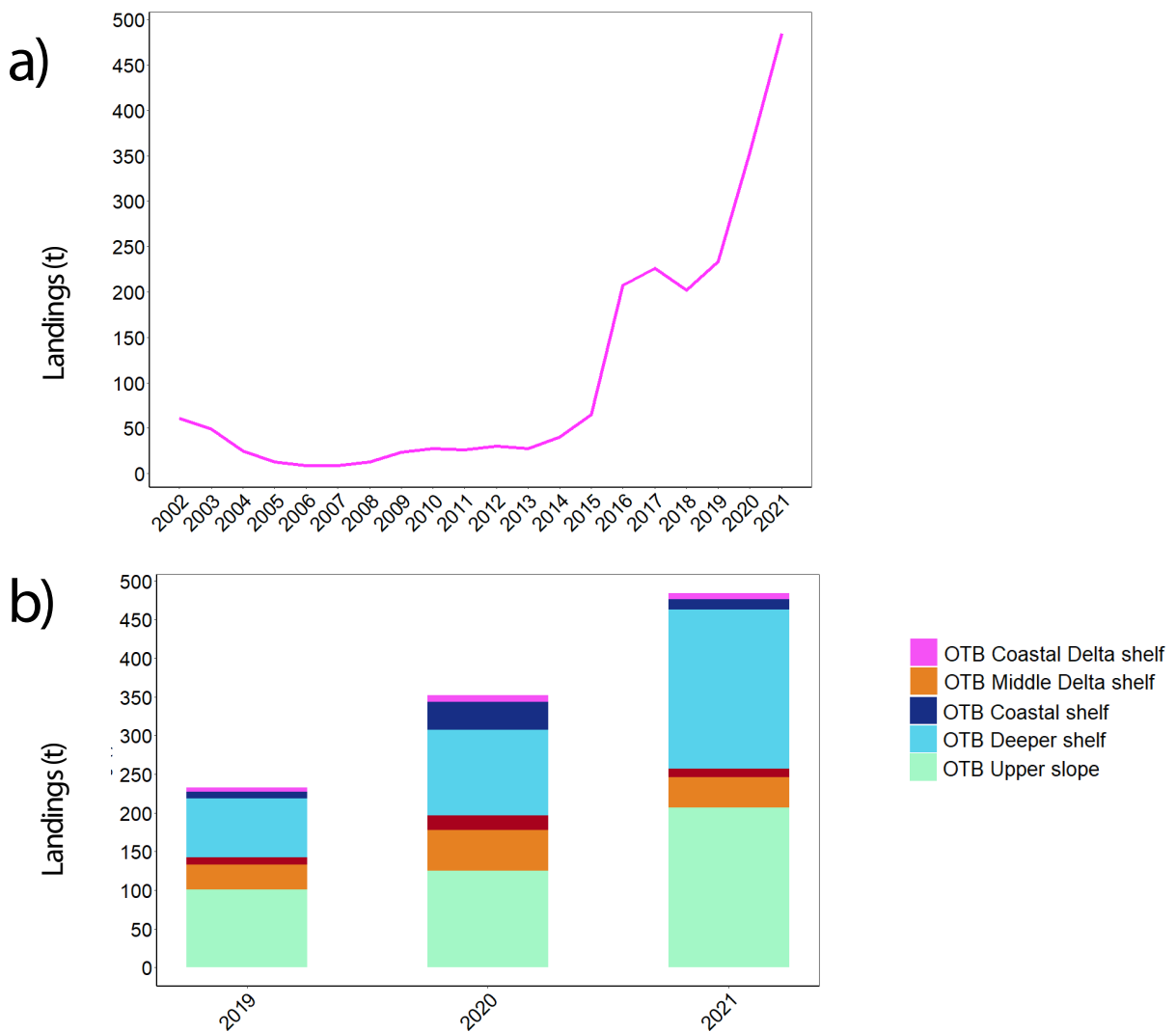


Figure 49. Characterization of deep-water rose shrimp landings. (a) Historical landings in Catalonia. (b) Landings per métier. (OTB) Bottom otter trawl.

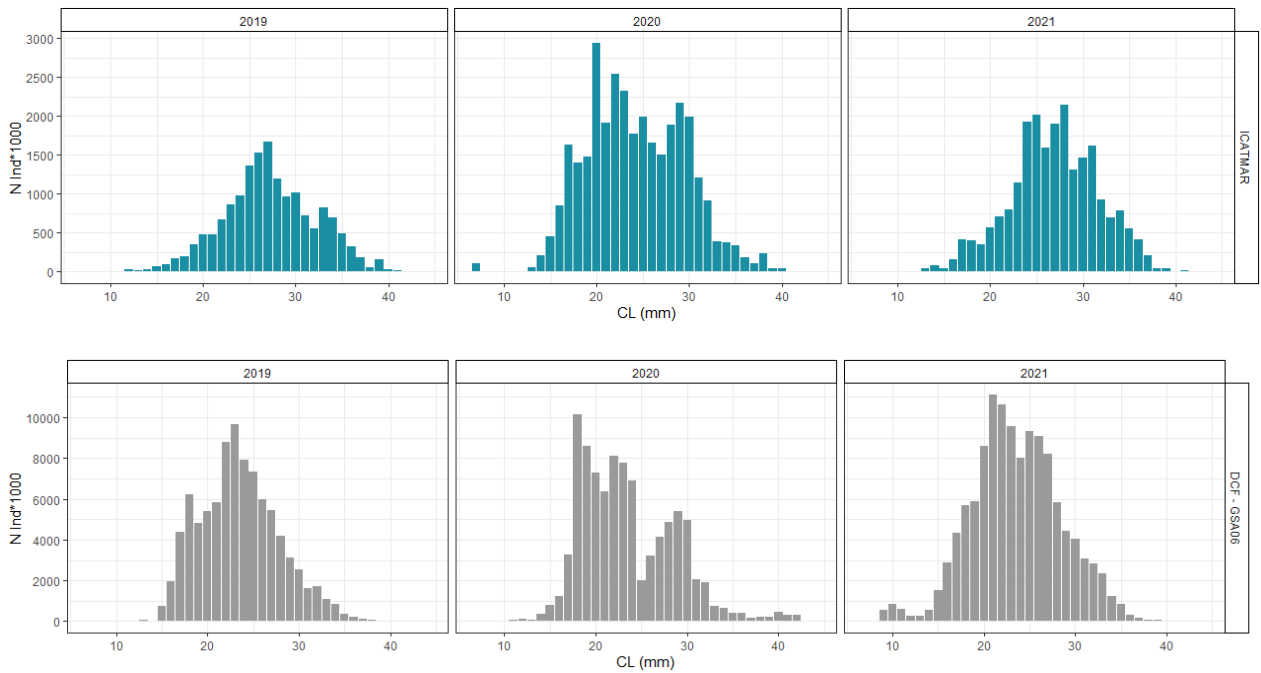


Figure 50. Annual length-frequency distributions for deep-water rose shrimp. Scenario 1 (top plots) using the ICATMAR data set and Scenario 2 (bottom plots) using DCF-GSA06 data data set. Data do not include discards.

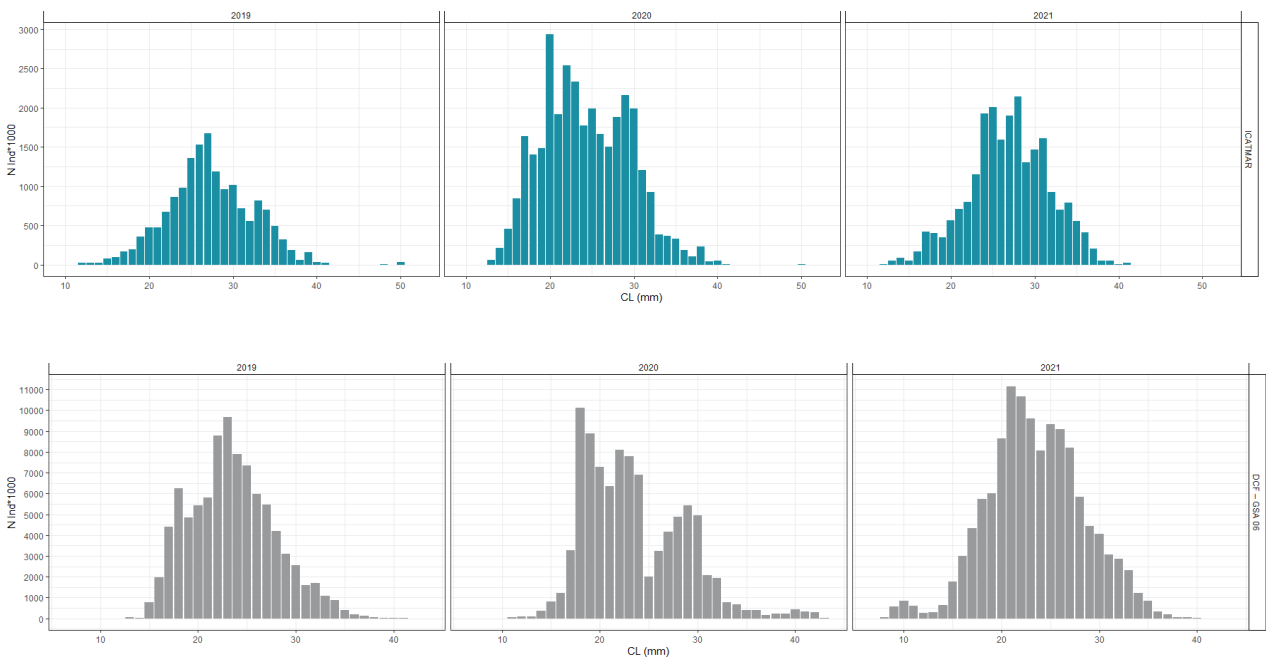


Figure 51. Annual length-frequency distributions for deep-water rose shrimp. Scenario 1 (top plots) using the ICATMAR data set and Scenario 2 (bottom plots) using DCF-GSA06 data data set. Data include discards.

Stock assessment by model (without discards)

LBSPR

Fitted data

The length frequency distribution fitted per year after raising the data for both scenarios, that is, using ICATMAR and DCF GSA6 data sets, are shown in Figure 52. In scenario 1, the best fit is for 2019 due to a more homogeneous size frequency. In 2020 the length frequency adjustment

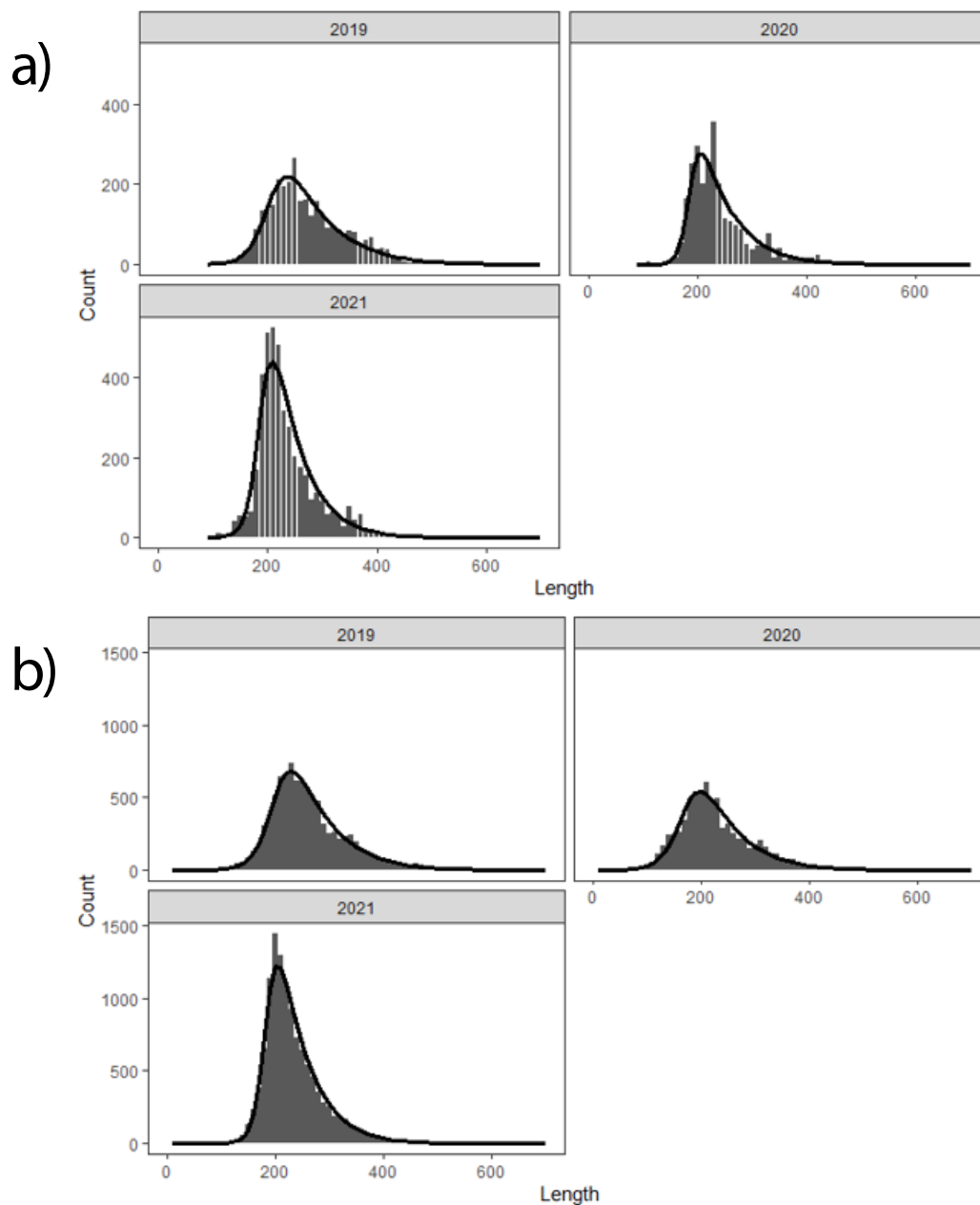


Figure 52. Fitting data by LBSPR by model for deep-water rose shrimp. (a) Scenario 1 (ICatMar data), (b) Scenario 2 (DCF-GSA06 data). Data do not include discards.

is the worst, especially for the central and larger size classes. In scenario 2, 2019 and 2021 have a better fit for in 2020 there are different length classes underestimated and overestimated.

Maturity vs. Selectivity (absolute and range of values)

The selectivity calculated by the model can be seen in Figure 53. In scenario 1, the calculated selectivity changes yearly. In detail, in 2019 it is on L_{mat50} , in 2020 reaches levels well below L_{mat50} but in 2021, selectivity is on L_{mat95} . In scenario 2, the calculated selectivity is always below L_{mat50} with 2020 being the year that is furthest away from all.

Precautionary advice based on SPR

The calculated SPR values are shown in Figure 54. Both scenarios have a similar trend through time. All years show a small number of drawings above the B_{tgt} . Most of them are below B_{lim} .

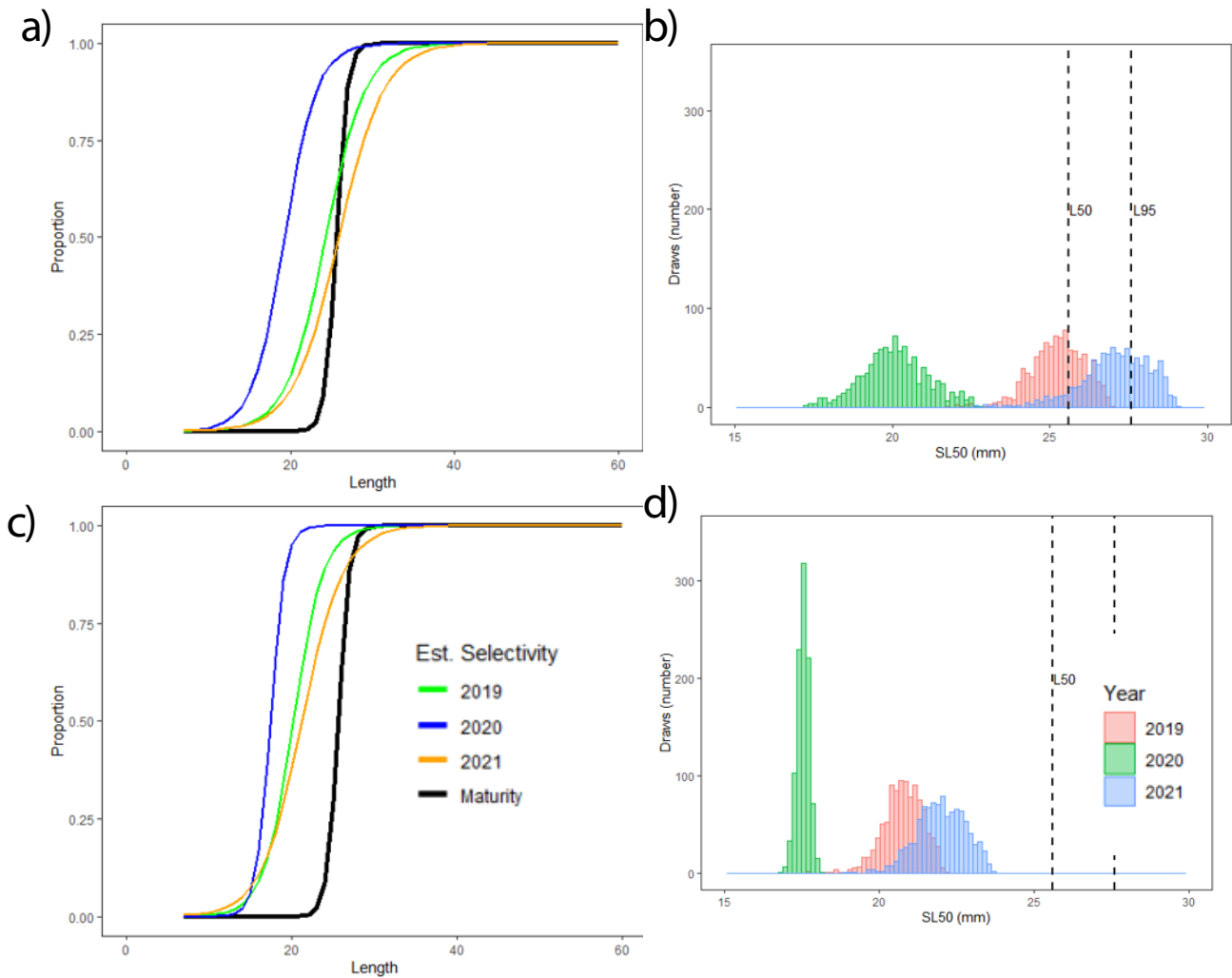


Figure 53. Left graphs plot the maturity-at-length curve and the estimated selectivity-at-length curve for each year by LBSPR for deep-water rose shrimp. Right graphs plot the SL50 values for each year; the bell shape is given by the number of draws estimated by the model. (a, b) Scenario 1 (ICatMar data), (c, d) Scenario 2 (DCF-GSA06 data). Data do not include discards.

Relative fishing mortality

F/M ratio values are shown in Figure 55. Both scenarios are very similar with a small proportion of the F/M ratio below 1 for years 2020 and 2021. There is no trend among years. In scenario 1, the range of values for the F/M ratio are very wide (0 to 20). However, in scenario 2, the values between years of the F/M ratio are more similar, ranging from 0 to 15.

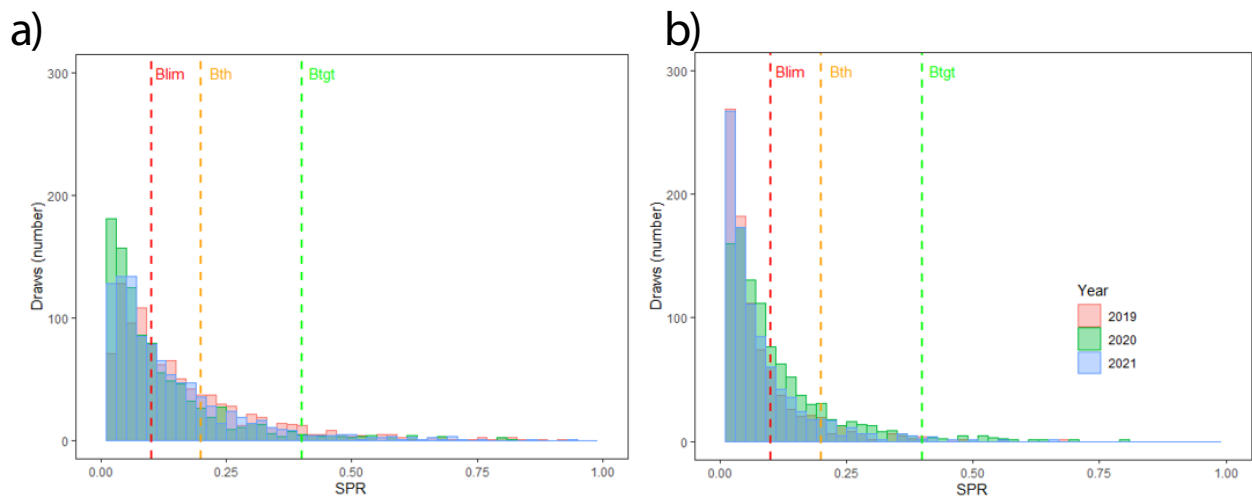


Figure 54. Estimated SPR values for deep-water rose shrimp. (a) Scenario 1 (ICatMar data), (b) Scenario 2 (DCF-GSA06 data). Data do not include discards.

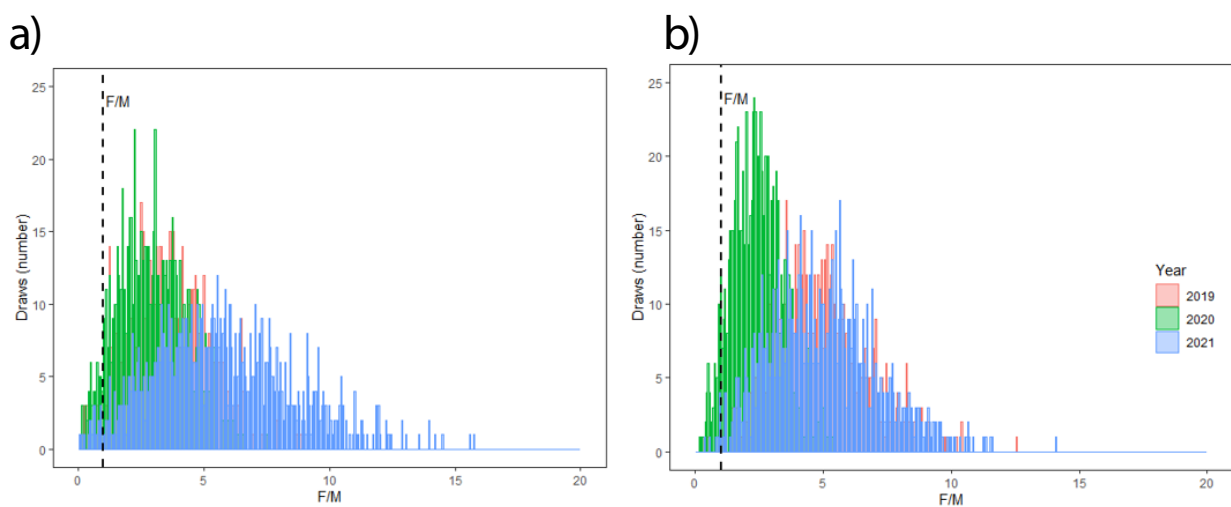


Figure 55. Estimated F/M values for deep-water rose shrimp. (a) Scenario 1 (ICatMar data), (b) Scenario 2 (DCF-GSA06 data). Data do not include discards.

LBPA

Fitted data

The length frequency distributions fitted per year after raising the data for both scenarios, that is, using ICATMAR and DCF GSA6 data sets, are shown in Figure 56. On both scenarios, sizes below the black line are underestimated and above the black line are overestimated. In scenario 1, the model underestimates small and large length classes and overestimates central length classes. In scenario 2, the model fits worse and overestimates the central length classes.

Maturity vs. Selectivity

Maturity and Selectivity curves for the deep-water rose shrimp are represented in Figure 57. In scenario 1, selectivity is below L_{mat50} but very close to it ($SL_{50}=23.4$ mm). In scenario 2, selectivity is further away from L_{mat50} ($SL_{50}=21.7$ mm).

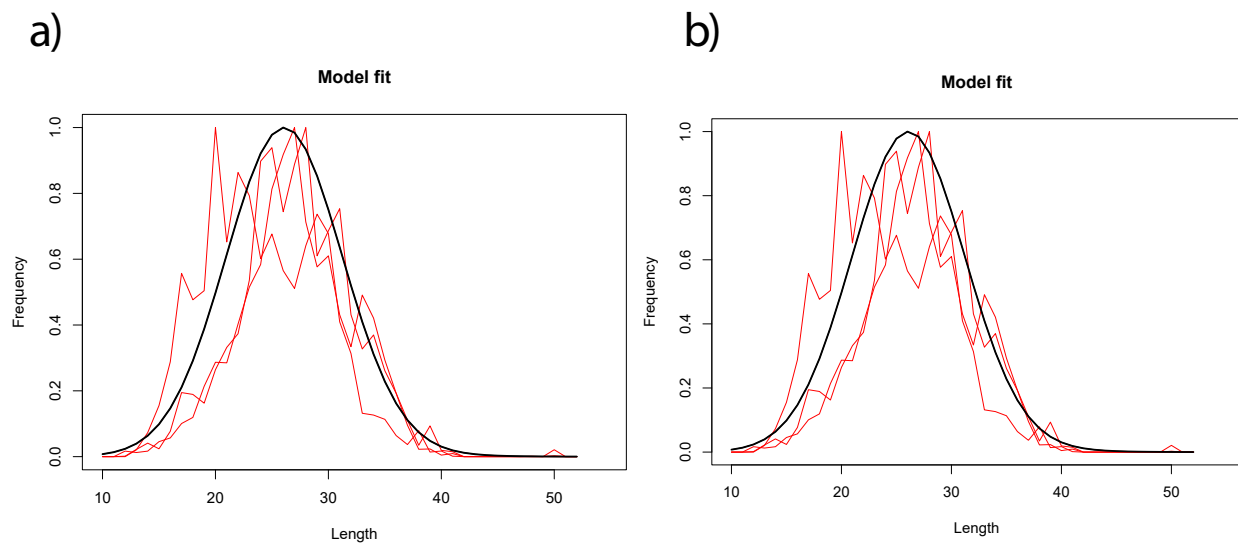


Figure 56. Fitting data by LBPR model for deep-water rose shrimp. (a) Scenario 1 (ICatMar data), (b) Scenario 2 (DCF-GSA06 data). Data do not include discards. Red lines represent the length frequency for the 3 studied years; the black line is the length frequency distribution estimated for the model.

SPR and Fishing mortality estimations

SPR and F estimations are shown in Figure 58. In scenario 1, the SPR values are below the SPR_{tgt} (0.4) but the uncertainty range is high. In turn, F is above the F_{tar} and its values range between 1 and 7.5, with high uncertainty. In scenario 2, SPR estimation is similar to scenario 1 but with less uncertainty. For fishing mortality, the model also shows high uncertainty values, with F ranging from 1 to 5.

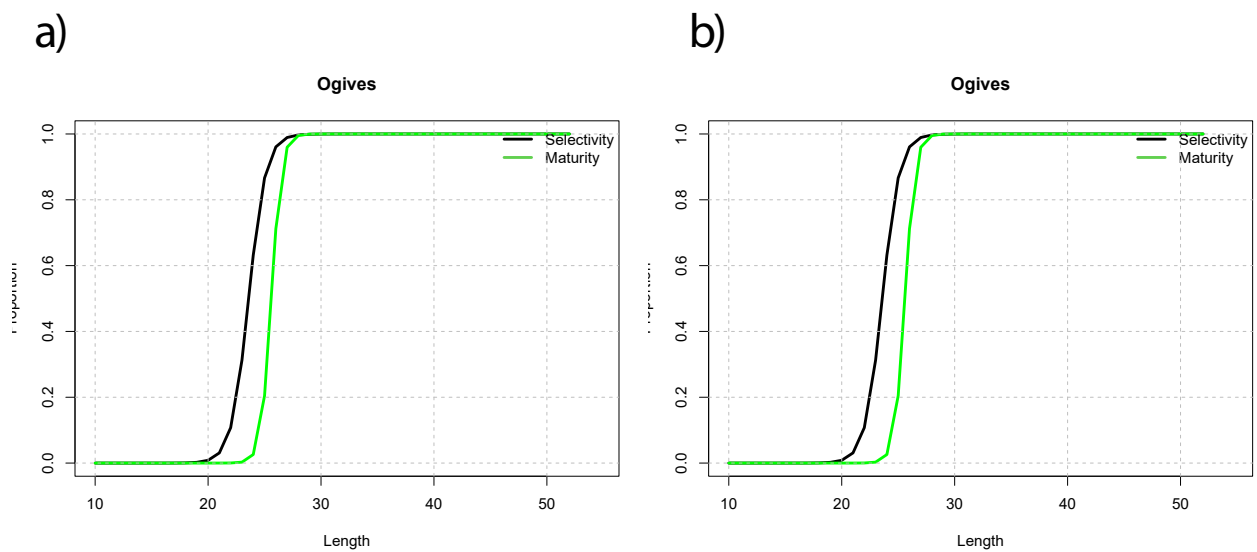


Figure 57. Graphs plotting the maturity-at-length curve and the estimated selectivity-at-length curve for each year by LBPR model for deep-water rose shrimp. (a) Scenario 1 (ICatMar data), (b) Scenario 2 (DCF-GSA06 data). Data do not include discards.

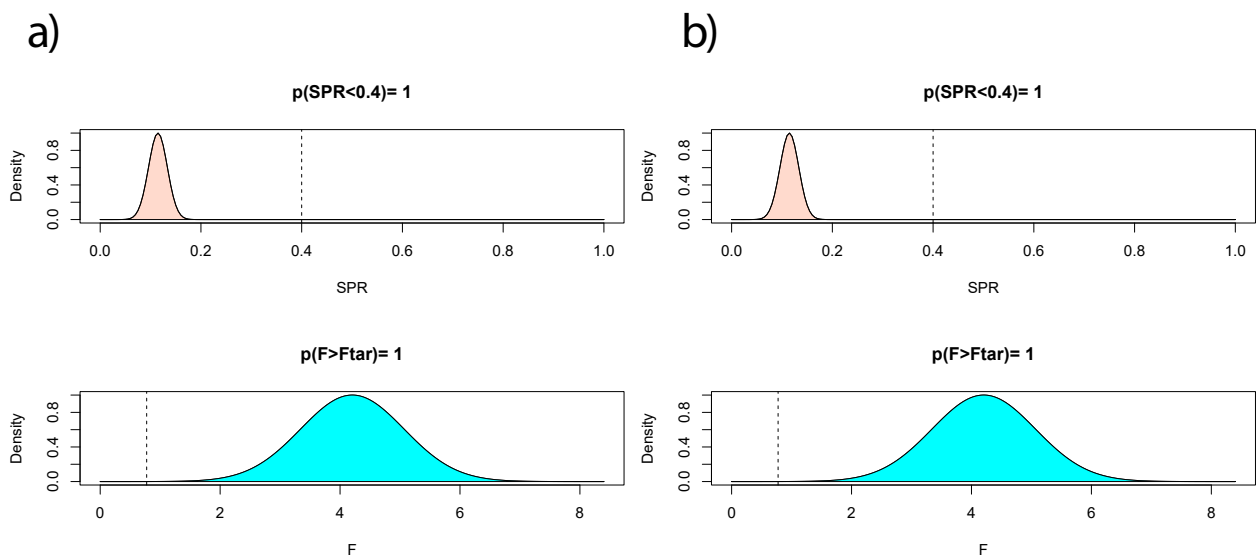


Figure 58. Graphs plotting the estimates of SPR and F by LBPR model for deep-water rose shrimp. (a) Scenario 1 (ICatMar data), (b) Scenario 2 (DCF-GSA06 data). Data do not include discards.

Stock assessment indicators

Table 10. Stock assessment indicators for deep-water rose shrimp. Detailed information of each parameter can be found in the Glossary. Data do not include discards.

Specie	Scenario	Method	Year	SPR	F/M or F/Fmsy*
DPS	ICATMAR	LBSPR	2019	0.16	3.64
DPS	ICATMAR	LBSPR	2020	0.12	3.04
DPS	ICATMAR	LBSPR	2021	0.14	5.68
DPS	ICATMAR	LBPA	2019	0.07	8.19*
DPS	ICATMAR	LBPA	2020	0.07	8.19*
DPS	ICATMAR	LBPA	2021	0.07	8.19*
DPS	DCF-GSA6	LBSPR	2019	0.07	4.63
DPS	DCF-GSA6	LBSPR	2020	0.11	2.48
DPS	DCF-GSA6	LBSPR	2021	0.07	4.96
DPS	DCF-GSA6	LBPA	2019	0.11	4.49*
DPS	DCF-GSA6	LBPA	2020	0.11	4.49*
DPS	DCF-GSA6	LBPA	2021	0.11	4.49*

Stock assessment by model (with discards)

LBSPR

Fitted data

The length frequency distribution fitted per year, including discards, after raising the data for both scenarios, that is, using ICATMAR and DCF GSA6 data sets, are shown in Figure 59. In scenario 1, the best fit is for year 2019, due to a more homogeneous size frequency, whereas the worst adjustment is in 2020. Central length classes are overestimated in 2020 and 2021. In sce-

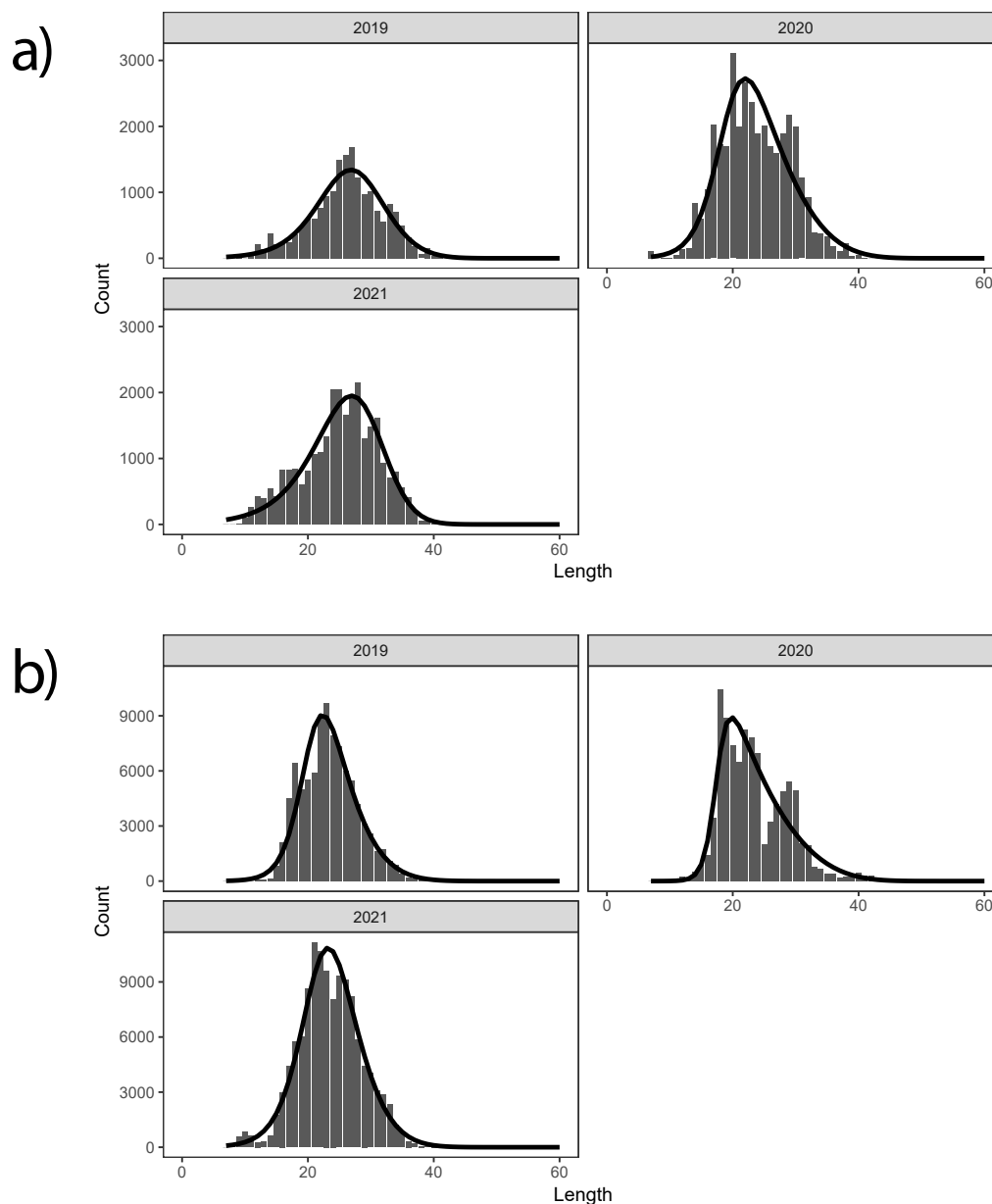


Figure 59. Fitting data by LBSPR model for deep-water rose shrimp. (a) Scenario 1 (ICatMar data), (b) Scenario 2 (DCF-GSA06 data). Data include discards.

nario 2, the best adjustment is in 2021, whereas the worst adjustment is in 2020, as in scenario 1.

Maturity vs. Selectivity (absolute and range of values)

The selectivity calculated by the model can be seen in Figure 60. In scenario 1, the calculated selectivity varies each year. In detail, it is on the L_{mat50} in 2019, it is below the L_{mat50} in 2020, and it is over L_{mat95} in 2021. Differently, in scenario 2, the calculated selectivity is below the L_{mat50} in the three years assessed.

Precautionary advice based on SPR

The calculated SPR values are shown in Figure 61. Both scenarios show a similar trend among years. All years show a small number of drawings above the B_{tgt} . Most of them are below B_{lim} .

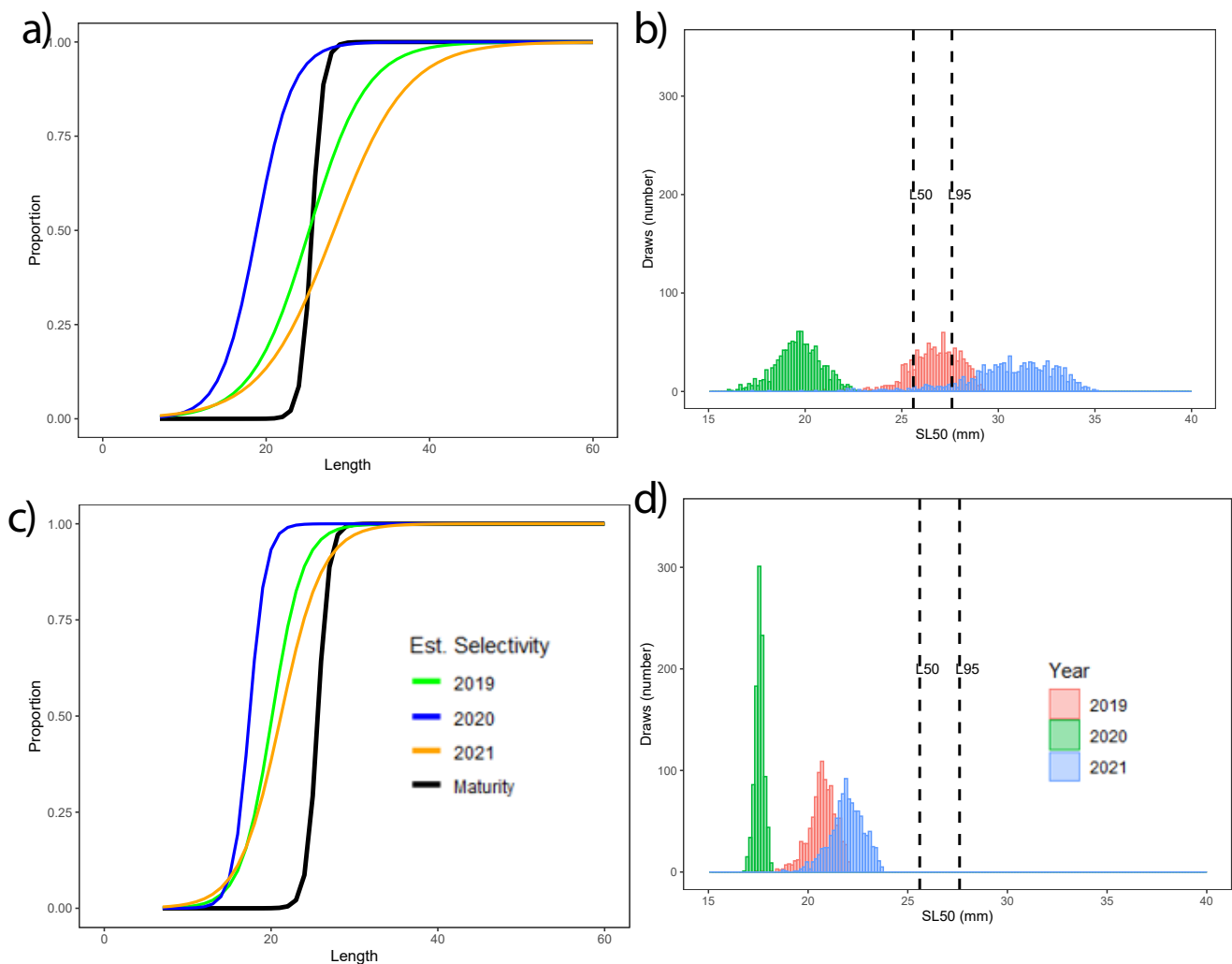


Figure 60. Left graphs plot the maturity-at-length curve and the estimated selectivity-at-length curve for each year by LBSPR for deep-water rose shrimp. Right graphs plot the SL50 values for each year; the bell shape is given by the number of draws estimated by the model. (a, b) Scenario 1 (lCatMar data), (c,d) Scenario 2 (DCF-GSA06 data). Data include discards.

Relative fishing mortality

F/M ratio values are shown in Figure 62. For both scenarios, a few proportion of the F/M ratio is under 1 in years 2020 and 2021, with no trend through time. In scenario 1, the range of values for the F/M ratio are very wide (0 to 35). In scenario 2, the values between years are more similar, ranging between 0 and 15.

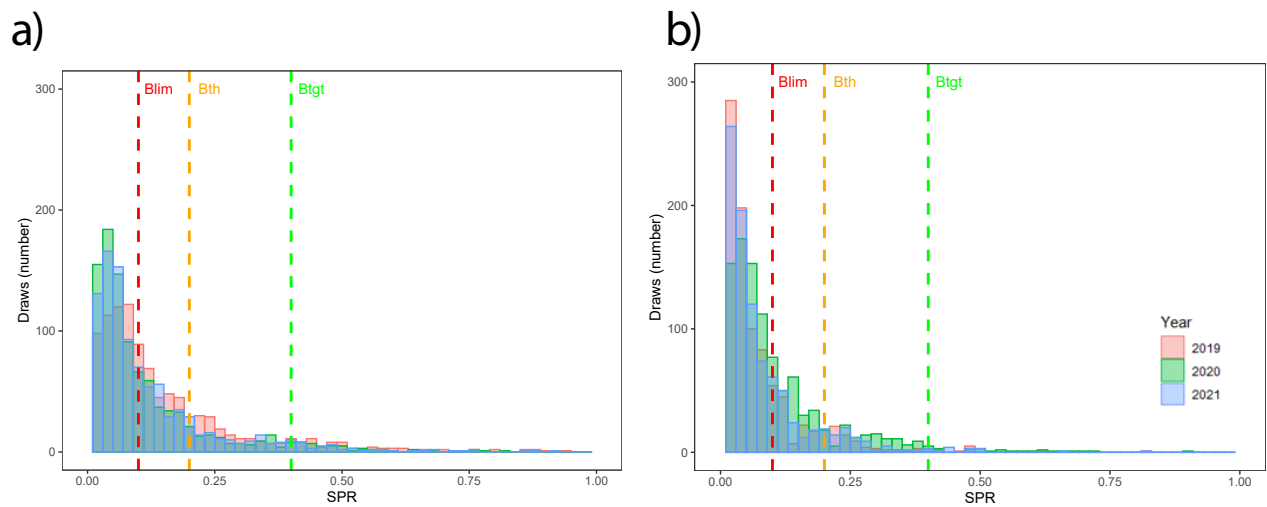


Figure 61. Estimated SPR values for deep-water rose shrimp. (a) Scenario 1 (ICatMar data), (b) Scenario 2 (DCF-GSA06 data). Data include discards.

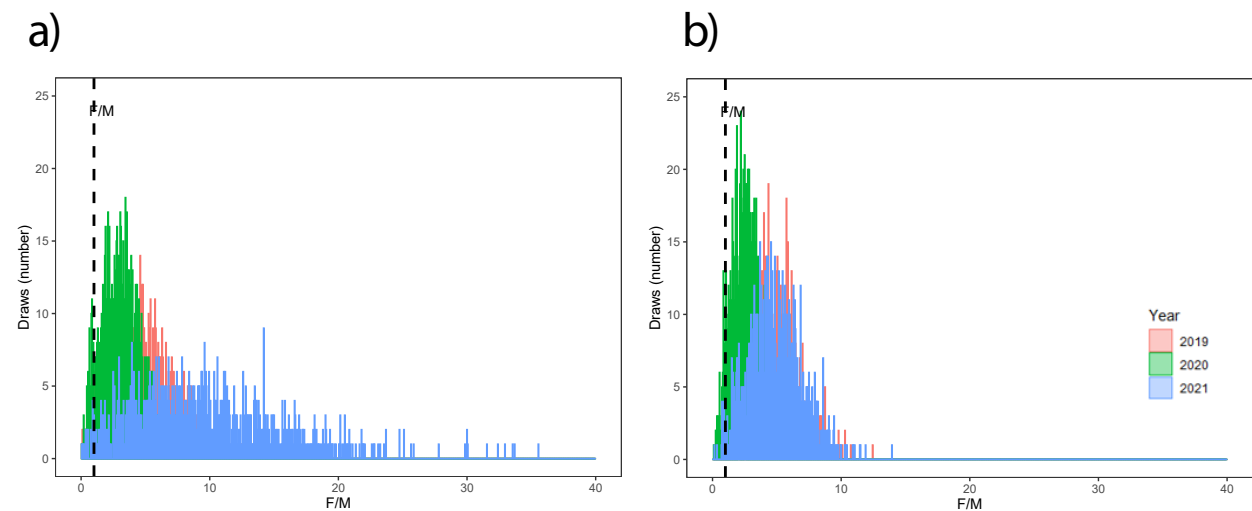


Figure 62. Estimated F/M values for deep-water rose shrimp. (a) Scenario 1 (ICatMar data), (b) Scenario 2 (DCF-GSA06 data). Data include discards.

LBPA

Fitted data

The length frequency distribution fitted per year, including discards, after raising the data for both scenarios, that is, using ICATMAR and DCF GSA6 data sets, are shown in Figure 63. On both scenarios, sizes below the black line are underestimated and above the black line are overestimated. For scenario 1, the model underestimates small and large length classes and overestimates central length classes. For scenario 2, the model fits worse and overestimates the central length classes.

Maturity vs. Selectivity

Maturity and Selectivity curves for the deep water rose shrimp are represented in Figure 64. In scenario 1, selectivity is just below L_{mat50} ($SL_{50} = 23.6$ mm). However, in scenarios 2, selectivity is further away from L_{mat50} ($SL_{50} = 21.8$ mm).

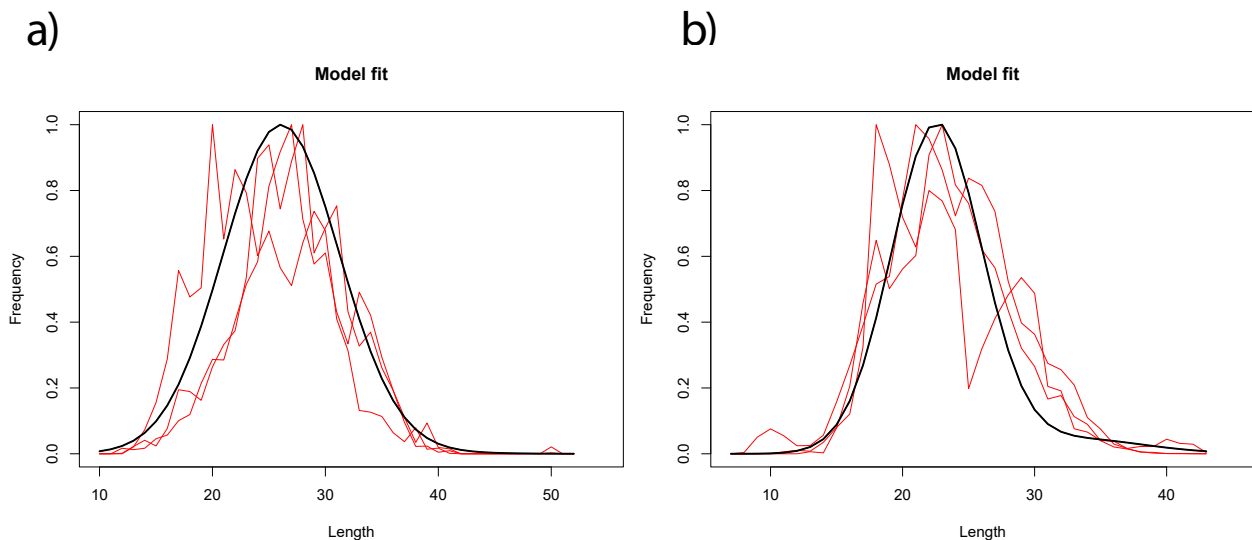


Figure 63. Fitting data by LBPR model for deep-water rose shrimp. (a) Scenario 1 (ICatMar data), (b) Scenario 2 (DCF-GSA06 data). Data include discards. Red lines represent the length frequency for the 3 studied years; the black line is the length frequency distribution estimated for the model.

SPR and Fishing mortality estimations

SPR and F estimations are shown in Figure 65. In both scenarios, there is overexploitation and overfishing. The SPR values are below the SPR_{tgt} (0.4) but the uncertainty range is high. For fishing mortality, the model shows very high uncertainty values, with F ranging from 2 to 6.

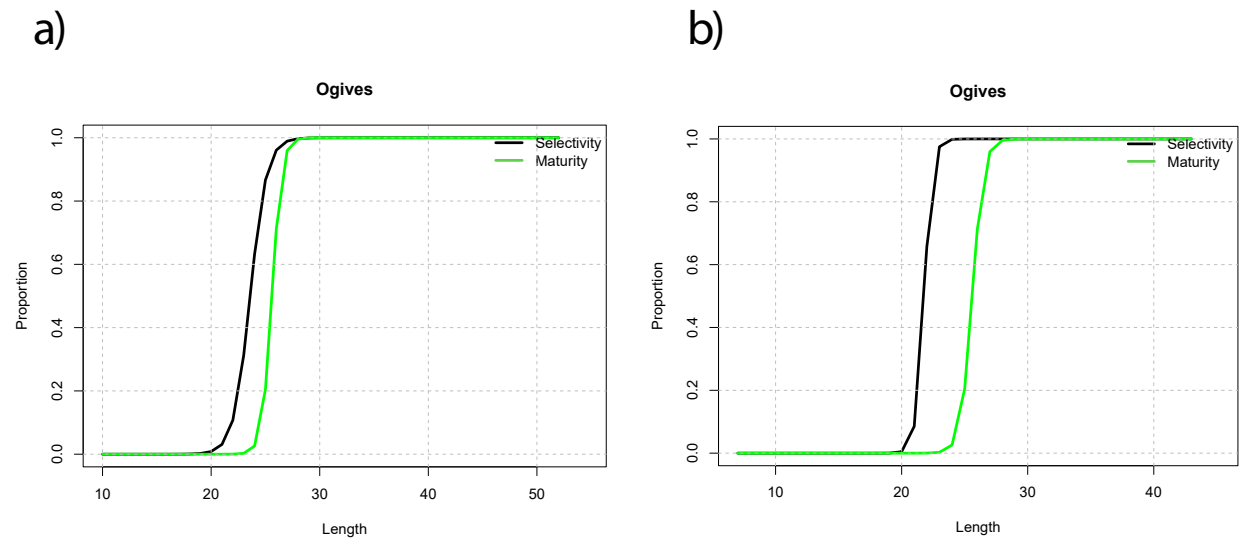


Figure 64. Graphs plotting the maturity-at-length curve and the estimated selectivity-at-length curve for each year by LBPR model for deep-water rose shrimp. (a) Scenario 1 (ICatMar data), (b) Scenario 2 (DCF-GSA06 data). Data include discards.

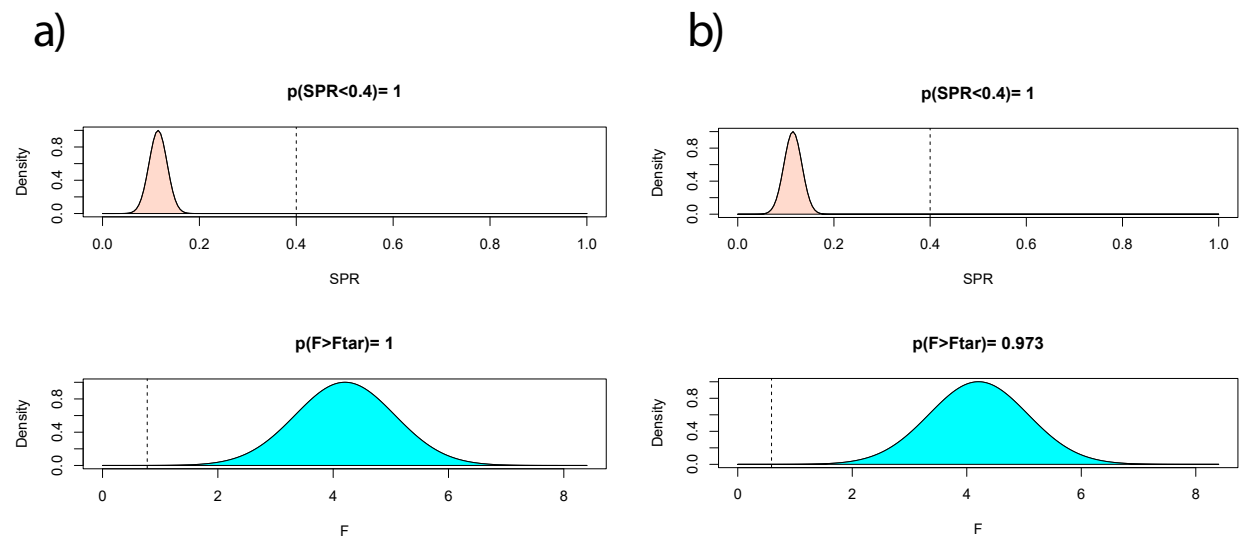


Figure 65. Graphs plotting the estimates of SPR and F by LBPR model for deep-water rose shrimp. (a) Scenario 1 (ICatMar data), (b) Scenario 2 (DCF-GSA06 data). Data include discards.

Stock assessment indicators

Table 11. Stock assessment indicators for deep-water rose shrimp. Detailed information of each parameter can be found in the Glossary. Data include discards.

Specie	Scenario	Method	Year	SPR	F/M or F/Fmsy*
DPS	ICATMAR	LBSPR	2019	0.15	4.61
DPS	ICATMAR	LBSPR	2020	0.11	3.07
DPS	ICATMAR	LBSPR	2021	0.12	9.62
DPS	ICATMAR	LBPA	2019	0.11	5.43*
DPS	ICATMAR	LBPA	2020	0.11	5.43*
DPS	ICATMAR	LBPA	2021	0.11	5.43*
DPS	DCF-GSA6	LBSPR	2019	0.07	4.59
DPS	DCF-GSA6	LBSPR	2020	0.11	2.51
DPS	DCF-GSA6	LBSPR	2021	0.08	4.89
DPS	DCF-GSA6	LBPA	2019	0.10	3.81*
DPS	DCF-GSA6	LBPA	2020	0.10	3.81*
DPS	DCF-GSA6	LBPA	2021	0.10	3.81*

Norway lobster (*Nephrops norvegicus*) NEP

The Norway lobster (*Nephrops norvegicus*; FAO code NEP) growth parameters, length-weight relationship and maturity at L_{mat50} and L_{mat95} are shown in Table 12. These data are used as inputs for the models used. Note that the inputs are the same for males and females (the parameters are not separated by sex).

The Norway lobster is known to have a dimorphic growth pattern, with males growing slower and reaching larger sizes than females. Reproduction occurs between April and September and recruitment is observed afterwards, in the seasons of autumn and winter.

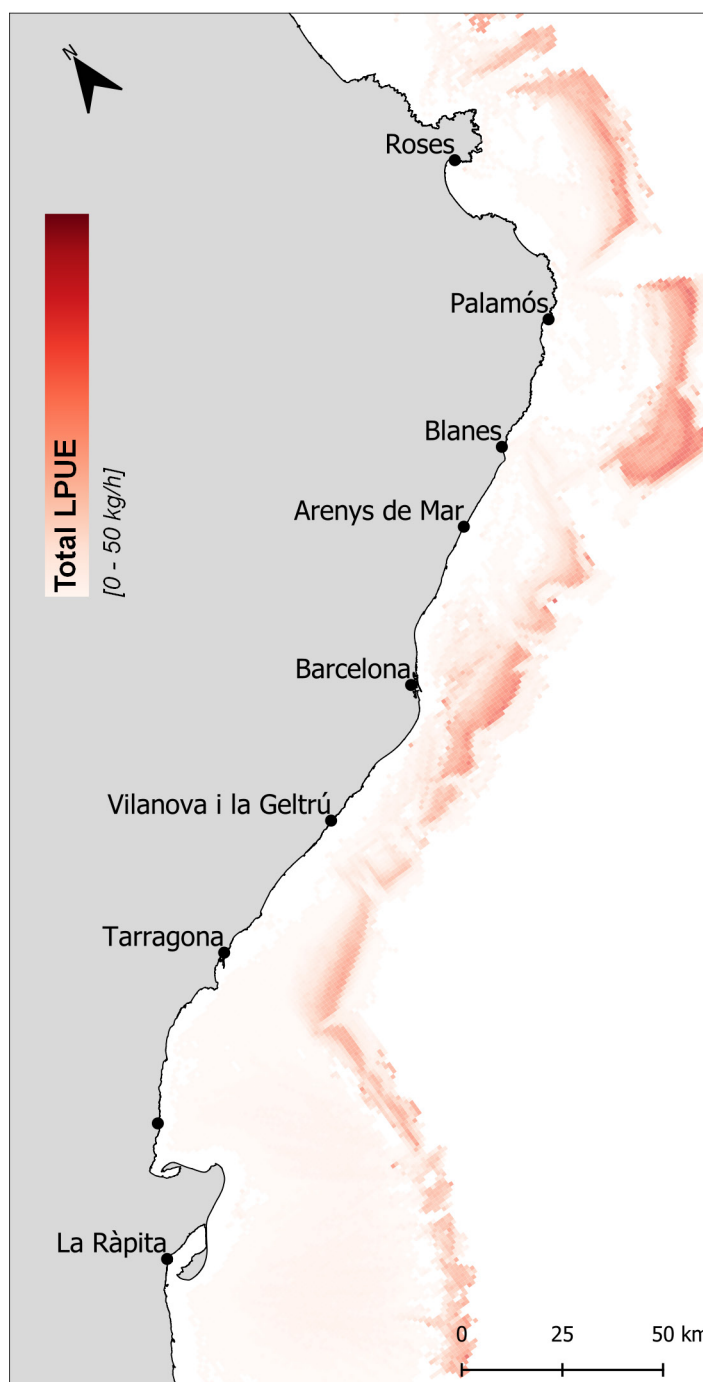


Figure 66. Spatial distribution of landings per unit effort (LPUE) for Norway lobster in the Catalan fishing grounds (N GSA6) in 2021.

Table 12. Biological parameters described for Norway lobster. Detailed information of each parameter can be found in the Glossary.

	L_{inf} (mm)	K	t_0	a	b	M	L_{mat50} (mm)	L_{mat95} (mm)
NEP	86.1	0.126	0	0.00048	3.25	0.5	32.5	36
Data source	DCF 2013-15		DCF 2017		Chen and Watanabe (1989)		GFCM RY2020	

Catch (landings and discards)

The catches of Norway lobster are produced exclusively by otter bottom trawl (OTB) at depths generally between 300 and 600 m. Discards of Norway lobster are negligible thus not included in the prediction models.

Historical data on Norway lobster landings show that they slightly increased until 2009. From then onwards, catches show a clear downward trend. Therefore, landings in Catalan fishing ports have decreased from almost 400 t to just over 100 t at present.

The total landings by *métier* and fishing gear are shown in Figure 67, confirming that OTB Upper slope is the *métier* that catches most Norway lobster.

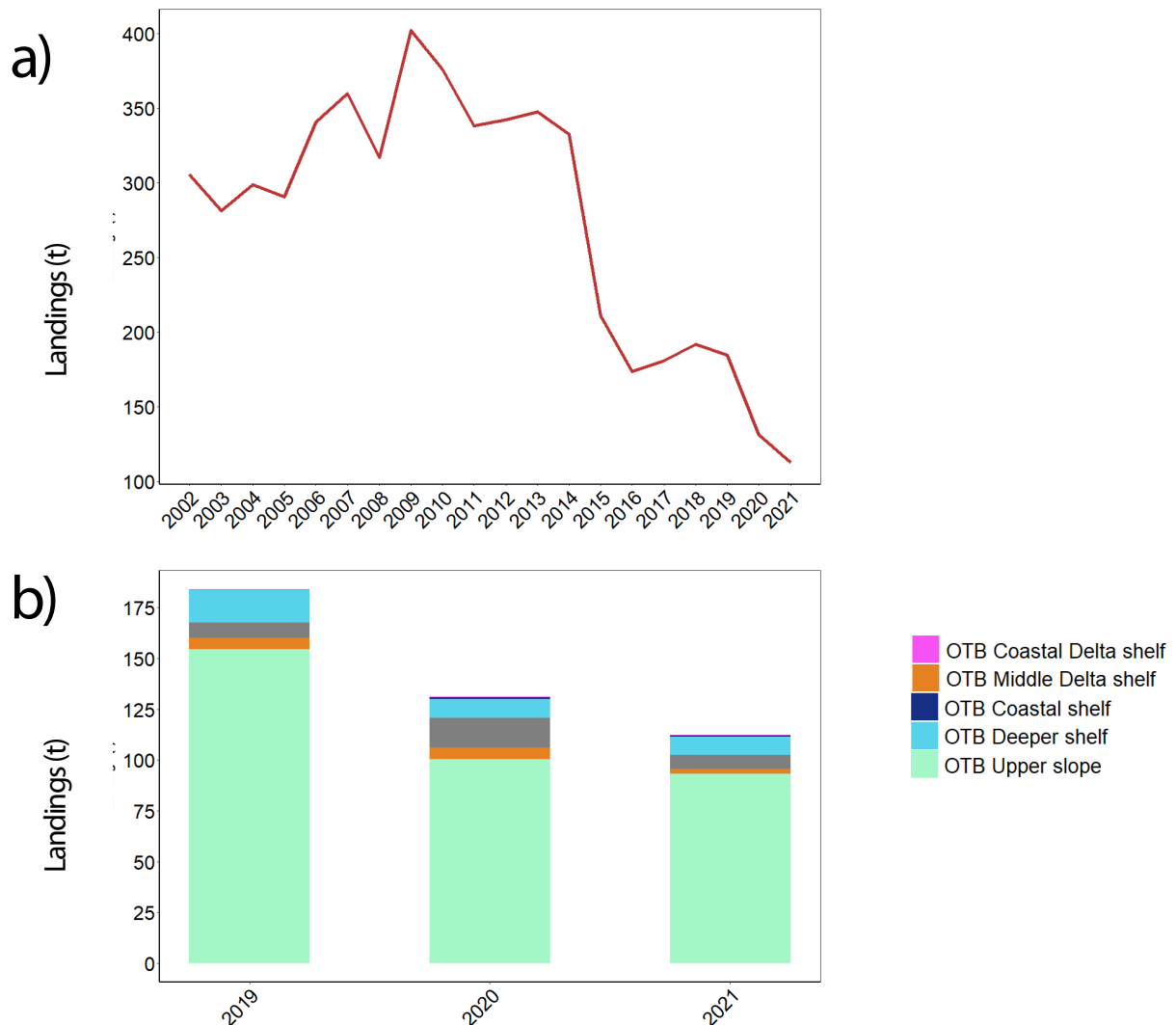


Figure 67. Characterization of Norway lobster landings. (a) Historical landings Catalan fishing grounds (N GSA6). (b) Landings per métier. (OTB) Bottom otter trawl.

The length frequency distribution per year and *métier* after raising the data for both scenarios, that is, using ICATMAR and DCF GSA6 data sets, are shown in Figure 68. For the first scenario (ICATMAR), there is a similar length structure among years, but with a decrease in the total numbers. For the second scenario (DCF GSA 6) there is no similarity among the length structure throughout the years, with less individuals in years 2020 and 2021 than in 2019.

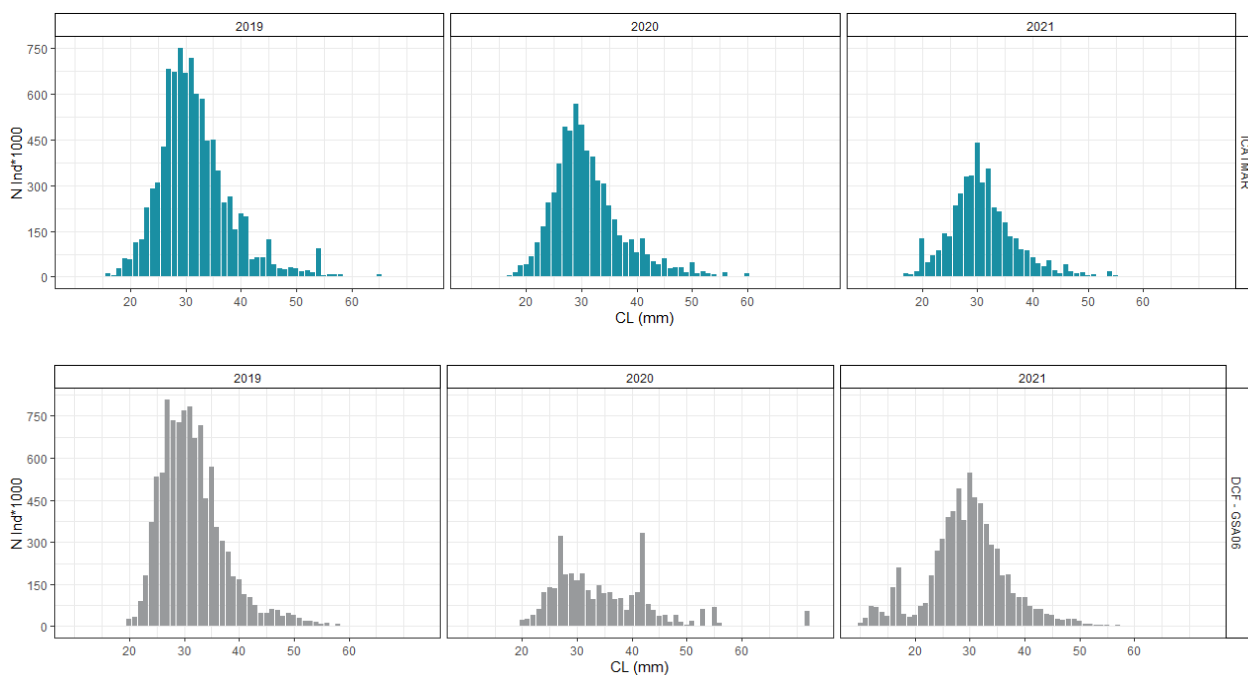


Figure 68. Annual length-frequency distributions for Norway lobster. Scenario 1 (top plots) using the ICATMAR data set and Scenario 2 (bottom plots) using DCF-GSA06 data data set. The data do not include discards.

Stock assessment by model

LBSPR

Fitted data

The fitting of the data varies with both studied scenarios (Fig. 69). For scenario 1, in general, there is a better fit with only a few length classes being over or subestimated by de model. In scenario 2, the model does not fit well data and over and subestimated length classes for all years.

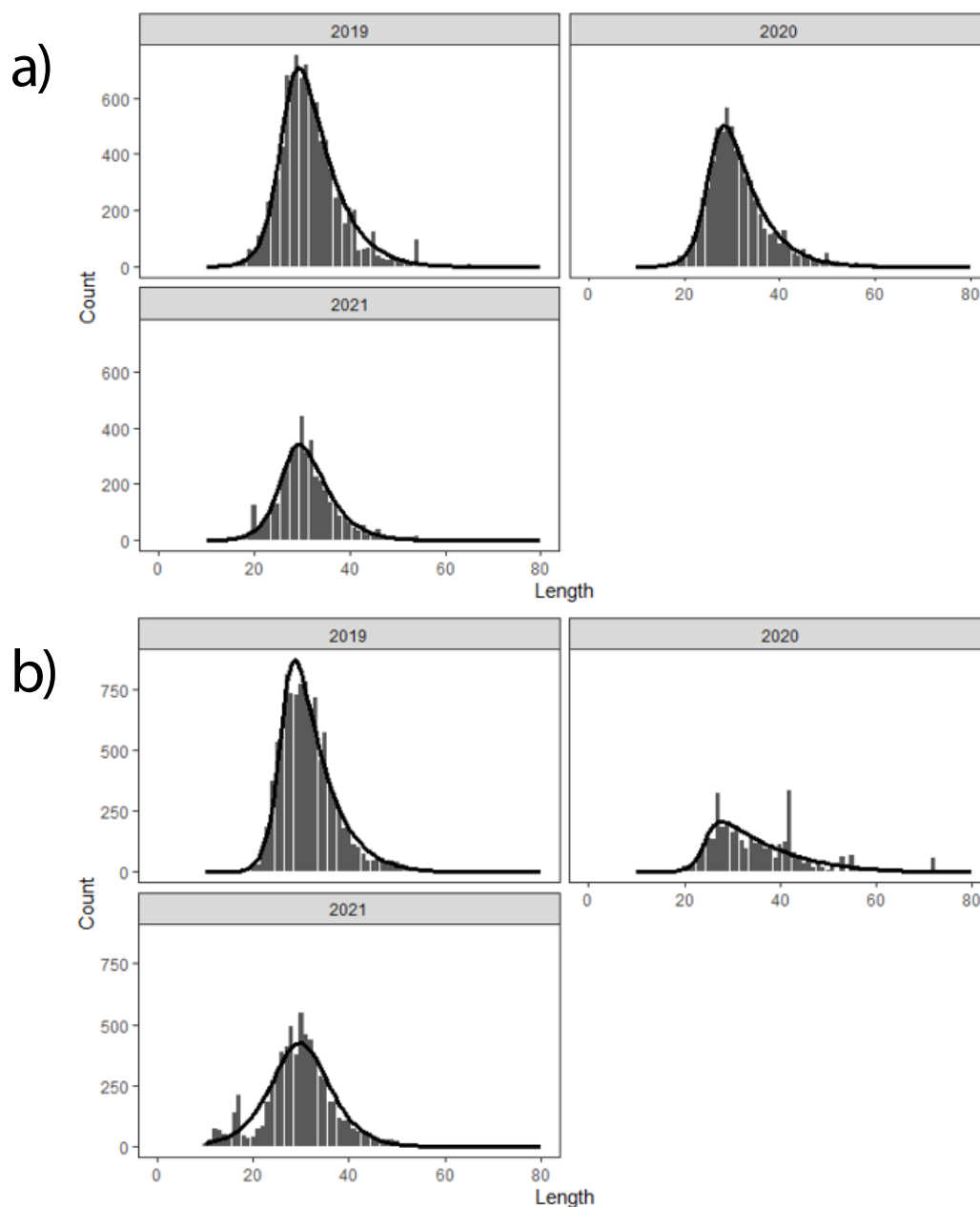


Figure 69. Fitting data by LBSPR model for Norway lobster. (a) Scenario 1 (ICatMar data), (b) Scenario 2 (DCF-GSA06 data). Data do not include discards.

Maturity vs. selectivity (absolute and range of values)

The selectivity estimated by the model, for both scenarios, indicates that the fishery catches individuals smaller than the L_{mat50} (Fig. 70). In detail, for scenario 1, the model estimates a similar selectivity among years. Scenario 2 is slightly different because the model estimates a different selectivity in 2021, due to the present of small individuals in the LFD.

Precautionary advice based on SPR

For scenario 1, most of the SPR values estimated by the model remain below B_{lim} for all years (Fig. 71). Due to the variability in the length structure for scenario 2, values of SPR for 2020 are different and reach values higher than 0.4 because of the presence of large individuals (Fig. 71).

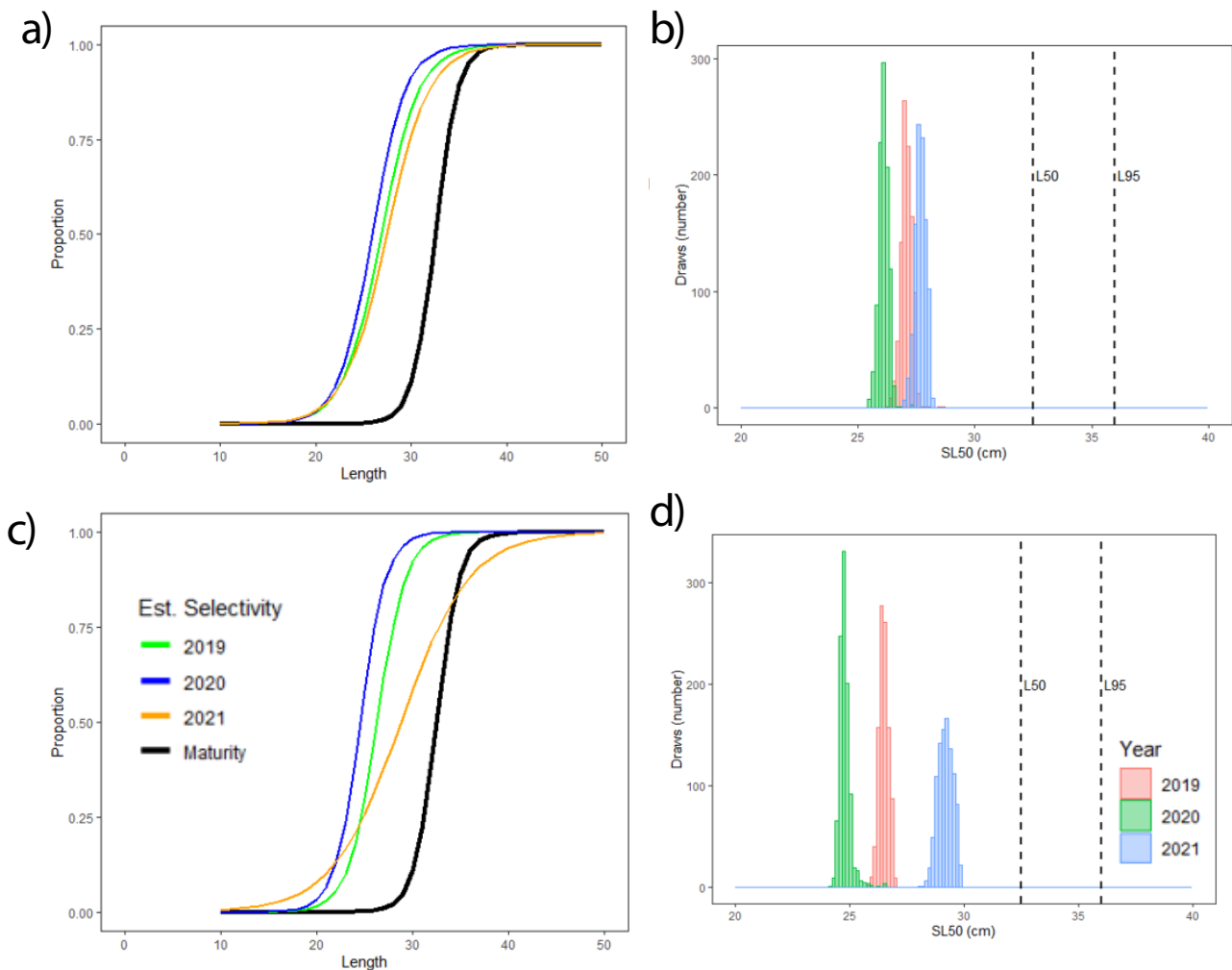


Figure 70. Left graphs plot the maturity-at-length curve and the estimated selectivity-at-length curve for each year by LBSPR for Norway lobster. Right graphs plot the SL50 values for each year; the bell shape is given by the number of draws. (a, b) Scenario 1 (ICatMar data), (c,d) Scenario 2 (DCF-GSA06 data). Data do not include discards.

Relative fishing mortality

For both scenarios, most of the F/M values estimated by the model remain above 1 for all years. The exception is for scenario 2 in year 2020, because the presence of larger individuals affects fishing mortality thus the model estimates values lower than 1 (Fig. 72).

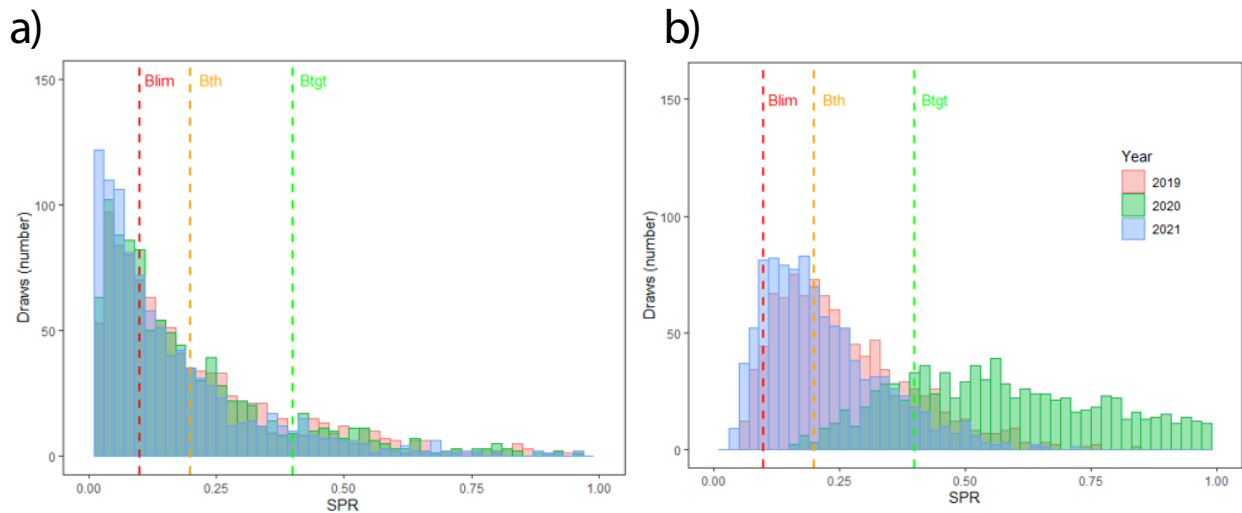


Figure 71. Estimated SPR values for Norway lobster. (a) Scenario 1 (ICatMar data), (b) Scenario 2 (DCF-GSA06 data). Data do not include discards.

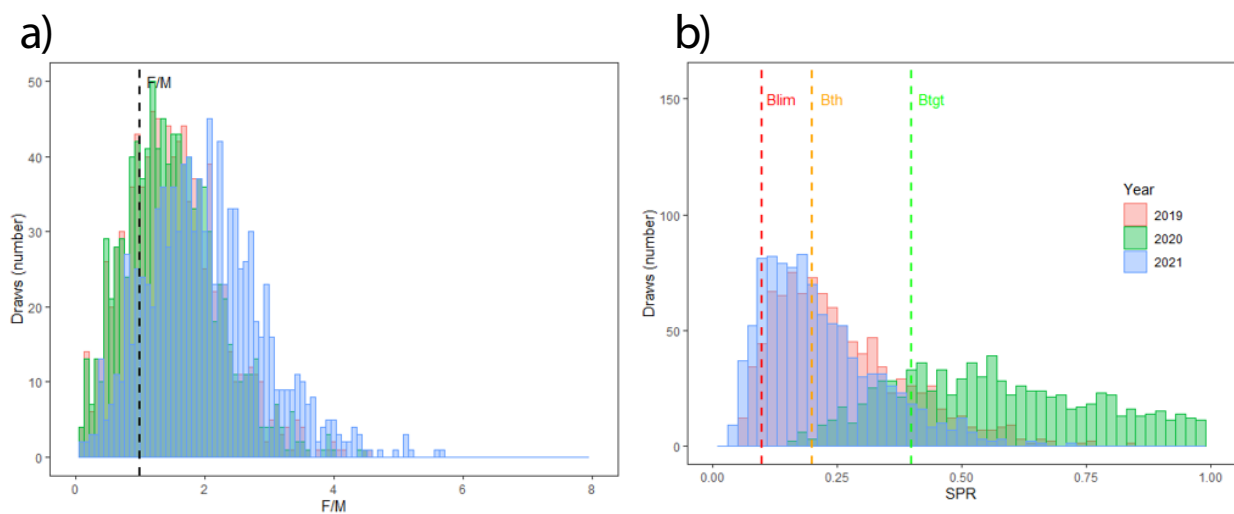


Figure 72. Estimated F/M values for Norway lobster. (a) Scenario 1 (ICatMar data), (b) Scenario 2 (DCF-GSA06 data). Data do not include discards.

LBPA

Fitted data

The fitting of the data varies with both studied scenarios (Fig. 73). For scenario 1, the model fit is similar among years. For scenario 2, the model does not seem to fit the data well, mainly overestimating it.

Maturity vs. Selectivity

The selectivity estimated by the model, for both scenarios, indicates that the fishery catches individuals that are below L_{mat50} (Figure 74). Scenario 1 seems to be further from maturity than scenario 2.

SPR and Fishing mortality estimations

In both scenarios, the model estimates SPR values below 0.4 and F values above 1 (Fig. 75). However, the model is more confident with the scenario 1 because there is less uncertainty. This is seen by the narrower bell shape from the graphs.

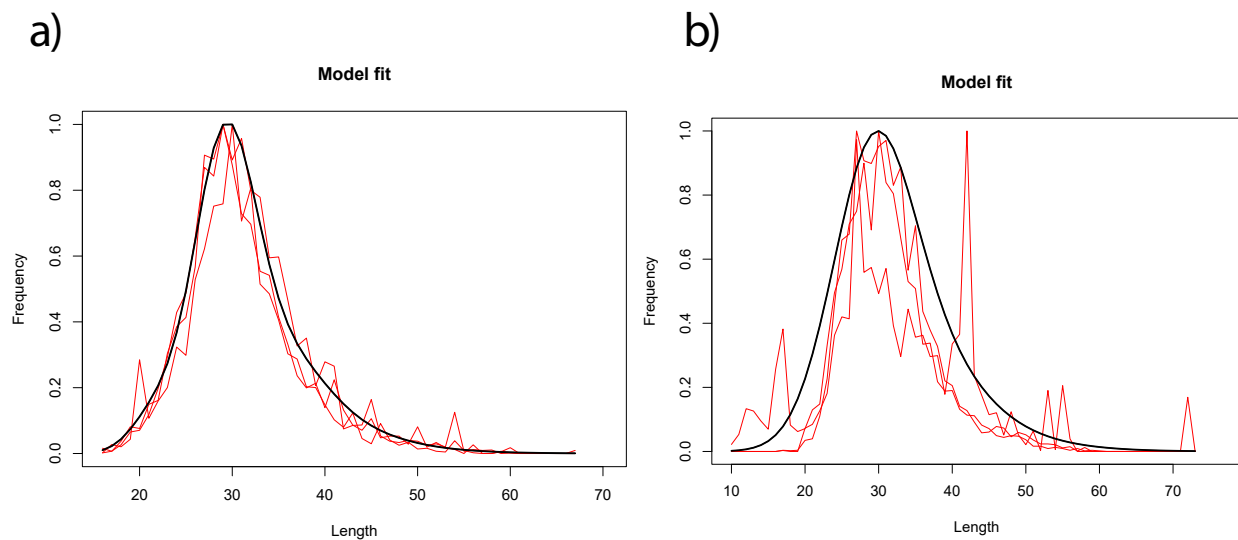


Figure 73. Fitting data by LBPR model Norway lobster. (a) Scenario 1 (ICatMar data), (b) Scenario 2 (DCF-GSA06 data). Red lines represent the length frequency for the 3 studied years; the black line is the length frequency distribution estimated for the model. Data do not include discards.

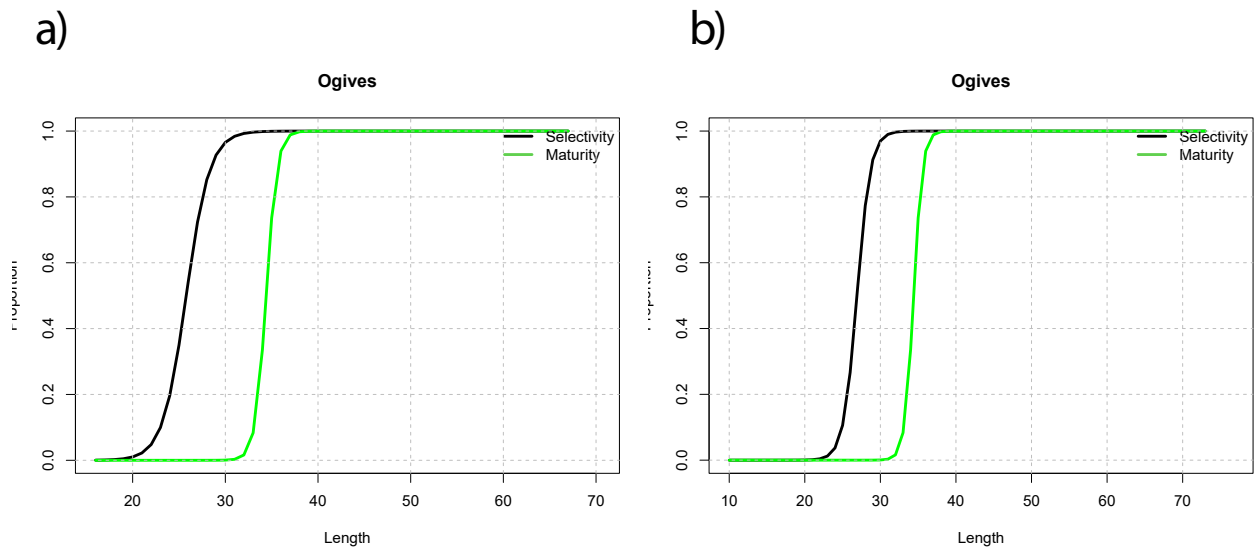


Figure 74. Graphs plotting the maturity-at-length curve and the estimated selectivity-at-length curve for each year by LBPR model for Norway lobster. (a) Scenario 1 (ICatMar data), (b) Scenario 2 (DCF-GSA06 data). Data do not include discards.

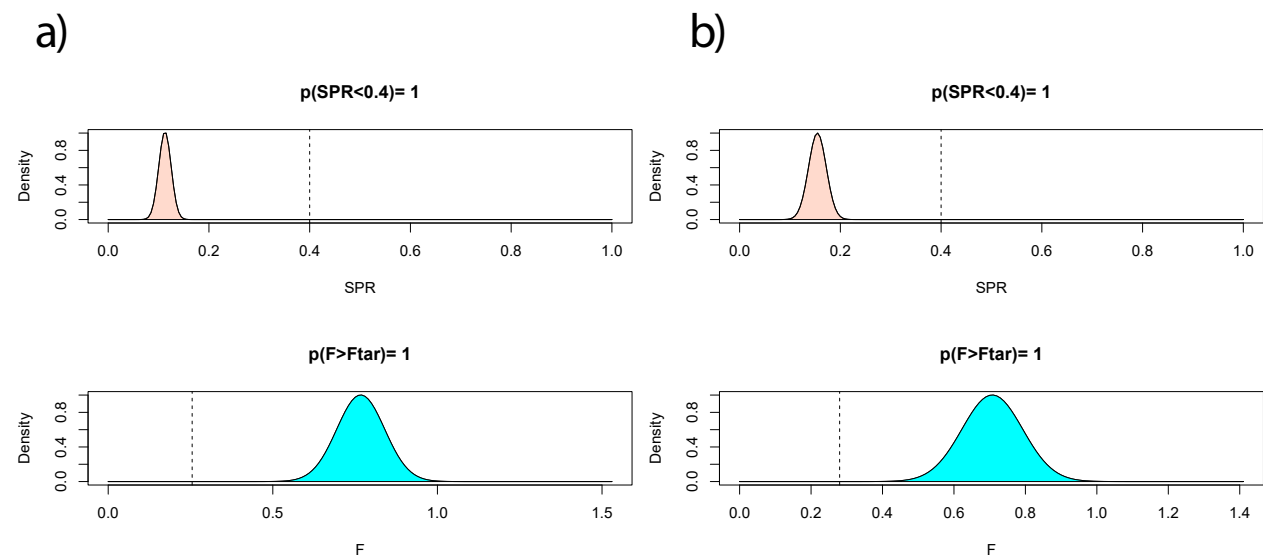


Figure 75. Graphs plotting the estimates of SPR and F by LBPR model for Norway lobster. (a) Scenario 1 (ICatMar data), (b) Scenario 2 (DCF-GSA06 data). Data do not include discards.

LIME

Fitted data

The fitting of the data varies with both studied scenarios (Fig. 76). For scenario 1, the model fit is well in general. For scenario 2, the model does not seem to fit the data, with sizes being underestimated and overestimating, especially for 2020.

Selectivity

The selectivity estimated by the model is different for both scenarios (Fig. 77). Whereas the selectivity for scenario 1 is below L_{mat50} for scenario 2 it is close to L_{mat50} .

For scenario 1, the SPR values estimated by the model are below 0.4 and remain stable through time. For scenario 2, values of SPR are close to 0.4 (Fig. 78).

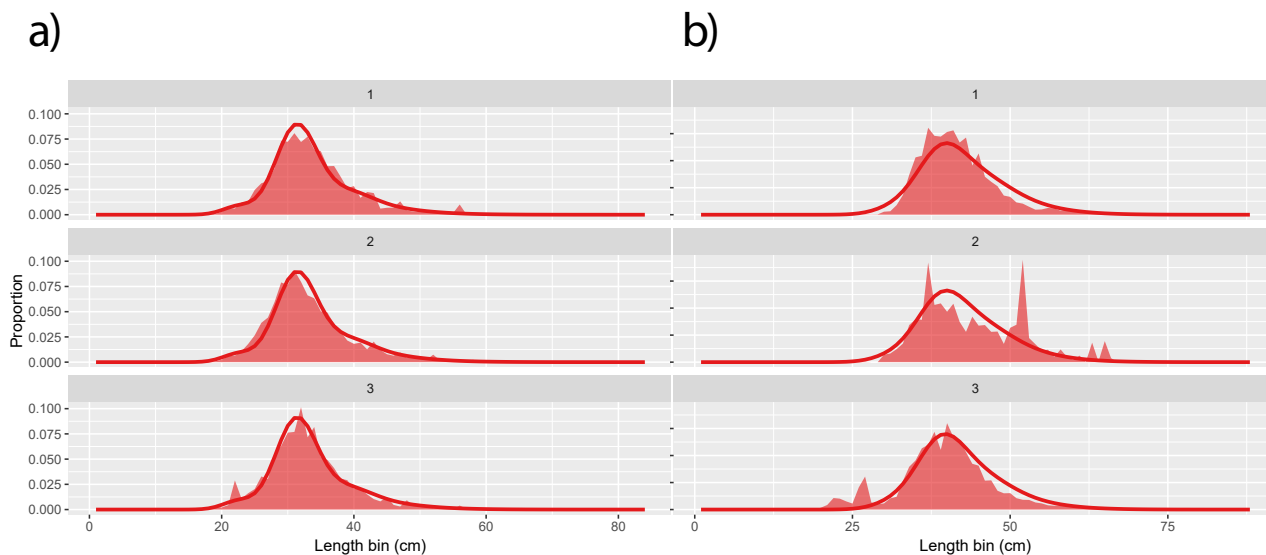


Figure 76. Fitting data by LIME model for Norway lobster. (a) Scenario 1 (ICatMar data), (b) Scenario 2 (DCF-GSA06 data). Top graph (1) plot year 2019, middle graphs (2) plot year 2020, and bottom graphs (3) plot year 2021. Data do not include discards.

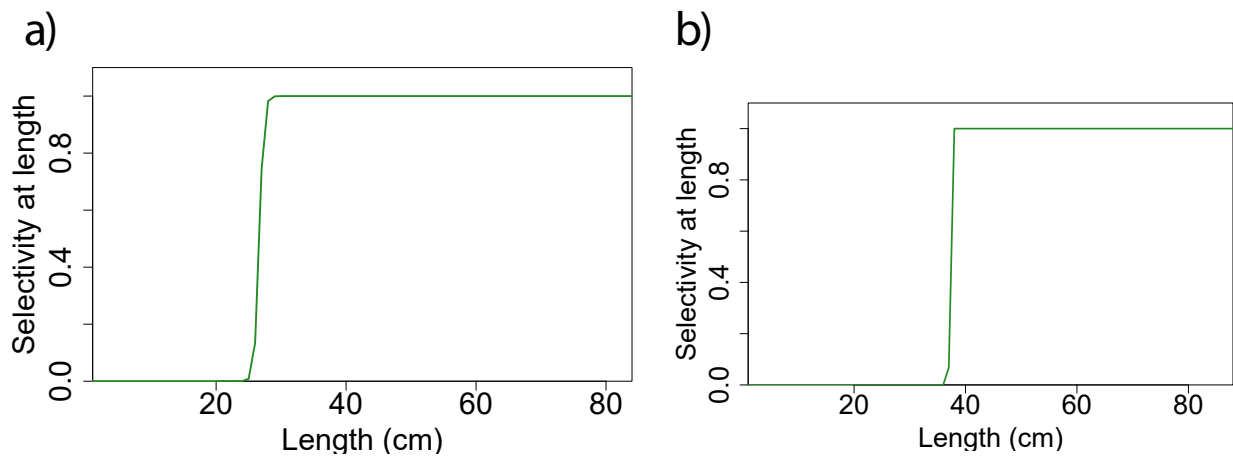


Figure 77. Graphs plotting the estimated selectivity-at-length curve by LIME model for Norway lobster. (a) Scenario 1 (ICatMar data), (b) Scenario 2 (DCF-GSA06 data). Data do not include discards.

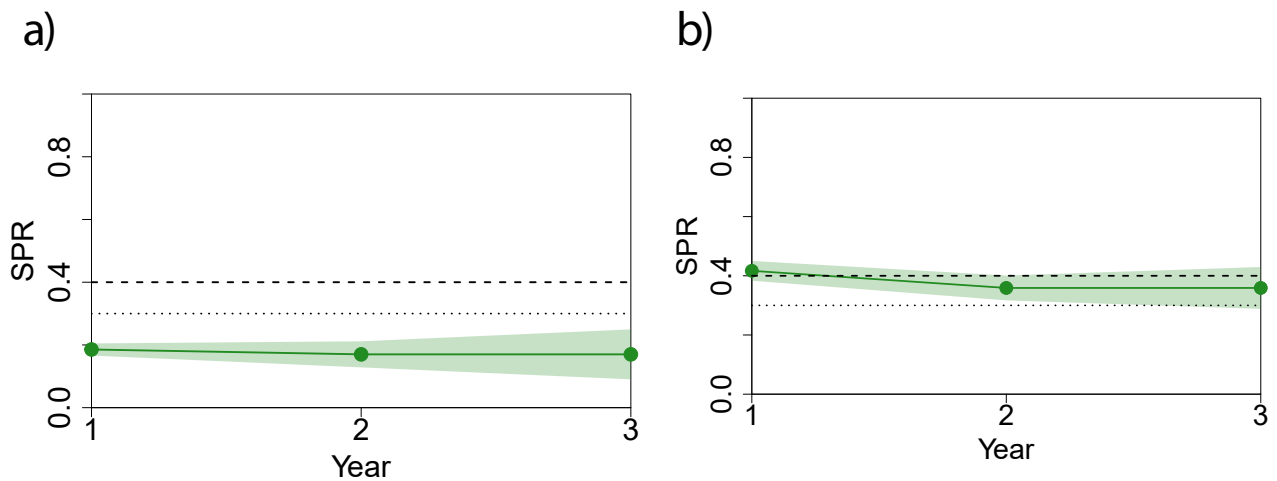


Figure 78. Graphs plotting the estimates of SPR by LIME model for Norway lobster. (a) Scenario 1 (ICatMar data), (b) Scenario 2 (DCF-GSA06 data). The uncertainty is shown by the green shade on both sides of the estimation. Data do not include discards.

Fishing mortality

For scenario 1 the fishing mortality is above the F_{msy} (Figure 79) whereas for scenario 2, the fishing mortality is close to F_{msy} .

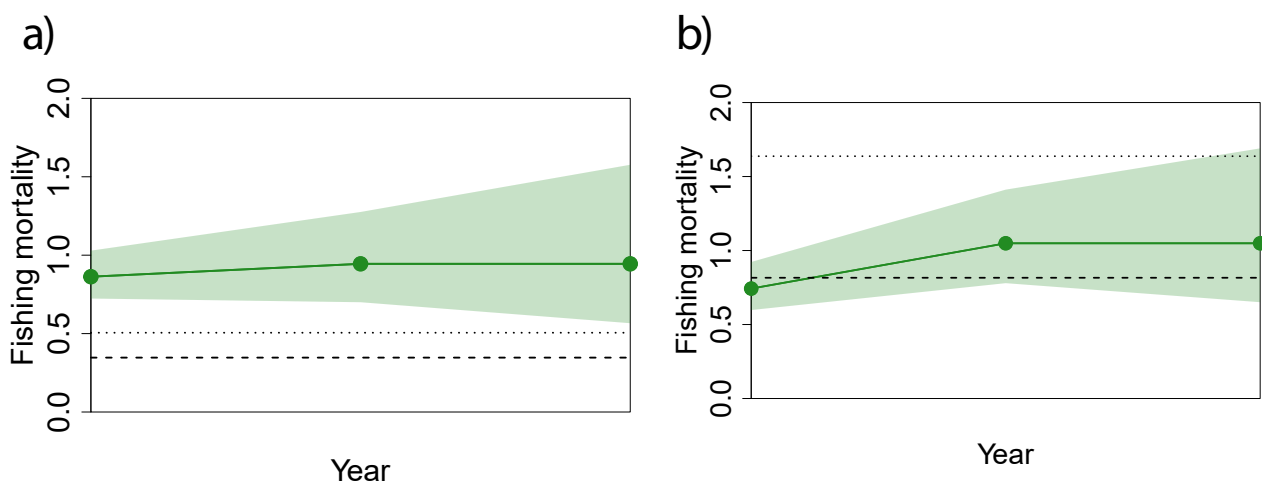


Figure 79. Estimated fishing mortality by LIME model for Norway lobster. (a) Scenario 1 (ICatMar data), (b) Scenario 2 (DCF-GSA06 data). The uncertainty is shown by the green shade on both sides of the estimation. Dotted line is the F_{msy} whereas the striped line is a precautionary F value. Data do not include discards.

Stock assessment indicators

Table 13. Stock assessment indicators for Norway lobster. Detailed information of each parameter can be found in the Glossary. Data do not include discards.

Specie	Scenario	Method	Year	SPR	F/M or F/Fmsy*
NEP	ICATMAR	LBSPR	2019	0.21	1.51
NEP	ICATMAR	LBSPR	2020	0.20	1.49
NEP	ICATMAR	LBSPR	2021	0.17	2.02
NEP	ICATMAR	LBPA	2019	0.11	3.01*
NEP	ICATMAR	LBPA	2020	0.11	3.01*
NEP	ICATMAR	LBPA	2021	0.11	3.01*
NEP	ICATMAR	LIME	2019	0.19	1.73
NEP	ICATMAR	LIME	2020	0.17	1.89
NEP	ICATMAR	LIME	2021	0.17	1.89
NEP	DCF-GSA6	LBSPR	2019	0.26	1.54
NEP	DCF-GSA6	LBSPR	2020	0.64	0.34
NEP	DCF-GSA6	LBSPR	2021	0.22	2.33
NEP	DCF-GSA6	LBPA	2019	0.15	2.53*
NEP	DCF-GSA6	LBPA	2020	0.15	2.53*
NEP	DCF-GSA6	LBPA	2021	0.15	2.53*
NEP	DCF-GSA6	LIME	2019	0.42	1.49
NEP	DCF-GSA6	LIME	2020	0.36	2.10
NEP	DCF-GSA6	LIME	2021	0.36	2.10

Blue and red shrimp (*Aristeus antennatus*) ARA

The blue and red shrimp (*Aristeus antennatus*; FAO code ARA) growth parameters, length-weight relationship and maturity at L_{mat50} and L_{mat95} are shown in Table 14. These data are used as inputs for the models used.

This species shows sexual dimorphism, with females reaching larger sizes than males. To analyse the data, though, only a combined set of growth parameters was used, thus the length data available was a dataset with both male and female parameters.

The reproduction of the blue and red shrimp occurs between April and September and recruitment is observed afterwards, in the seasons of autumn and winter.

The blue and red shrimp is a deep-water species caught exclusively by bottom trawl. It has a wide

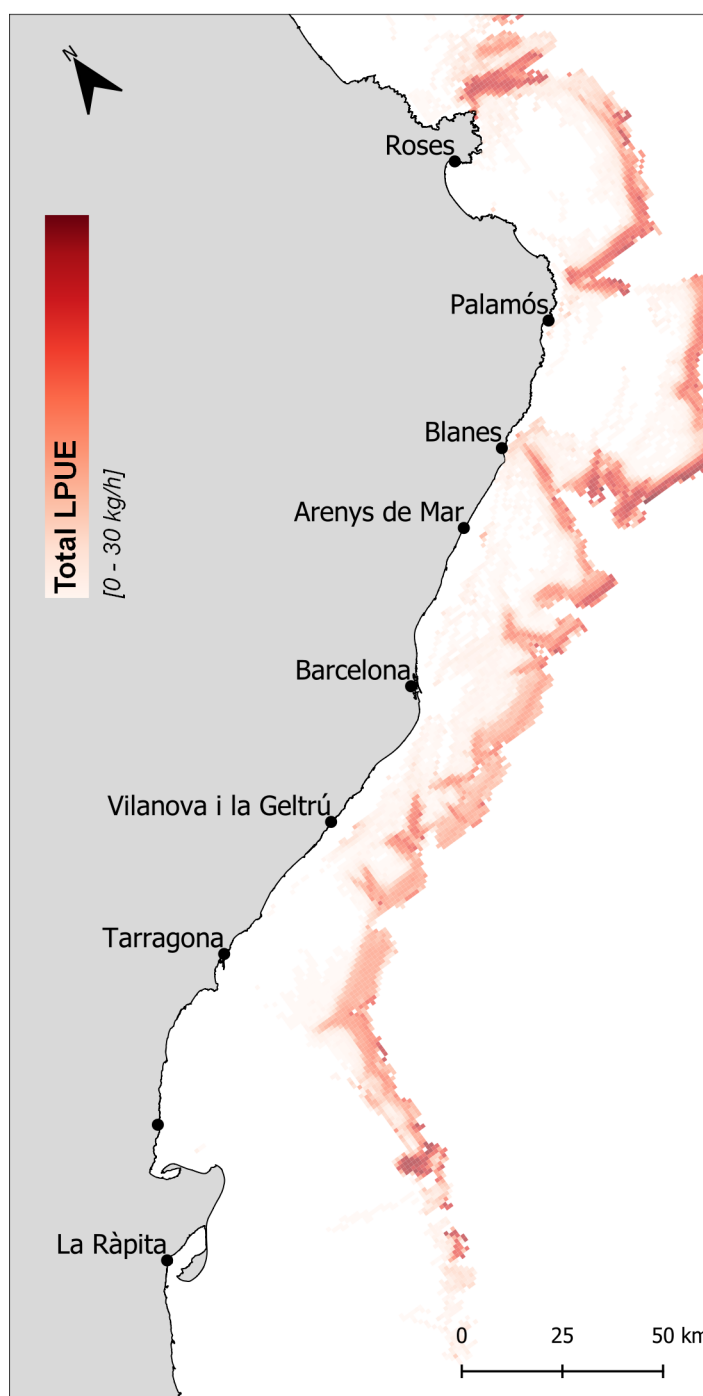


Figure 80. Spatial distribution of landings per unit effort (LPUE) for blue and red shrimp in the Catalan fishing grounds (N GSA6) in 2021.

Table 14. Biological parameters described for blue and red shrimp. Detailed information of each parameter can be found in the Glossary.

	L_{inf} (mm)	K	t_0	a	b	M	L_{mat50} (mm)	L_{mat95} (mm)
ARA	77	0.38	-0.065	0.00203	2.512	0.46	23.4	27
Data source	Garcia-Rodriguez (2003)			DCF 2017		Chen and Watanabe (1989)	GFCM RY2020	

bathymetric distribution, between 80 and 3300 m depth (Sardà et al., 2004), although commercial fishing grounds are located between 450 and 900 m depth (Figure 80)

Catch (landings and discards)

The historical landings for the blue and red shrimp are plotted from 2002 to 2021 in Figure 81. The landings have a clear downward trend until 2006, caused by a downwelling process as reported by Company et al (2008). The following year, 2007, the catches increased to a maximum of almost 700 t. From 2008 onwards, the catches have shown a negative trend until the present time. There are barely any discards for the blue and red shrimp because of the high commercial value of the species and no minimum catch size. Thus, for stock assessment, no discards have been accounted for the model input data.

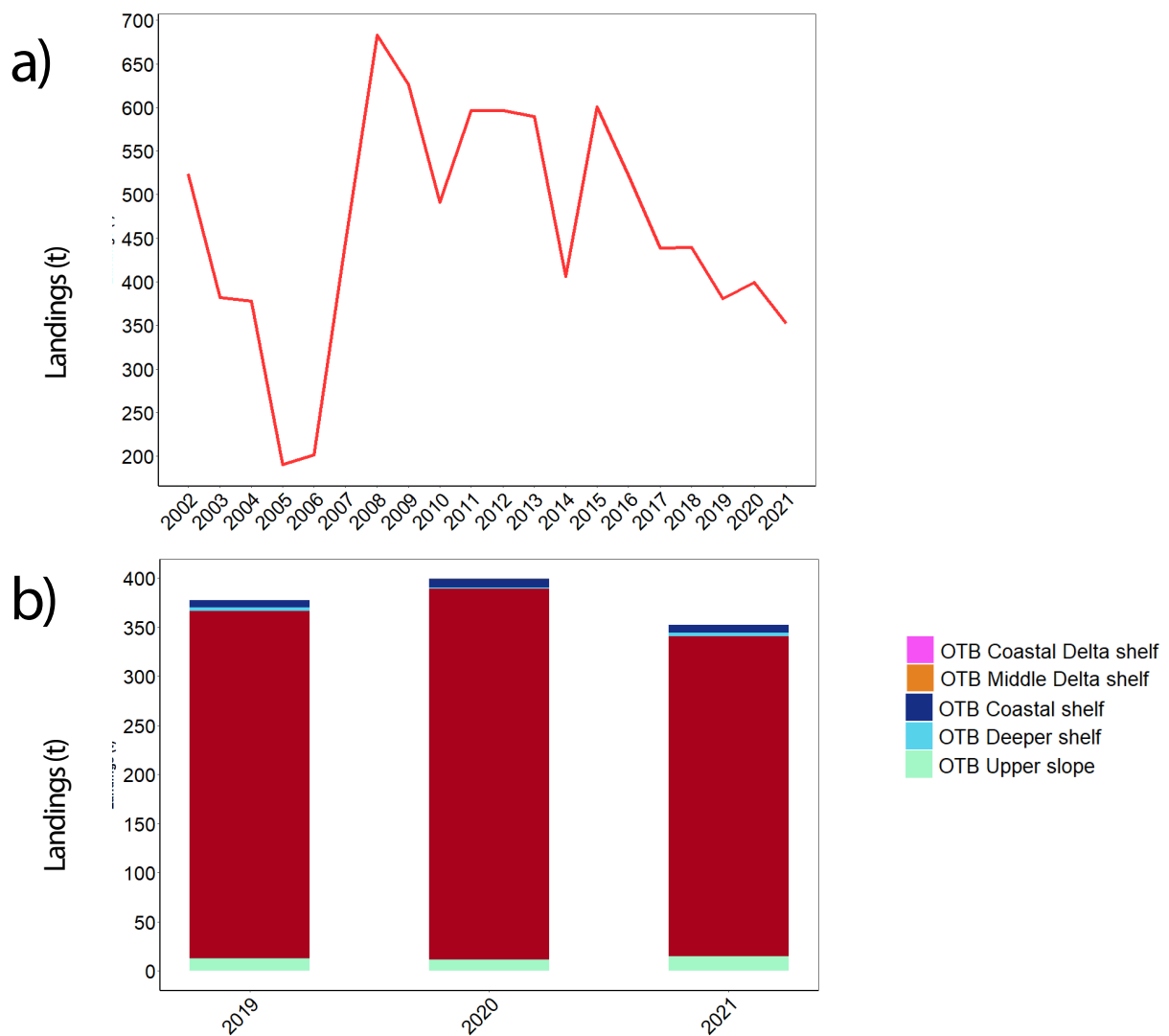


Figure 81. Characterization of blue and red shrimp landings. (a) Historical landings in Catalonia. (b) Landings per metier. (OTB) Bottom otter trawl.

The total landings by métier and fishing gear are shown in Figure 81. OTB Upper slope is the *métier* of the Catalan fishing fleet that catches the most blue and red shrimp.

The length frequency distribution per year and métier after raising the data for both scenarios, that is, using ICATMAR and DCF GSA6 data sets, are shown in Figure 82. For the first scenario (ICATMAR), there is a similar length structure among years, despite that there were larger individuals in 2021. On the contrary, for the second scenario (DCF GSA 6) there is no similarity among the length structure throughout the years and there are less individuals in years 2020 and 2021 than in 2019.

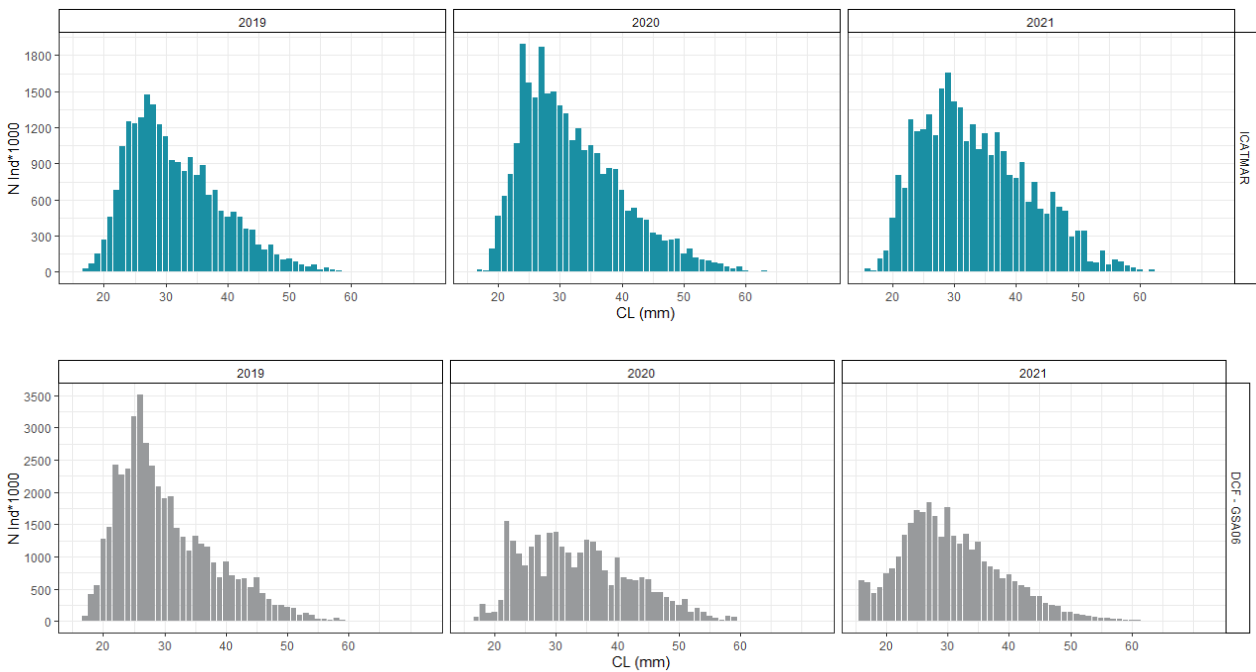


Figure 82. Annual length-frequency distributions for Blue and red shrimp. Scenario 1 (top plots) using the ICATMAR data set and Scenario 2 (bottom plots) using DCF-GSA06 data data set. The data do not include discards.

Stock assessment by model

LBSPR

Fitted data

The Fitting of the data varies with both studied scenarios (Figure 83). For scenario 1, there is a better fit in 2019. In general, a few length classes are overestimated or sub-estimated by the model, especially in 2020 and 2021. In scenario 2, the model has a good fit, in general, in 2019 and 2021 but not in 2020 where the length structure differs from the other years.

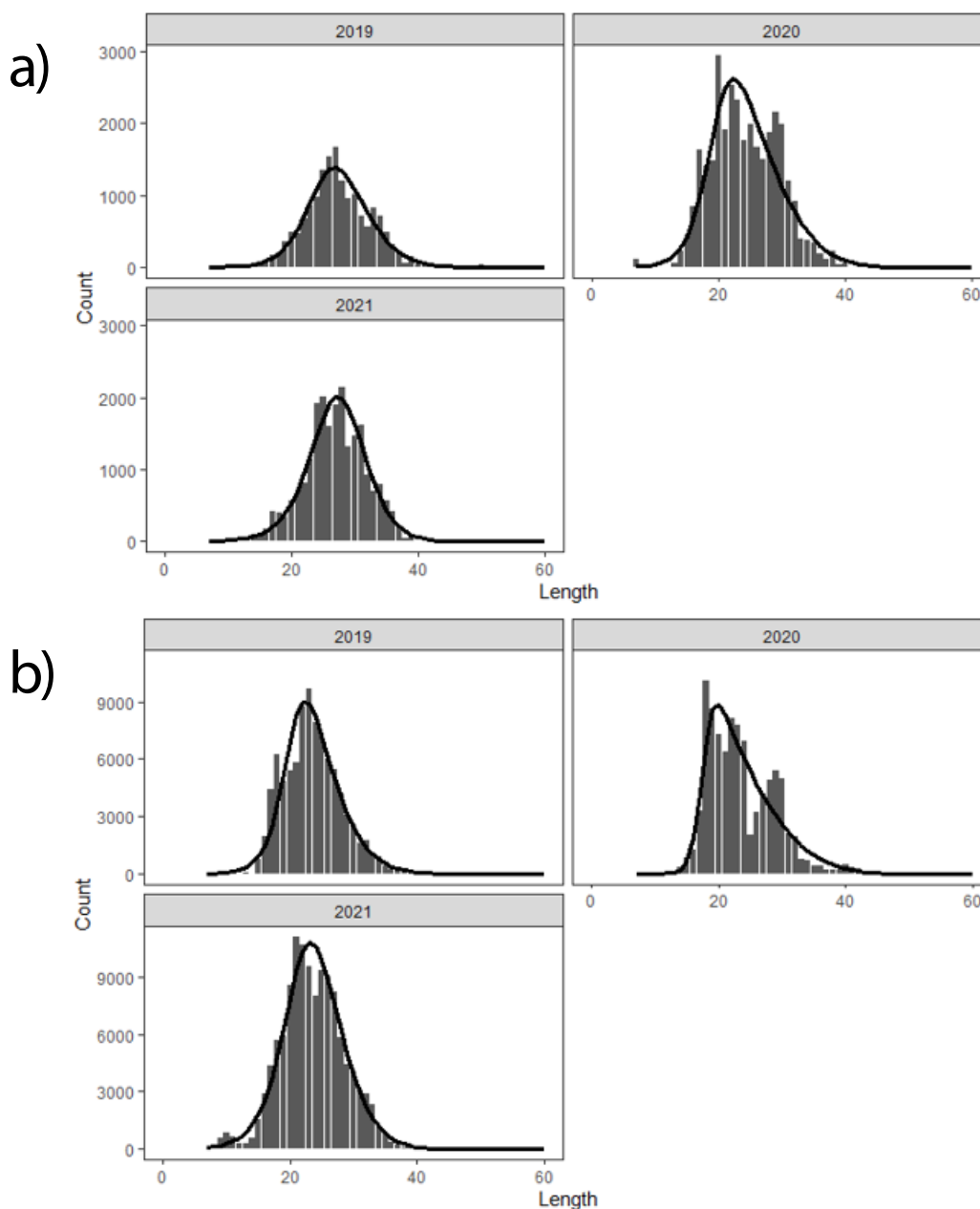


Figure 83. Fitting data by LBSPR model for blue and red shrimp. (a) Scenario 1 (ICatMar data), (b) Scenario 2 (DCF-GSA06 data). Data do not include discards.

Maturity vs. selectivity (absolute and range of values)

The selectivity estimated by the model, for both scenarios, indicates that the fishery catches individuals smaller than the L_{mat50} (Figure 84). In detail, for scenario 1, the model estimates selectivity close to the L_{mat50} maturity value for all years. Scenario 2 is slightly different because the model estimates selectivity close to the L_{mat50} maturity for 2020 and 2021 but not for 2019.

Precautionary advice based on SPR

For scenario 1, most of the SPR values estimated by the model remain below B_{lim} for all years. There seems to be a slight increasing trend from 2019 to 2021 (Figure 85). Similarly, for scenario 2, most of the SPR values estimated by the model remain below B_{lim} for years 2019 and 2021 (Figure 85). However, in 2020, most values are between B_{lim} and B_{th} . Differently than in scenario 1, there is no clear trend for the SPR values in scenario 2.

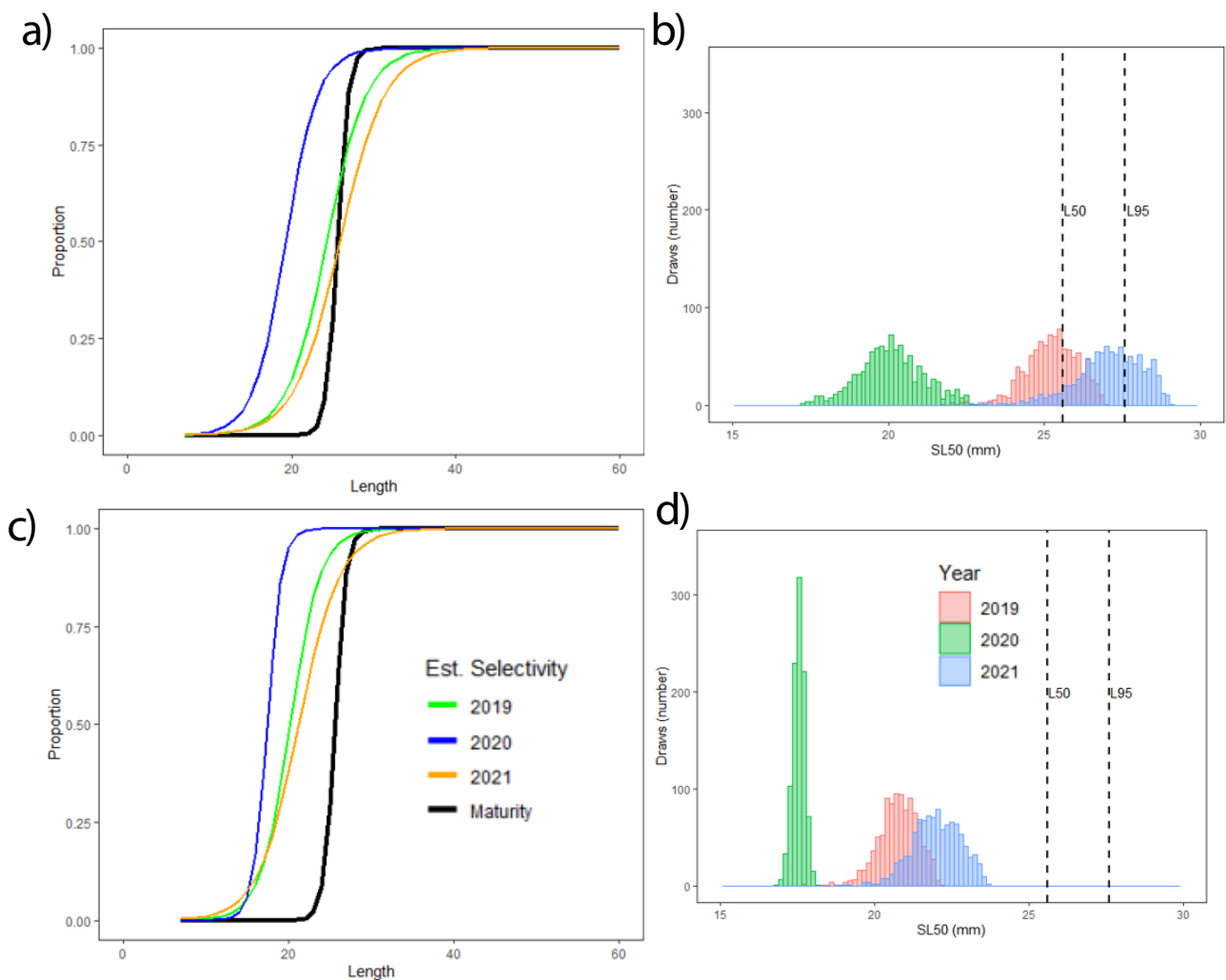


Figure 84. Left graphs plot the maturity-at-length curve and the estimated selectivity-at-length curve for each year by LBSPR for blue and red shrimp. Right graphs plot the SL50 values for each year; the bell shape is given by the number of draws estimated by the model. (a, b) Scenario 1 (ICatMar data), (c, d) Scenario 2 (DCF-GSA06 data). Data do not include discards.

Relative fishing mortality

For scenario 1, most of the F/M values estimated by the model for all years remain above 1, with a decreasing trend from 2019 to 2021. Similarly, for scenario 2, most of the F/M values estimated by the model for all years remain above 1. However, in this case, there is no clear trend with time (Figure 86).

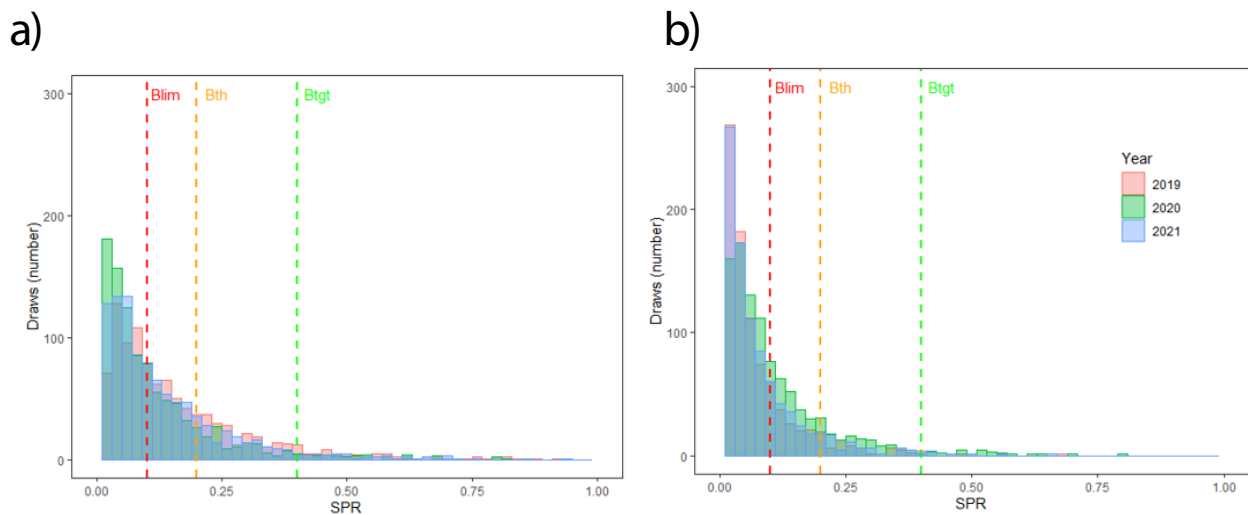


Figure 85. Estimated SPR values for blue and red shrimp. (a) Scenario 1 (ICatMar data), (b) Scenario 2 (DCF-GSA06 data). Data do not include discards.

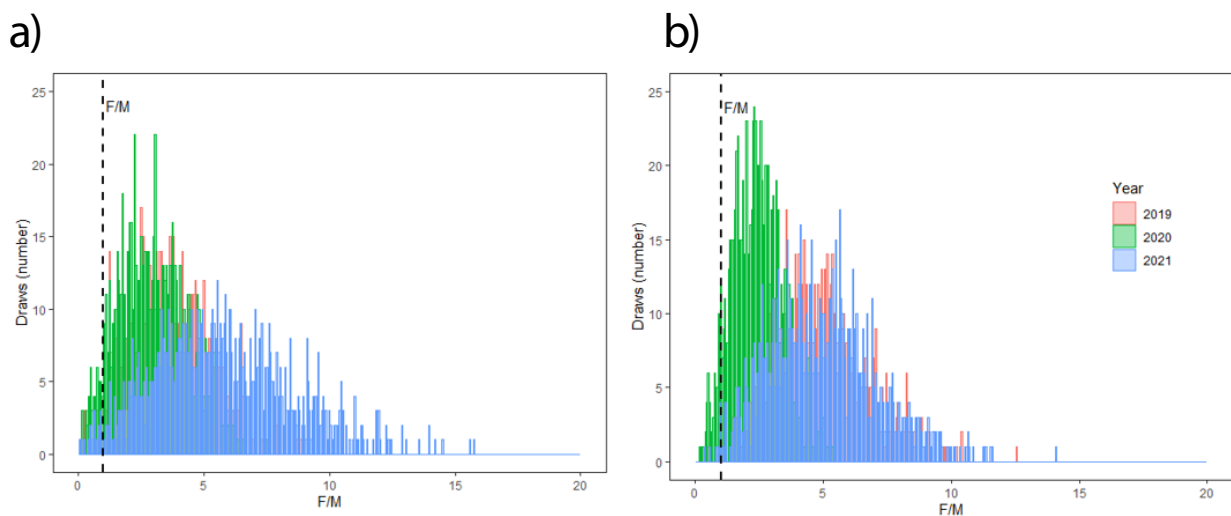


Figure 86. Estimated F/M values for blue and red shrimp. (a) Scenario 1 (ICatMar data), (b) Scenario 2 (DCF-GSA06 data). Data do not include discards.

LBPA

Fitted data

The fitting of the data varies with both studied scenarios (Figure 87). For scenario 1, the model fit is similar among years but mismatches with the estimated mode as this one is higher than those from the three studied years. On the contrary, for scenario 2, the model does not seem to fit the data well, mainly overestimating it.

Maturity vs. Selectivity

The selectivity estimated by the model, for both scenarios, indicates that it is nearby the L_{mat50} maturity but the fishery catches individuals are still below L_{mat50} (Figure 88).

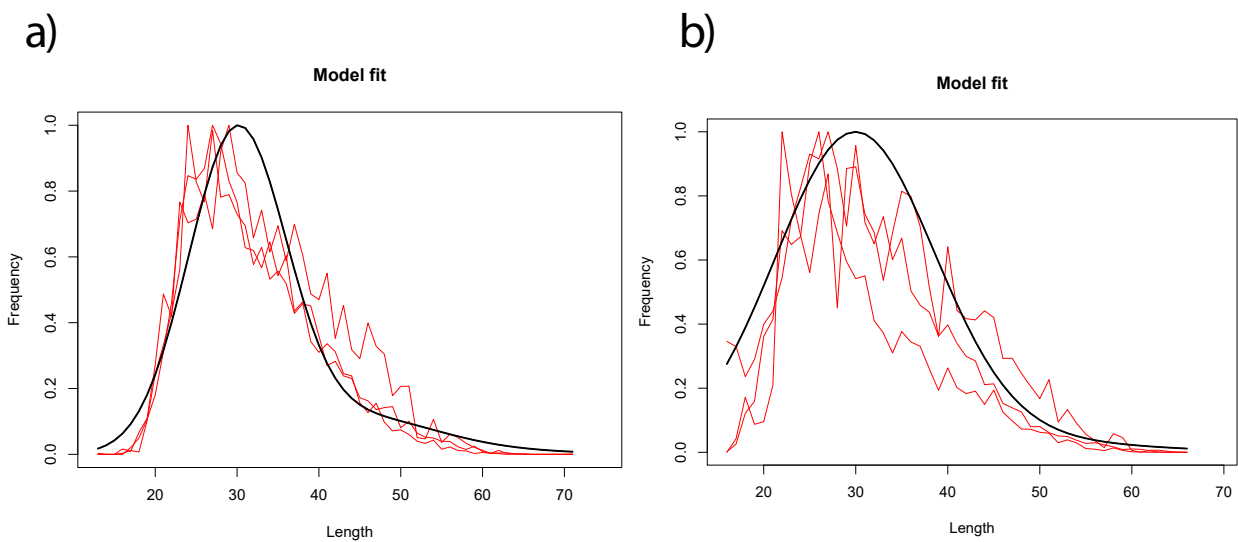


Figure 87. Fitting data by LBPR model for blue and red shrimp. (a) Scenario 1 (ICatMar data), (b) Scenario 2 (DCF-GSA06 data). Red lines represent the length frequency for the 3 studied years; the black line is the length frequency distribution estimated for the model. Data do not include discards.

SPR and Fishing mortality estimations

In both scenarios, the model estimates SPR values below 0.4 and F values above 1 (Figure 89). However, the model is more confident with the scenario 1 values because there is less uncertainty. This is seen by the narrower bell shape from the graphs.

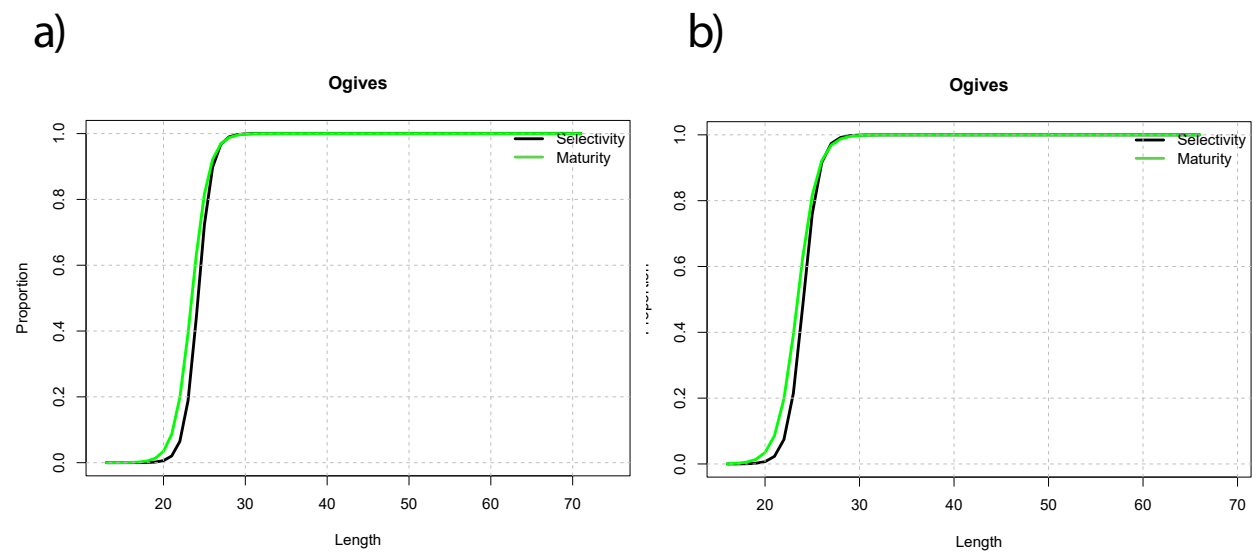


Figure 88. Graphs plotting the maturity-at-length curve and the estimated selectivity-at-length curve for each year by LBPR model for blue and red shrimp. (a) Scenario 1 (ICatMar data), (b) Scenario 2 (DCF-GSA06 data). Data do not include discards.

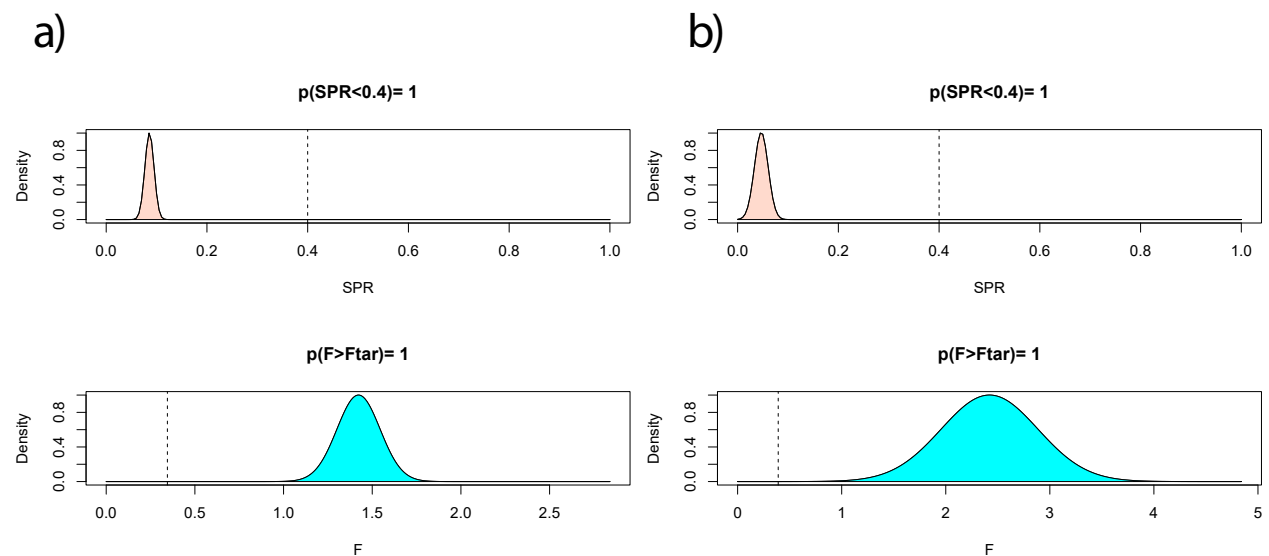


Figure 89. Graphs plotting the estimates of SPR and F by LBPR model for blue and red shrimp. (a) Scenario 1 (ICatMar data), (b) Scenario 2 (DCF-GSA06 data). Data do not include discards.

LIME

Fitted data

The fitting of the data varies with both studied scenarios (Figure 90). For scenario 1, the model fit is better for 2020 and 2021 because in 2019, the mode is mismatched and estimated with lower values. For scenario 2, the model does not seem to fit the data well, with sizes being underestimated and overestimating, especially for 2020.

Selectivity

The selectivity estimated by the model is different for both scenarios (Figure 91). Whereas the selectivity for scenario 1 is below L_{mat50} for scenario 2 it is close L_{mat50} .

Precautionary advice based on SPR

For both scenarios, the SPR values estimated by the model are below 0.4 and remain stable through time (Figure 92). There seems to be a lower uncertainty in scenario 2.

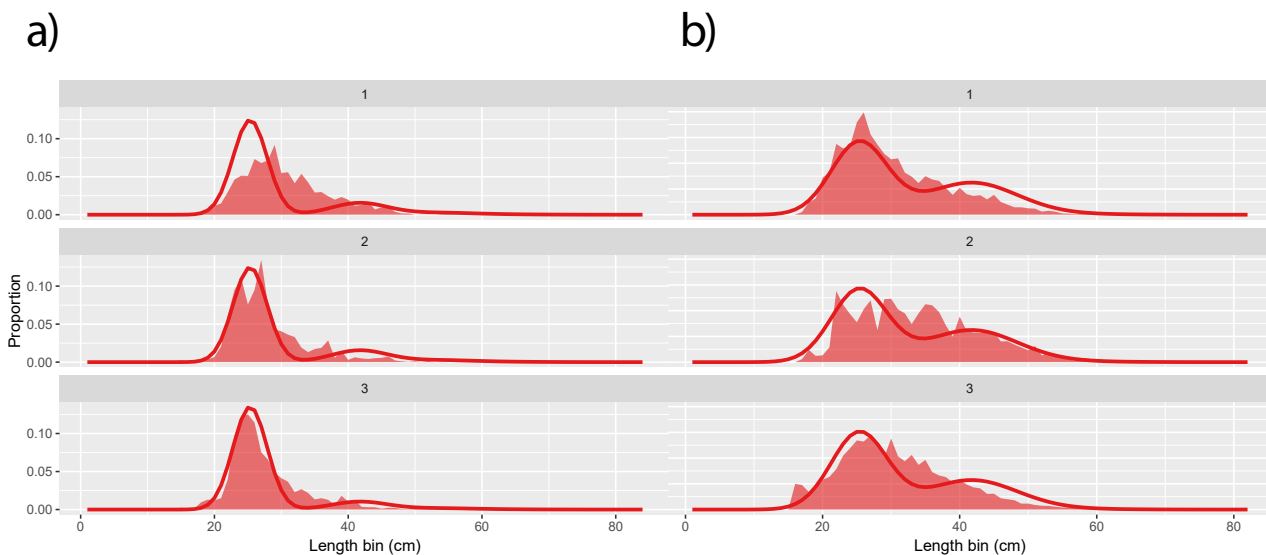


Figure 90. Fitting data by LIME model for blue and red shrimp. (a) Scenario 1 (ICatMar data), (b) Scenario 2 (DCF-GSA06 data). Top graphs (1) plot year 2019, middle graphs (2) plot year 2020, and bottom graphs (3) plot year 2021. Data do not include discards.

Fishing mortality

For both scenarios, 1 and 2, the fishing mortalities are above the F_{msy} (Figure 93). However, the values and uncertainty are much higher in scenario 2 than in scenario 1.

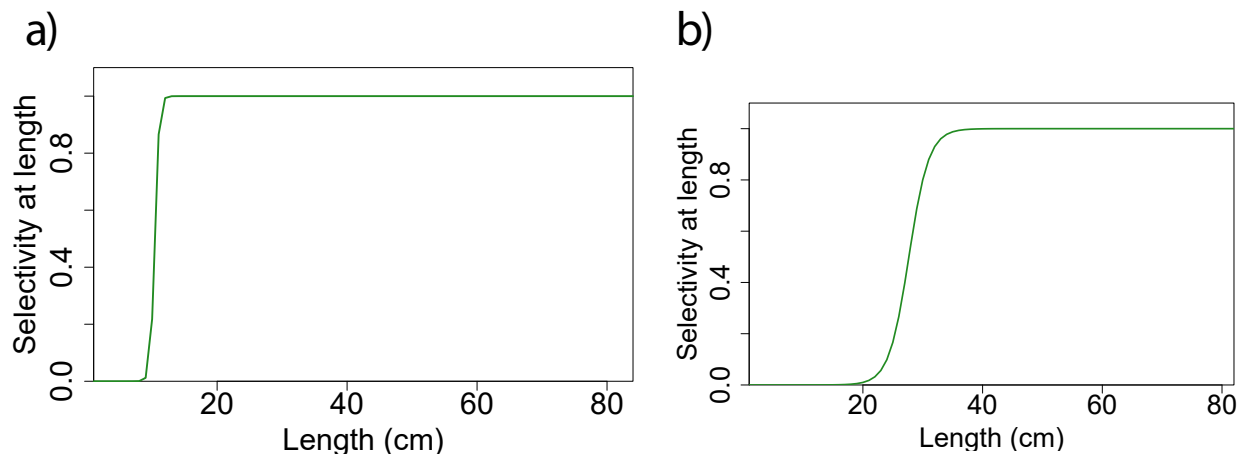


Figure 91. Graphs plotting the estimated selectivity-at-length curve by LIME model for blue and red shrimp. (a) Scenario 1 (ICatMar data), (b) Scenario 2 (DCF-GSA06 data). Data do not include discards.

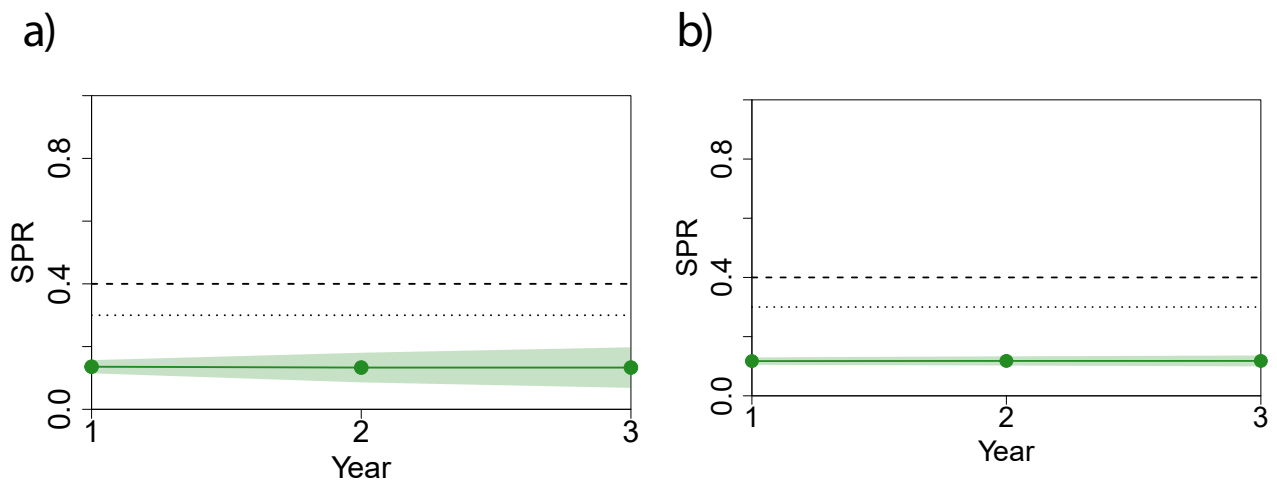


Figure 92. Estimated SPR values by LIME model for blue and red shrimp. (a) Scenario 1 (ICatMar data), (b) Scenario 2 (DCF-GSA06 data). The uncertainty is shown by the green shade on both sides of the estimation. Data do not include discards.

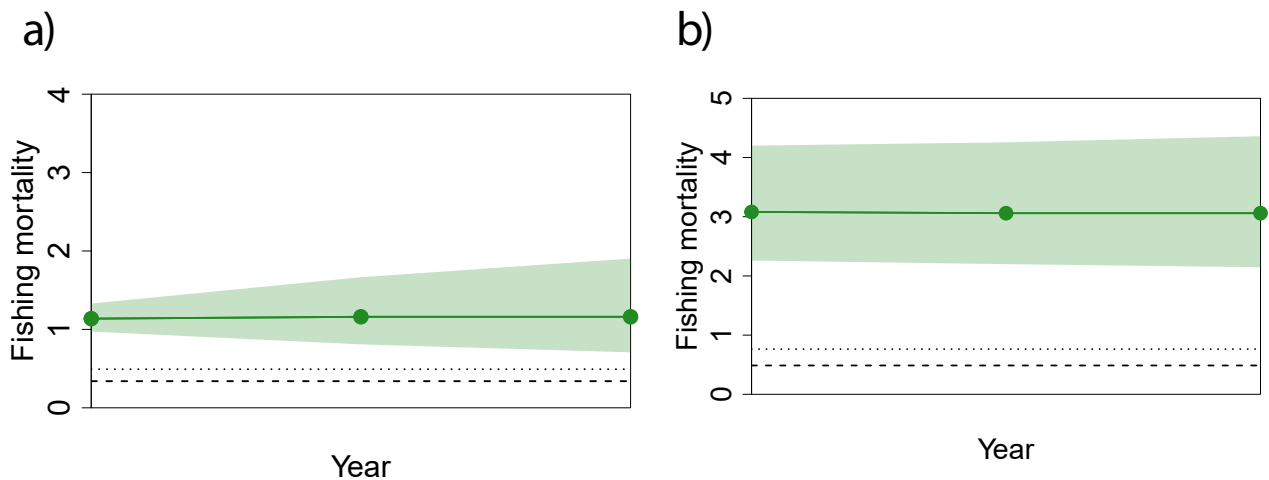


Figure 93. Estimated fishing mortality by LIME model for blue and red shrimp. (a) Scenario 1 (ICatMar data), (b) Scenario 2 (DCF-GSA06 data). The uncertainty is shown by the green shade on both sides of the estimation. Dotted line is the F_{msy} whereas the striped line a precautionary F value. Data do not include discards.

Stock assessment indicators

Table 15. Stock assessment indicators for blue and red shrimp. Detailed information of each parameter can be found in the Glossary. Data do include discards.

Specie	Scenario	Method	Year	SPR	F/M or F/Fmsy*
ARA	ICATMAR	LBSPR	2019	0.07	3.60
ARA	ICATMAR	LBSPR	2020	0.09	3.14
ARA	ICATMAR	LBSPR	2021	0.11	2.69
ARA	ICATMAR	LBPA	2019	0.05	5.69*
ARA	ICATMAR	LBPA	2020	0.05	5.69*
ARA	ICATMAR	LBPA	2021	0.05	5.69*
ARA	ICATMAR	LIME	2019	0.14	2.47
ARA	ICATMAR	LIME	2020	0.13	2.52
ARA	ICATMAR	LIME	2021	0.13	2.52
ARA	DCF-GSA6	LBSPR	2019	0.07	3.50
ARA	DCF-GSA6	LBSPR	2020	0.13	2.42
ARA	DCF-GSA6	LBSPR	2021	0.07	3.68
ARA	DCF-GSA6	LBPA	2019	0.05	6.21*
ARA	DCF-GSA6	LBPA	2020	0.05	6.21*
ARA	DCF-GSA6	LBPA	2021	0.05	6.21*
ARA	DCF-GSA6	LIME	2019	0.12	6.70
ARA	DCF-GSA6	LIME	2020	0.12	6.65
ARA	DCF-GSA6	LIME	2021	0.12	6.65



4

Conclusions and Comments

From this report, two main conclusions can be highlighted. First, a more detailed sampling can generate better length frequency distributions meaning that these are more stable over the years, which is of interest for stock assessments. Moreover, the results obtained with ICATMAR length data for Catalonia are consistent with those presented by the STECF for the GSA06.

The second main conclusion is that all the studied stocks are overexploited and in overexploitation on a precautionary basis. However, modelling results differ among the studied fishing stocks. In detail, the red mullet and the European hake SPR are always under Blim for the three years evaluated and with the three models tested. The deep-water rose shrimp and the blue and red shrimp results varied according to each model evaluated, being below or above Blim. Finally, the Norway lobster estimates for all the models resulted in a SPR above the Blim.

It is worth mentioning that the models LBSPR, LBPA and LIME are *data-limited* and cannot provide a quantitative assessment, with three years of data and the presented temporal resolution. Ideally, stock assessments would require long term data sets. For example, for the European hake, the time series should include, at least, the life span of the species, which is about 10 years. Another limitation of the models is the apparent inaccuracy in estimating fishing mortality; thus, it is recommended SPR to be considered as the stock indicator. The model fit also affects the reliability of the results.

In summary, the main objective of this report was to explore the use of data-limited stock assessment models with the three years of data collected from ICATMAR. The next step is to continue the intense monitoring program in the area to establish a long-term data collection, and fill in potential information gaps that might arise with the current sampling European monitoring system.

References

Abella, A.J., Caddy, J.F., Serena, F., 1997. Do natural mortality and availability decline with age? An alternative yield paradigm for juvenile fisheries, illustrated by the hake *Merluccius merluccius* fishery in the Mediterranean. *Aquat Liv Res.* 10, 257–269.

Canales, C.M., Punt, A.E., Mardones, M., 2021. Can a length-based pseudo-cohort analysis (LBPA) using multiple catch length-frequencies provide insight into population status in data-poor situations? *Fish Res.* 234, 105810.

Chen, S., Watanabe, S., 1989. Age dependence of natural mortality coefficient in fish population dynamics. *Nippon Suisan Gakk.* 55, 205–208.

Company, J.B., Puig, P., Sardà, F., Palanques, A., Latasa, M., Scharek, R., 2008. Climate influence on deep sea populations. *PLoS ONE.* 3, e1431.

García-Rodríguez, M., 2003. Characterisation and standardisation of a red shrimp, *Aristeus antennatus* (Risso, 1816), fishery off the Alicante gulf (SE Spain). *Sci Mar.* 67, 63–74.

García-Rodríguez, M., Barcala, E., Gil, J.P., 2009. Some biological aspects of *Parapenaeus longirostris* (Lucas, 1846) (Decapoda, Dendrobranchiata) in the gulf of Alicante (SE Spain). *Crustaceana.* 82, 293–310.

García-Rodríguez, M., Fernández, Á.M., 2005. Influence of cod-end mesh geometry on catches, selectivity and yields of some commercial fish species in the Gulf of Alicante (Southeastern Iberian Peninsula). IEO, Madrid, pp. 26.

Hordyk, A., Ono, K., Prince, J.D., Walters, C.J., 2016. A simple length-structured model based on life history ratios and incorporating size-dependent selectivity: application to spawning potential ratios for data-poor stocks. *Can J Fish Aquat Sci.* 13, 1–13.

Lombarte, A., Recasens, L., González, M., Gil de Sola, L., 2000. Spatial segregation of two species of Mullidae (*Mullus surmuletus* and *M. barbatus*) in relation to habitat. *Mar Ecol Prog Ser.* 206, 239–249.

Mellon-Duval, C., de Pontual, H., Métral, H., Quemener, L., 2009. Growth of European hake (*Merluccius merluccius*) in the Gulf of Lions based on conventional tagging. *ICES J Mar Sci.* 67, 62–70.

Recasens, L., Chiericoni, V., Belcari, P., 2008. Spawning pattern and batch fecundity of the European hake (*Merluccius merluccius* (Linnaeus, 1758)) in the western Mediterranean. *Sci Mar.* 72, 721–732.

Rudd, M.B., Thorson, J.T., 2018. Accounting for variable recruitment and fishing mortality in length-based stock assessments for data-limited fisheries. *Can J Fish Aquat Sci.* 75, 1019–1035.

Sardà, F., D'Onghia, G., Politou, C.Y., Company, J.B., Maiorano, P., Kapiris, K., 2004. Deep-sea distribution, biological and ecological aspects of *Aristeus antennatus* (Risso, 1816) in the western and central Mediterranean Sea. *Sci Mar.* 68, 117–127.

